

Drew University
College of Liberal Arts

**Some Reactions of Triosmium Decacarbonyl Bisethoxide,
 $\text{Os}_3(\text{CO})_{10}(\mu^2\text{-OEt})_2$, with Amides**

A Thesis in Chemistry

by

Katherine Marak

Submitted in Partial Fulfillment of the Requirements for the Degree of Bachelor in Arts
With Specialized Honors in Chemistry

Examining Committee:

Mary-Ann Pearsall, Thesis Advisor

Chemistry

Alan Rosan, Member

Chemistry

Minjoon Kouh, Member

Physics

MAY 2017

Abstract

In our investigation of the unique and unexplored dibridged triosmium cluster, $\text{Os}_3(\text{CO})_{10}(\mu^2\text{-OEt})_2$, reactions with amides were performed. The reactions with acetamide (CH_3CONH_2) and benzamide ($\text{C}_6\text{H}_5\text{CONH}_2$) were analogous to the reaction of the cluster with carboxylic acids forming a diosmium complex, but there exists the possibility of isomers. Spectroscopic NMR and IR data with supporting DFT frequency calculations used to characterize the coordination of the ligands to the clusters as well as chromatographic data indicates that under thermodynamic conditions both isomers of $\text{Os}_2(\text{CO})_6(\text{RCONH})_2$ ($\text{R} = \text{C}_6\text{H}_5, \text{CH}_3$) were observed in almost equal amounts for $\text{R} = \text{CH}_3$ (52:48) but, favored the less polar (H,T) isomer when $\text{R} = \text{C}_6\text{H}_5$ (61:39). The proposed reaction scheme for the reaction with acetamide is below:

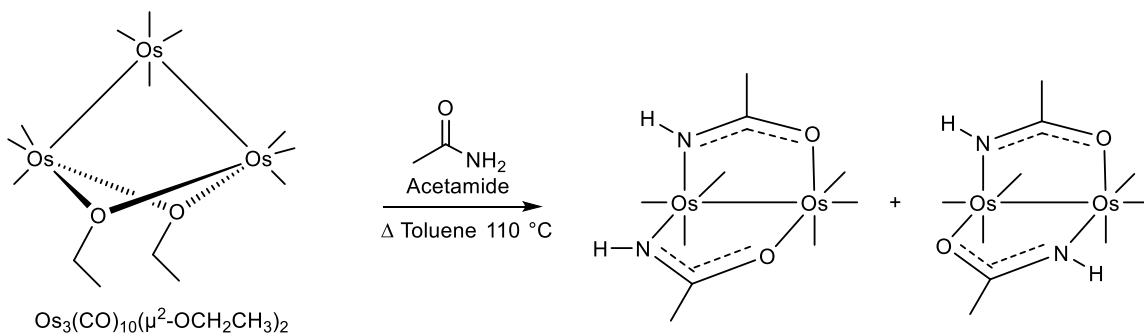


Table of Contents

1. Introduction	1
a. General Chemistry of Osmium Carbonyl Clusters	10
b. Osmium Carbonyl Clusters with Carboxylate Ligands	19
c. Reactions of Osmium Carbonyl Clusters with Amides	22
2. Experimental	
a. $Os_3(CO)_{10}(\mu^2-OEt)_2$ and acetamide in hexanes (68 °C)	25
b. Synthesis of new clusters of the type $[Os_2(CO)_6(RCONH)_2]$ using $Os_3(CO)_{10}(\mu^2-OEt)_2$ and acetamide in toluene (110 °C)	25
c. Synthesis of new clusters of the type $[Os_2(CO)_6(RCONH)_2]$ using $Os_3(CO)_{10}(\mu^2-OEt)_2$ and benzamide in toluene (110 °C)	26
d. Gaussian09 DFT Calculations on optimized structure of the type $[Os_2(CO)_6(HCONH)_2]$	27
3. Methods	
a. FT-Infrared Spectroscopy	28
b. Thin Layer Chromatography	30
c. Nuclear Magnetic Resonance	32
d. DFT Vibrational Calculations	34
4. Results and Discussion	
a. Reaction of $Os_3(CO)_{10}(\mu^2-OEt)_2$ and acetamide	36
b. Reaction of $Os_3(CO)_{10}(\mu^2-OEt)_2$ and benzamide	44
c. Reaction comparison of amides and carboxylic acids as ligands	47

d. Computational Vibrational Analysis	48
e. $^1\text{H-NMR}$ analysis of products I-IV	60
f. D_2O exchange to find exchangeable protons	64
g. Interconversion of the isomers cis-(H,T) and cis-(H,H) $\text{Os}_3(\text{CO})_6(\mu^2\text{-PhCONH})_2$ in solution of CDCl_3	66
5. Conclusion	70
6. Works Cited	72
7. Spectral Appendix	75

Tables

01	Bidentate ligand reactivity summary table	48
02	Summary of computational bond lengths and angles	54
03	Frequency calculation summary table for clusters the three clusters	58
04	Reactions summary of $\text{Os}_3(\text{CO})_{10}(\mu^2\text{-OEt})_2$ with bidentate ligands	71

Figures

01	Structure of $\text{Os}_3(\text{CO})_{10}(\mu^2\text{-L})_2$	1
02	Structure of trinuclear cluster $\text{Os}_3(\text{CO})_{12}$ (left) and mononuclear metal complex $\text{Os}(\text{CO})_5$ (right).	2
03	Structure of osmium pentacarbonyl $\text{Os}(\text{CO})_5$ and its electron count	2
04	Structure and electron count for $\text{Os}_3(\text{CO})_{10}(\mu^2\text{-OEt})_2$	3
05	Simple metal-ligand interactions arranged in order of field strength	4
06	CO acting as a ligand with generic metal (M).	5
07	Synthetic scheme of Fe, Ru and Os nanoparticles formation in ionic liquids	6
08	Triosmium carbonyl clusters acting a molecular switched via linking ligands	7
09	Os_3 clusters shown to induce apoptosis	7
10	Novel cluster head-to-tail (H,T) of $\text{cis-}[\text{Rh}_2(\text{HNOCCCH}_3)_2(\text{CH}_3\text{CN})_6]^{2+}$ and subsequent photo-activated product which can bind to DNA	8
11	General structure of amides as well as examples of primary secondary and tertiary amides	9
12	The formation of peptide bonds from amino acids	10
13	Structure of $\text{Os}_3(\text{CO})_{12}$	11
14	Reaction scheme for $\text{Os}_3(\text{CO})_{12}$ with isobutanol	11
15	Clusters with 3 Os-Os bonds	12
16	Typical product class of clusters $\text{Os}_3(\text{CO})_{10}(\text{CH}_3\text{CN})_2$ and $\text{Os}_3(\text{CO})_{10}(\mu^2\text{-H})(\mu^2\text{-OH})$	13
17	Reaction scheme of hydrogenation of $\text{Os}_3(\text{CO})_{12}$ to give $\text{Os}_3(\text{CO})_{10}(\mu^2\text{-H})_2$	13
18	Typical product structure and electron count of reactions of $\text{Os}_3(\text{CO})_{10}(\mu^2\text{-H})_2$ with nucleophiles	14

19	$\text{Os}_3(\text{CO})_{10}(\mu^2\text{-OEt})_2$ as a minor product of $\text{Os}_3(\text{CO})_{12}$ synthesis	15
20	Electron count for $\text{Os}_3(\text{CO})_{10}(\mu^2\text{-OEt})_2$	15
21	The cluster $\text{Os}_3(\text{CO})_{10}(\mu^2\text{-OEt})_2$ with the two reactive sites demonstrated	16
22	Reaction of $\text{Os}_3(\text{CO})_{10}(\mu^2\text{-OEt})_2$ with trimethyl phosphite	17
23	Reactions of $\text{Os}_3(\text{CO})_{10}(\mu^2\text{-OEt})_2$ with alcohols and strong acids HX	17
24	Synthetic routes to clusters of the form $\text{Os}_3(\text{CO})_{10}(\mu^2\text{-X})_2$ from $\text{Os}_3(\text{CO})_{12}$ passing through linear $\text{Os}_3(\text{CO})_{12}(\text{X})_2$ intermediate	18
25	Reaction of $\text{Os}_3(\text{CO})_{10}(\mu^2\text{-OEt})_2$ with carboxylic acid in heptane	19
26	Products of the reaction of $\text{M}_3(\text{CO})_{12}$ (M=Os, Ru) with carboxylic acids	20
27	Intermediates of the reaction of $\text{Os}_3(\text{CO})_{10}(\mu^2\text{-OEt})_2$ with carboxylic acid	21
28	Microwave reaction of $\text{Os}_3(\text{CO})_{12}$ in carboxylic acids to produce osmium hexacarbonyl dicarboxylate products	21
29	Monomeric and polymeric products of the reaction of $\text{Ru}_3(\text{CO})_{12}$ with amides	22
30	The major product of $\text{Os}_3(\text{CO})_{10}(\text{CH}_3\text{CN})_2$ with amides	23
31	The major product of $\text{Os}_3(\text{CO})_{10}(\text{CH}_3\text{CN})_2$ with carboxylic acids	23
32	Some potential bonding modes of the reaction of $\text{Os}_3(\text{CO})_{10}(\mu^2\text{-OEt})_2$ with an amide	24
M.1	Calculated vibrational band patterns of $\text{Mo}(\text{CO})_6$ and $\text{Mo}(\text{CO})_4(\text{PH}_3)_2$	29
M.2	Example of band patterns $\text{Os}_3(\text{CO})_{10}(\mu^2\text{-X})_2$ class of cluster and $\text{cis-Os}_2(\text{CO})_6(\mu^2\text{-X})_2$ class of cluster	30
M.3	TLC plate set	
	up	31
M.4	Sample TLC plate with R_f parameters shown.	32
M.5	The Harmonic Oscillator approximation as it relates to Morse potential	35
R.1	IR of crude reaction mixture of $\text{Os}_3(\text{CO})_{10}(\mu^2\text{-OEt})_2$ and acetamide in hexanes (68°C) showing no reaction	36
R.2	Reaction of $\text{Os}_3(\text{CO})_{10}(\mu^2\text{-OEt})_2$ and acetamide IR and TLC of crude reaction mixture after 6 hours in toluene against impure $\text{Os}_3(\text{CO})_{10}(\mu^2\text{-OEt})_2$	38
R.3	Overlaid spectra of crude reaction mixture of $\text{Os}_3(\text{CO})_{10}(\mu^2\text{-OEt})_2$ and	

acetamide in toluene (110°C) at 0 minutes and 6 hours	39
R.4 IR Comparison of product(s) of acetamide reaction to a cis-Os ₂ (CO) ₆ (μ ² -RCOO) ₂ both in hexanes	40
R.5 The possible isomer configurations of cis-[Os ₂ (CO) ₆ (μ ² -CH ₃ CONH) ₂] of mixture A	41
R.6 TLC of crude reaction mixture of Os ₃ (CO) ₁₀ (μ ² -OEt) ₂ and acetamide 360 minutes	42
R.7 IR and TLC of purified product A in hexanes	43
R.8 Crude IR of reaction mixture of benzamide and Os ₃ (CO) ₁₀ (μ ² -OEt) ₂ after 150 minutes in toluene	45
R.9 Isomers in mixture D of the form cis-[Os ₂ (CO) ₆ (μ ² -PhCONH) ₂]	46
R.10 Overlaid IR spectra of isomers of cis-[Os ₂ (CO) ₆ (μ ² -PhCONH) ₂] along with TLC III blue and IV red in hexanes	47
R.11 Gaussian 09 unoptimized structures and theoretical frequency calculations for both isomers, cis-(H,T) Os ₂ (CO) ₆ (HCONH) ₂ (left) and cis-(H,H) Os ₂ (CO) ₆ (HCONH) ₂ (right).	49
R.12 Frequency calculation of modified structure of cis-(H,T) Os ₂ (CO) ₆ (HCONH) ₂ showing similar pattern to experimental but poor wavenumber correlation	50
R.13 Optimized structures of (cis H,T) Os ₂ (CO) ₆ (HCONH) ₂ and (cis H,H) Os ₂ (CO) ₆ (HCONH) ₂	51
R.14 Theoretical vibrational frequencies for (cis H,T) Os ₂ (CO) ₆ (HCONH) ₂	51
R.15 Theoretical vibrational frequencies for (cis H,H) Os ₂ (CO) ₆ (HCONH) ₂	52
R.16 Optimized structure of cis- Os ₂ (CO) ₆ (μ ² -HCOO) ₂	53
R.17 Theoretical vibrational spectrum of cis- Os ₂ (CO) ₆ (HCOO) ₂	53
R.18 General regions of hypothesized band shifting as evident by the difference in experimental pattern between Os ₂ (CO) ₆ (RCOO) ₂ and [cis- Os ₂ (CO) ₆ (RCONH) ₂] clusters	55
R.19 Theoretical mid intensity band of Os ₂ (CO) ₆ (RCOO) ₂ shifting to become	

lower energy shoulder in [cis- Os ₂ (CO) ₆ (RCONH) ₂] clusters.	56
R.20 Experimental band shifting to become lower energy shoulder	57
R.21 LUMO of cis-(H,T) Os ₂ (CO) ₆ (HCONH) ₂ and to cis- Os ₂ (CO) ₆ (HCOO) ₂	59
R.22 ¹ H NMR of isomer III, cis (H,T) Os ₂ (CO) ₆ (μ ² -C ₆ H ₅ CONH) ₂ with relative integrations and chemical shifts (δ).	61
R.23 ¹ H NMR of IV cis (H,H) Os ₂ (CO) ₆ (μ ² -C ₆ H ₅ CONH) ₂ with relative integrations and chemical shifts (δ).	62
R.24 ¹ H-NMR of mixture D, cis (H,H) and cis (H,T) Os ₂ (CO) ₆ (μ ² -C ₆ H ₅ CONH) ₂ with relative integrations of NH peaks	63
R.25 ¹ H-NMR of mixture A highlighting peaks corresponding to isomer I in red and peaks corresponding to isomer II in blue	64
R.26 Graphs of D ₂ O shakes' ¹ H-NMR integration ratio data to a grease reference	66
R.27 Evidence of isomers III (H,T) and IV (H,H) interconversion in solution over four weeks	67
R.28 Isomer ratios of solutions A and B as they change across four weeks.	68
R.29 Potential mechanism for interconversion of isomers III and IV	69
33 Proposed products of reaction of Os ₃ (CO) ₁₀ (μ ² -OEt) ₂ with acetamide and benzamide in toluene	70-71
IR1- IR of crude reaction mixture of Os ₃ (CO) ₁₀ (μ ² -OEt) ₂ and acetamide in hexanes	75
IR2- IR of crude reaction mixture of Os ₃ (CO) ₁₀ (μ ² -OEt) ₂ and acetamide after 6 hours in toluene	75
IR3- IR spectrum of Os ₂ (CO) ₆ (μ ² -RCOO) ₂ in hexanes	76
IR 4- IR purified mixture of cis-(H,H) and (H,T) Os ₂ (CO) ₆ (μ ² - CH ₃ CONH) ₂ in hexanes	76
IR5- Crude IR of reaction mixture of benzamide and Os ₃ (CO) ₁₀ (μ ² -OEt) ₂ after 150 minutes in toluene	77
IR6- Computational unoptimized cis-(H,T) Os ₂ (CO) ₆ (HCONH) ₂ without solvation	77
IR7- Computational unoptimized cis-(H,H) Os ₂ (CO) ₆ (HCONH) ₂ without solvation	78
IR8- Frequency calculation of modified structure of cis-(H,T) Os ₂ (CO) ₆ (HCONH) ₂ without solvation	78
IR9- Theoretical vibrational frequencies for (cis H,T) Os ₂ (CO) ₆ (HCONH) ₂ solvation heptanes	79

IR10- Theoretical vibrational frequencies for (cis H,H) Os ₂ (CO) ₆ (HCONH) ₂ solvation heptanes	79
IR11- Theoretical vibrational spectrum of cis- Os ₂ (CO) ₆ (HCOO) ₂ solvation heptanes	80
NMR1- ¹ H NMR of isomer III, cis (H,T) Os ₂ (CO) ₆ (μ ² -C ₆ H ₅ CONH) ₂	80
NMR2- ¹ H NMR of IV cis (H,H) Os ₂ (CO) ₆ (μ ² -C ₆ H ₅ CONH) ₂	81
NMR3- ¹ H-NMR of mixture D, cis (H,H) and cis (H,T) Os ₂ (CO) ₆ (μ ² -C ₆ H ₅ CONH) ₂	81
NMR4- ¹ H-NMR of mixture A cis (H,H) and cis (H,T) Os ₂ (CO) ₆ (μ ² -CH ₃ CONH) ₂	82

Introduction-

This work will focus on novel reactions of amides with $\text{Os}_3(\text{CO})_{10}(\mu^2\text{-OEt})_2$ to further understand the chemistry of osmium carbonyl clusters of the form $\text{Os}_3(\text{CO})_{10}(\mu^2\text{-L})_2$ (figure 1).

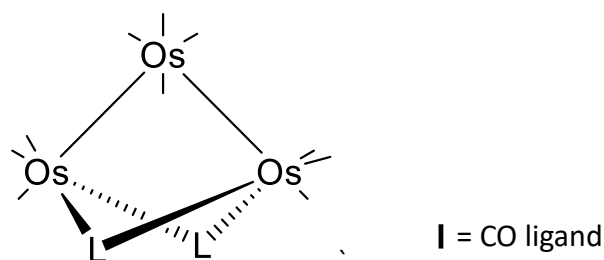


Figure 1- Structure of $\text{Os}_3(\text{CO})_{10}(\mu^2\text{-L})_2$. Lines emanating from metal atoms represent CO ligands for clarity and will be used frequently throughout this text.

Organometallic compounds are various, defined only to contain metal-carbon bonds, and organometallic clusters are a class of these compounds defined by two or more metal atoms covalently bonded.¹ With no limit on the number or the size and variety of these clusters there exist molecules with unique and unusual structural motifs. Clusters have unique chemistry due to the presence of covalent metal-metal bonds, lying somewhere in between the chemistry of mononuclear metal complexes and bulk metal (figure 2).

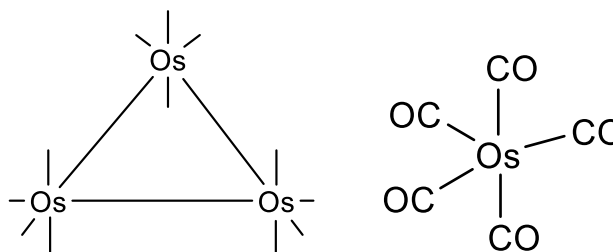


Figure 2- Structure of trinuclear cluster $\text{Os}_3(\text{CO})_{12}$ (left) and mononuclear metal complex $\text{Os}(\text{CO})_5$ (right).

An organometallic cluster's reactivity and structure is dependent mainly on the electron count and ligands coordinated, therefore electron counting is being introduced in this paper to provide support and understanding of the variety of structures and chemistries in organometallic clusters. The rule that governs the structure of small organometallic clusters is the 18 electron rule. It dictates that each metal atom will have all valence orbitals filled to maximize bonding and therefore stabilize the metal. With each transition metal having 9 valence orbitals, that means each metal atom must have 18 electrons. An example of electron counting is shown in figure 3 below.

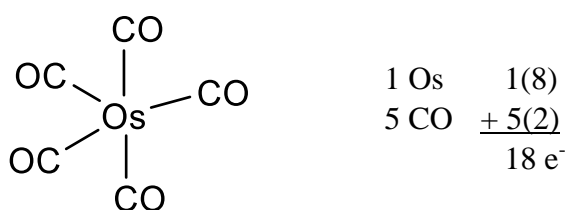


Figure 3- structure of osmium pentacarbonyl $\text{Os}(\text{CO})_5$ and its electron count demonstrating the 18 electron rule

The 18 electron rule can be applied to clusters to determine the number and type of metal-metal bonds, giving considerable insight to structure and reactivity. For

example, the cluster $\text{Os}_3(\text{CO})_{10}(\mu^2\text{-OEt})_2$ is shown in figure 4. The μ in this formula represents the number of atoms bridged by the ligand as shown by the superscript, in this case 2. It is general practice to not include the μ for terminal ligands, or ligands coordinated to one metal center ($\mu=1$). When the electron count is performed as with mononuclear molecules the count comes to $50 e^-$ which is 4 short of satisfying the $18e^-$ rule for three independent metal atoms, or $54 e^-$. This makes the cluster electron deficient and this suggests that 2 Os-Os bonds are formed to satisfy the 18 electron rule. Thus the 18 electron rule is shown to be useful in determining structural elements of a transition metal cluster.

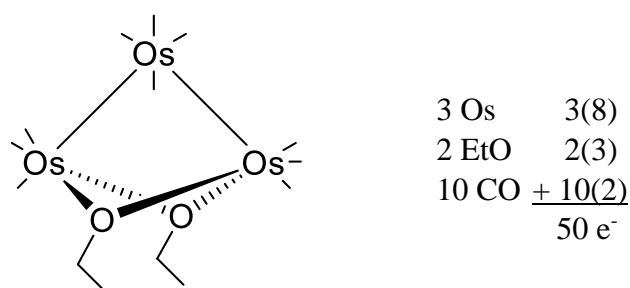


Figure 4- Structure and electron count for $\text{Os}_3(\text{CO})_{10}(\mu^2\text{-OEt})_2$ demonstrating the need for M-M bonding and the use of the $18e^-$ rule in clusters

It is also important to consider ligand properties when thinking about the structure and reactivity of a metal cluster. There are several types of metal-ligand interactions with the most significant being σ and π . These classifications have to do with the type of orbital overlap achieved in the interaction, with σ being head on overlap and π being side on overlap as seen in figure 5. Generally, π , due to the nature of the overlap, is considered a weaker interaction. There are two types of π interactions in transition metal complexes,

π -accepting and π -donating ligands. Transition metals are electron deficient so they can accept σ or π -donation into their vacant valance orbitals as seen in figure 5. Additionally, in the case of CO and other π -acceptor ligands, π -back donation of metal electron density into the ligand is possible. This type of interaction stabilizes the cluster and allows for neutral metal clusters such as the ones that will be presented in the paper. This can also be visualized in figure 5.

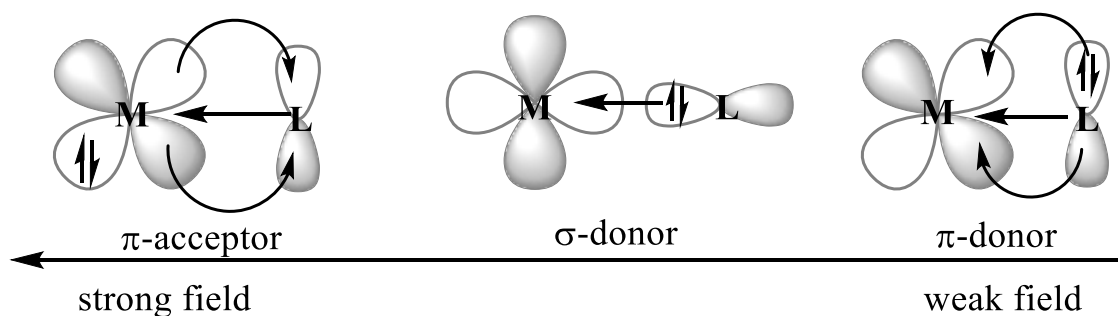


Figure 5- Simple metal-ligand interactions arranged in order of field strength

This work is concerned with clusters where the majority of ligands are carbonyl ligands, CO coordinated to a metal, which act as σ -donor and π -acceptor ligands. The σ -donation under a hybridization model comes from an sp non-bonding orbital lone pair on the carbon into a vacant d^2sp^3 orbital on the M. The π interaction between the metal and CO comes from back donation from a filled d orbital on the metal into the π^* antibonding orbital on the CO. This can be better visualized in figure 6, where the π interacting orbitals are shown.

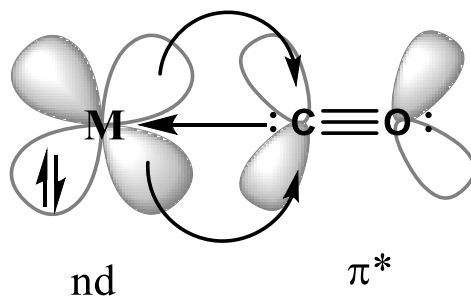


Figure 6- CO acting as a ligand with generic metal (M). σ -bonding shown with straight arrow and π -accepting property demonstrated with orbitals and curved arrows.

Molecular orbital analysis is possible and is sufficient for mononuclear and homoleptic systems, where there is only one type of ligand, and therefore the energy effects are easily quantified. However, using simple molecular orbital theory to understand binding and reactivity in clusters, especially ones that are heteroleptic, a system with a combination of different ligands, becomes too complex without computational aid. Therefore, our understanding of small clusters with small organic ligands remains not fully understood as even with computations there remain problems computing smaller clusters.² Therefore a systematic series of reactions of a cluster type with small organic molecules can provide different insights into the reaction of transition metal clusters with potential ligands.

Understanding the reactivity of transition metal clusters with small organic molecules can have countless potential applications in a variety of fields. For example, in fields like nanotechnology producing transition metal nanoparticles (MNPs) for use in catalysis or chemical sensors that are stable and defined has been a challenge.³ One route found by researchers at Institut für Anorganische and Analytische Chemie was to utilize metal

carbonyl clusters, $\text{Fe}_2(\text{CO})_9$, $\text{Ru}_3(\text{CO})_{12}$, and $\text{Os}_3(\text{CO})_{12}$ in the ionic liquid, n-butylmethylimidazolium tetrafluoroborate. An ionic liquid is a salt where the ions are poorly coordinated resulting in these solvents being liquid at certain temperatures. This facilitated the decomposition of the clusters under high heat in order to obtain nanoparticles of each respective metal which ranged in size from 1.5-2.5 nm (figure 7).³

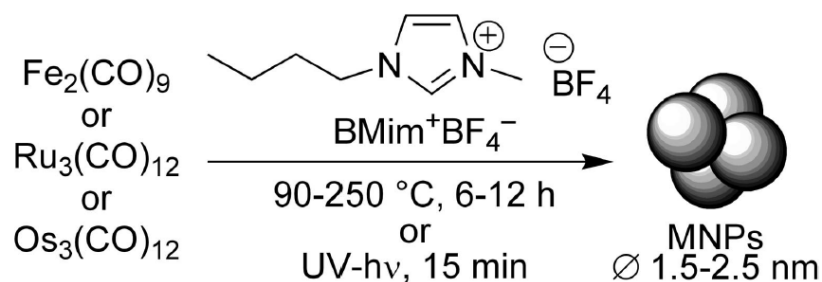


Figure 7- Synthetic scheme of Fe, Ru and Os nanoparticles formation in ionic liquids from their respective carbonyl cluster.³

Additional applications of transition metal clusters are in molecular switches, where clusters could potentially be linked via two or more organic ligands which have been designed with electron transfer in mind. In such a system with enough potential difference these linked clusters could act as molecular switches as seen in figure 8.

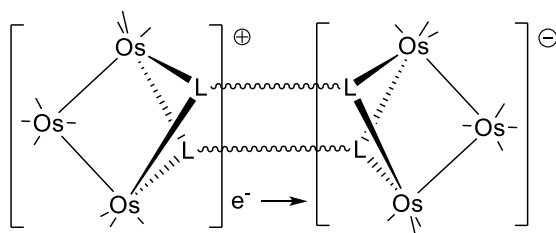


Figure 8- Triosmium carbonyl clusters acting a molecular switched via linking ligands L which facilitate electron transfer between clusters.

In the field of medicine transition metal clusters are being investigated as anti-cancer agents after the successful use of mononuclear cisplatin. More recently, osmium carbonyl clusters have been shown to exhibit cytotoxic properties by researchers from the Chemistry and Physiology Departments of The National University of Singapore⁴. This group found that in order to induce apoptosis, the cluster needs to have at least two coordination sites available⁴. In order to have coordination sites available the cluster must have non-carbonyl ligands which enhance reactivity by being more labile. This means that the clusters must be activated either through substitution of CO ligands or bridging ligands. For example $\text{Os}_3(\text{CO})_{10}(\text{CH}_3\text{CN})_2$ is labilized by the CH_3CN ligands, and $\text{Os}_3(\text{CO})_{10}(\mu^2\text{-H})(\mu^2\text{-OH})$ and $\text{Os}_3(\text{CO})_{10}(\mu^2\text{-H})_2$ are activated by bridging ligands and exchangeable carbonyl ligands (figure 9). All of these clusters have been shown to induce apoptosis, but non activated clusters like $\text{Os}_3(\text{CO})_{12}$ did not⁴. The diosmium hexacarbonyl diamidato or dicarboxylate clusters presented in this work have not been investigated for their abilities to induce apoptosis. However, the synthesis of novel osmium carbonyl clusters with functionalized ligands adds to the library of potential anti-cancer organometallic molecules.

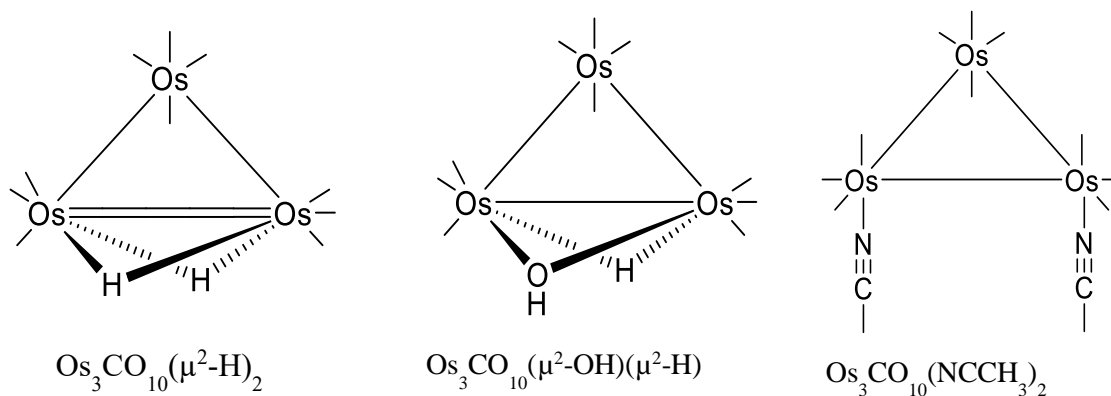


Figure 9- Os_3 clusters shown to induce apoptosis

Additional support for the investigation of osmium carbonyl clusters with bridging amidato ligands as anti-cancer agents comes from a cluster motif that is being explored which bears resemblance to the product structures presented in this paper. A research group from Ohio State University synthesized two novel dirhodium complexes, the head-to-tail (H,T) and head-to-head (H,H) isomers of cis- $[\text{Rh}_2(\text{HNOCCCH}_3)_2(\text{CH}_3\text{CN})_6]^{2+}$. These cluster were then activated with light and water, exchanging the two CH_3CN trans to the NH groups for water ligands. This suggests the NH coordination site has a labilizing effect relative to the O. These clusters were found to bind to DNA as seen in figure 10 which has potential applications in anticancer treatments.⁵

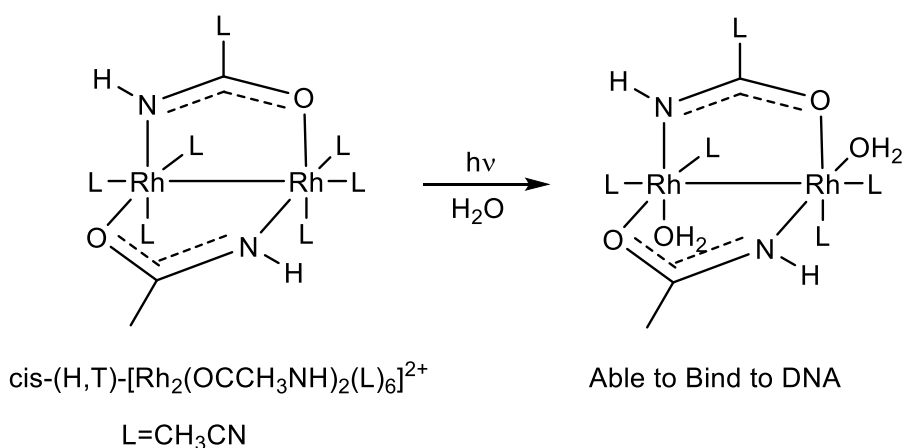


Figure 10- Novel cluster head-to-tail (H,T) of cis- $[\text{Rh}_2(\text{HNOCCCH}_3)_2(\text{CH}_3\text{CN})_6]^{2+}$ and subsequent photo-activated product which can bind to DNA⁵

The structural similarities to the products presented in this paper are apparent, though the clusters presented in this paper have 6 CO ligands instead of CH_3CN ligands. The significance of the notation head-to-head (H,H) and head-to-tail (H,T), which will be

used throughout this work, is the orientation of the amides on the isomers. Looking at the coordinated amides in figure 10, one can see that the nitrogen groups (the tails) and oxygens (heads) are located on the opposite side of the cluster. If one were to look at the coordination on one Rh atom they would find a head and a tail therefore the name head-to-tail, or H,T is used. The opposite is true for head-to-head (H,H) where both oxygens are coordinated to the same Rh.

The significance of studying the reactivity of amides as ligands with this class of cluster is partially due to the biological relevance of amides. Amides, have a general formula $RCONR'R''$ as seen in figure 11. For the purposes of this investigation, only primary amides are considered, meaning R' and R'' are hydrogens, though it is conceivable that a secondary amide could also achieve similar results, but tertiary amide would likely not react or only coordinate through the oxygen (figure 11).

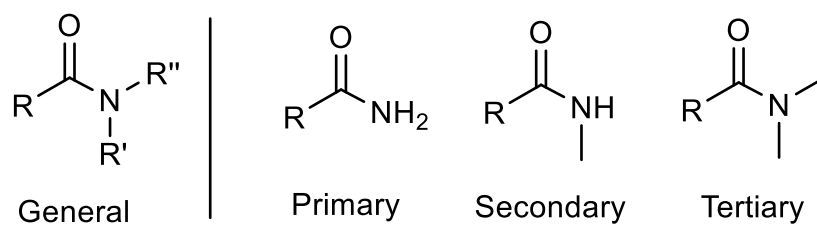


Figure 11- General structure of amides as well as examples of primary secondary and tertiary amides

The biological significance of amides can be seen in amino acids which come together to form peptide chains and ultimately proteins. When they come together an amide group is formed which becomes the rigid backbone of the peptide sequence as explained in figure 12.

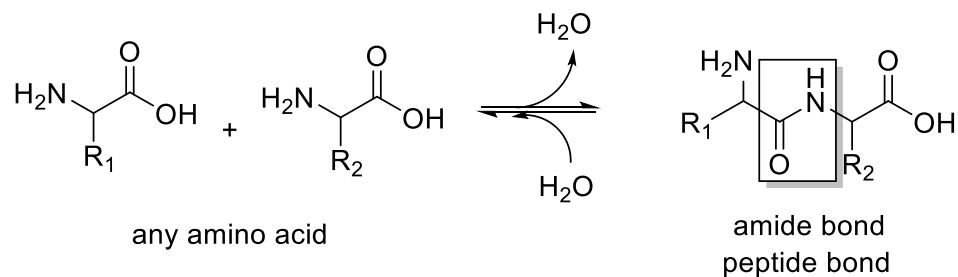


Figure 12- The formation of peptide bonds from amino acids with the amide bond boxed.

Although there are potential implications of biological amides reacting with this cluster motif, this work is mainly a fundamental exploration of amides reacting with this dibridged class of cluster. This is particularly interesting because amides have not been studied significantly with many osmium carbonyl cluster motifs.

General Chemistry of Osmium Carbonyl Clusters

The study of osmium carbonyl clusters has been used to gain a better understanding of transition metal clusters and their chemistry for decades⁶. The reason why osmium clusters are particularly useful for the study of transition metal clusters is because they form strong Os-Os bonds in comparison to other metal-clusters in the group. They are therefore significantly less reactive than many other transition metals which allows them to react with organic and inorganic substrates without any change of nuclearity⁶.

The starting material for the formation of many of these clusters is “osmium carbonyl”, Os₃(CO)₁₂ (figure 13) which has afforded over 100 new clusters, many of

which have the same tri-metal framework which allows for direct comparison and analysis of new ligands^{6,7}.

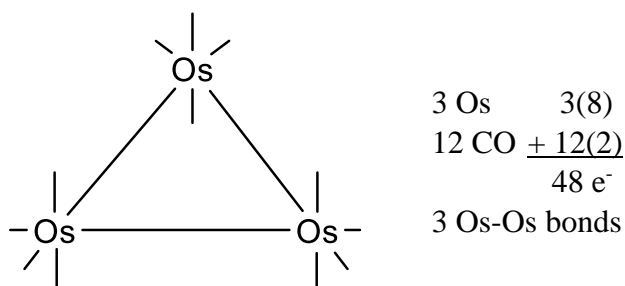


Figure 13: Structure of $\text{Os}_3(\text{CO})_{12}$ for simplicity sake CO ligands represented as |

However, osmium carbonyl is not very reactive on its own and the high temperatures and pressure needed for the reactions to occur lead to fragmentation and several different products. For example, the reaction of $\text{Os}_3(\text{CO})_{12}$ with isobutanol gives 6 unique products, many of which involve significant cluster buildup and fragmentation (figure 14).⁸

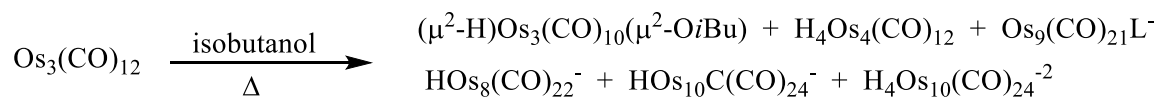


Figure 14- reaction scheme for $\text{Os}_3(\text{CO})_{12}$ with isobutanol, showing several products

Generally, derivatives of osmium carbonyl are synthesized with organic ligands to activate the cluster. By replacing 2 carbonyl ligands with a more labile organic ligand, such as MeCN, a more reactive cluster is formed. Triosmium decacarbonyl bisacetonitrile, $\text{Os}_3(\text{CO})_{10}(\text{CH}_3\text{CN})_2$ (figure 15), with 3 M-M bonds and two organic activating ligands is an example of the most common class of triosmium clusters.⁶ This

cluster type is better studied than the cluster type explored by this laboratory, $\text{Os}_3(\text{CO})_{10}(\mu^2\text{-L})_2$, making it the foundation that we compare the results of our reactions to.

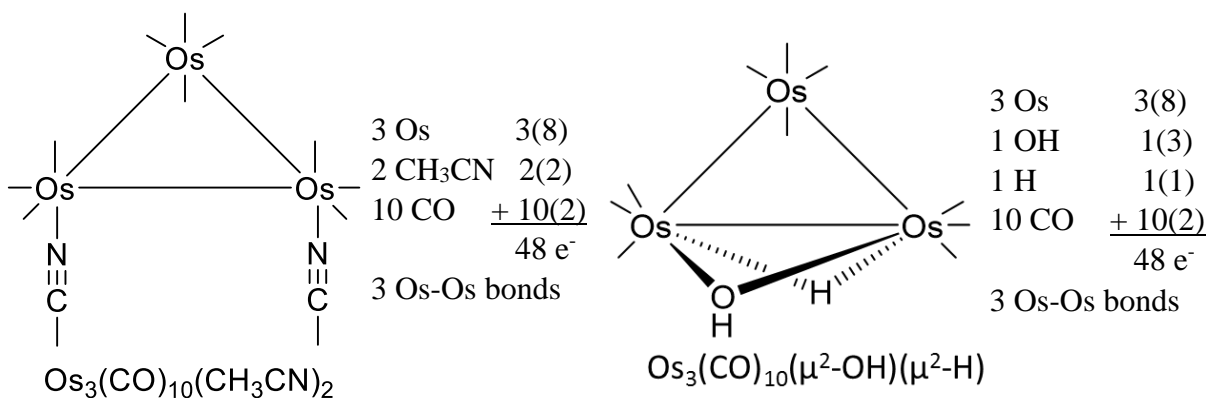


Figure 15- Clusters with 3 Os-Os bonds

This cluster can react to substitute the MeCN ligands for other ligands, such as PR_3 , maintaining the same cluster symmetry. When the incoming ligand has an available acidic proton, the cluster may react further via oxidative addition to give a bridged product of the type $\text{Os}_3(\text{CO})_{10}(\mu^2\text{-H})(\mu^2\text{-L})$, where L includes {OH, COOR, RCONH} (figure 16).^{7,9,10} Oxidative addition involves the reduction of the hydrogen of the alcohol (+1 oxidation state) as it becomes a bridging hydride (-1 oxidation state) while the triosmium core Os_3 is oxidized. Additionally, under extreme reaction conditions, such as high temperature and pressure, the cluster can build up or break down.^{8,11}

Another route to activate osmium carbonyl is through bridging ligands, such as $\text{Os}_3(\text{CO})_{10}(\mu^2\text{-H})(\mu^2\text{-OH})$ (figure 15), which typically only substitutes the bridging OH ligand which is more labile than the H ligand because bridging hydride ligands are fairly

unreactive and do not exchange^{12,6} thus forming similar clusters to that of $\text{Os}_3(\text{CO})_{10}(\text{CH}_3\text{CN})_2$ (Figure 16).

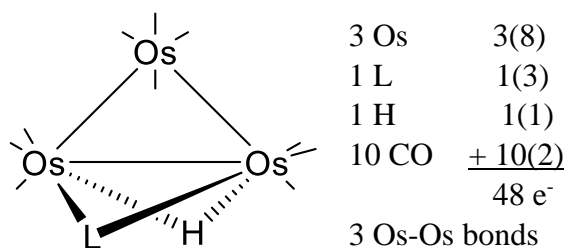


Figure 16- Typical product class of clusters $\text{Os}_3(\text{CO})_{10}(\text{CH}_3\text{CN})_2$ and $\text{Os}_3(\text{CO})_{10}(\mu^2\text{-H})(\mu^2\text{-OH})$ where L includes {OH, COOR, RCONH}

A unique class of osmium carbonyl cluster are ones with 4 Os-Os bonds.⁶ The most well studied cluster of this type is $\text{Os}_3(\text{CO})_{10}(\mu^2\text{-H})_2$ (figure 17) which undergoes two main types of reaction, simple insertion and more complex insertion. This cluster is formed in high yield by hydrogenation of $\text{Os}_3(\text{CO})_{12}$ to give a deep purple cluster (figure 17).¹³

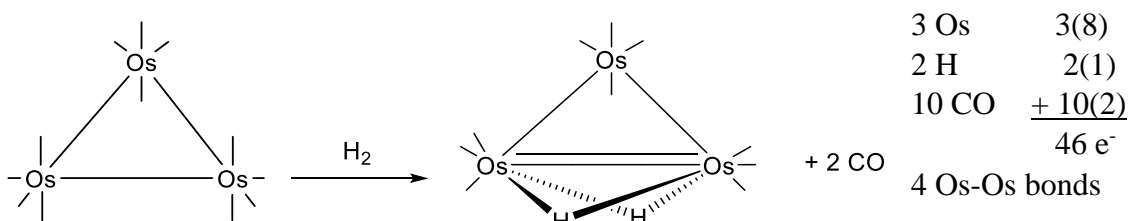


Figure 17- Reaction scheme of hydrogenation of $\text{Os}_3(\text{CO})_{12}$ to give $\text{Os}_3(\text{CO})_{10}(\mu^2\text{-H})_2$ whose electron count is shown right.¹³

Due to the enhanced electron density from the additional M-M bond, nucleophilic addition of organic ligands can occur forming clusters of the type $\text{Os}_3(\text{CO})_{10}(\mu^2\text{-H})\text{LH}$ (Figure 18).^{6,14}

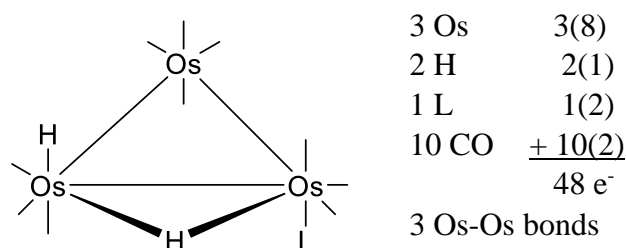


Figure 18- Typical product structure and electron count of reactions of $\text{Os}_3(\text{CO})_{10}(\mu^2\text{-H})_2$ with nucleophiles such as L=acetylene

Alternatively, clusters similar to the products of clusters with 3 Os-Os bonds discussed earlier can also be observed with complex insertion reactions as one L is protonated and leaves as LH as a second L binds leaving one remaining bridging H and the organic ligand (as Figure 16).^{6,15} It is important to note that the second bridging hydrogen is not reactive and will not substitute so this is not a route to the cluster type of interest in this paper, $\text{Os}_3(\text{CO})_{10}(\mu^2\text{-L})_2$.

The class of osmium carbonyl clusters that is used as the parent molecule for the majority of reactions in this lab is the activated cluster is $\text{Os}_3(\text{CO})_{10}(\mu^2\text{-OEt})_2$ which was discovered as a byproduct in the synthesis of $\text{Os}_3(\text{CO})_{12}$ from Os_4O_4 in ethanol in 1984 (figure 19).⁷ Our group has found this cluster to be activated towards substitutions by several classes of organic compounds. This cluster is unique in its structure compared to other activated clusters used as starting materials because it only has two metal-metal

bonds in the triosmium frame (compared to the 3 or 4 that have been well studied). The two bridging ethoxy ligands occupying the third edge of the triangular backbone and the ten carbonyl ligands, three on each osmium adjacent to the bridging face and four on the remaining osmium maintains the $18e^-$ rule for each osmium atom (figure 20).

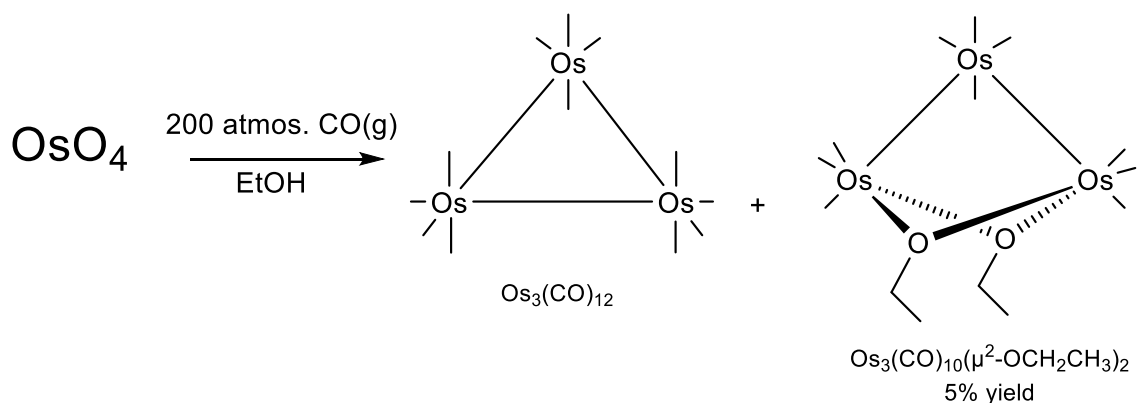


Figure 19- $\text{Os}_3(\text{CO})_{10}(\mu^2\text{-OEt})_2$ as a minor product of $\text{Os}_3(\text{CO})_{12}$ synthesis

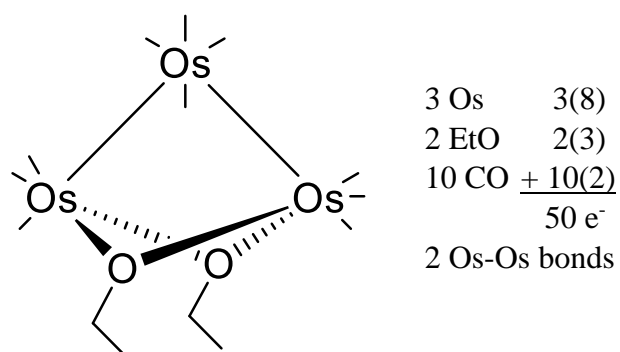


Figure 20-Electron count for $\text{Os}_3(\text{CO})_{10}(\mu^2\text{-OEt})_2$

The synthesis of clusters with two functionalized bridging ligands has been a challenge and an interest in osmium carbonyl cluster research because its two functional bridging ligands cause it to yield different products than the other activated clusters discussed above. To date it has shown two reactive sites with organic molecules as demonstrated in

figure 21. The carbonyl ligands trans to the Os-Os bonds can be displaced, or the bridging ethoxide ligands can be substituted. Additionally, like $\text{Os}_3(\text{CO})_{12}$, this cluster has been shown to break down to a diosmium cluster, as well as build up to a tetraosmium cluster and higher during reactions with carboxylic acids and diols respectively.^{16,17,18,19} In contrast to $\text{Os}_3(\text{CO})_{12}$, this system produces single products which makes it a more desirable precursor in synthetic design of novel clusters.

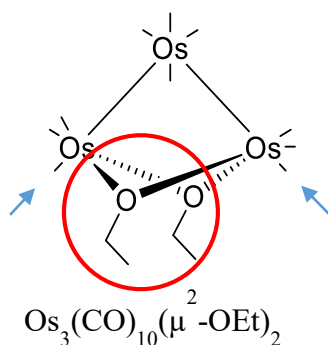


Figure 21- the cluster $\text{Os}_3(\text{CO})_{10}(\mu^2\text{-OEt})_2$ with the two reactive sites demonstrated. The displaced carbonyls are indicated by the arrows (blue) and the bridging ethoxide ligands are circled (red)

One of the reaction pathways observed is the disubstitution of the CO ligands trans to the Os-Os bonds for a trimethyl phosphite ligand²⁰ (figure 22). This was observed at relatively low temperatures not only with $\text{Os}_3(\text{CO})_{10}(\mu_2\text{-OEt})_2$ but also with $\text{Os}_3(\text{CO})_{10}(\mu_2\text{-X})_2$ ($\text{X} = \text{Cl}, \text{Br}, \text{I}, \text{OH}, \text{OMe}, \text{OiPr}$) to form the product $\text{Os}_3(\text{CO})_8(\text{P}(\text{OCH}_3)_3)_2(\mu_2\text{-X})_2$ ²⁰. In contrast, $\text{Os}(\text{CO})_{12}$ requires higher temperature and leads to several products.⁶

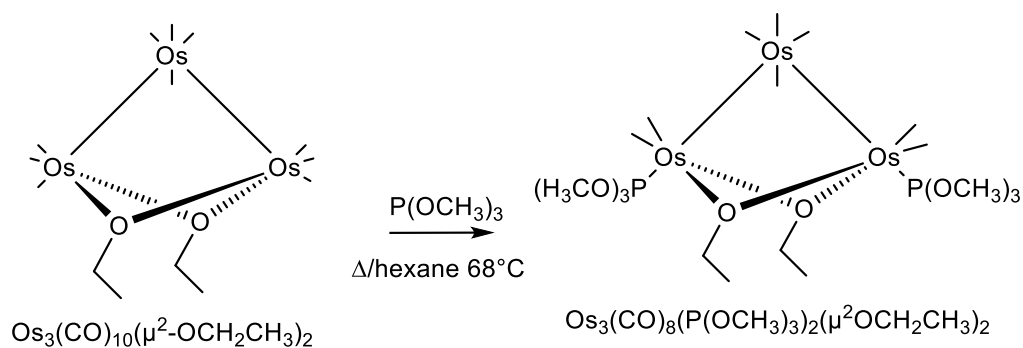


Figure 22 – Reaction of $\text{Os}_3(\text{CO})_{10}(\mu^2\text{-OEt})_2$ with trimethyl phosphite showing disubstitution of CO ligands for $\text{P}(\text{OCH}_3)_3$ ligands

Additionally, direct substitution of both bridging ethoxide groups was observed in reactions of $\text{Os}_3(\text{CO})_{10}(\mu^2\text{-OEt})_2$ with various alcohols and strong acids (HX , $\text{X}=\text{Cl}$, Br , I) to form $\text{Os}_3(\text{CO})_{10}(\mu^2\text{-X})_2$ ($\text{X}=\text{I}$, Br , Cl , OR).^{20,21} These reversible reactions go at fairly mild conditions and products are formed in a relatively short amount of time (figure 23). In order to isolate $\text{Os}_3(\text{CO})_{10}(\mu^2\text{-OEt})_2$ in the reverse reaction, a solid state base is used to quench the HX byproduct and eliminate the possibility of reverting back to $\text{Os}_3(\text{CO})_{10}(\mu^2\text{-X})_2$.

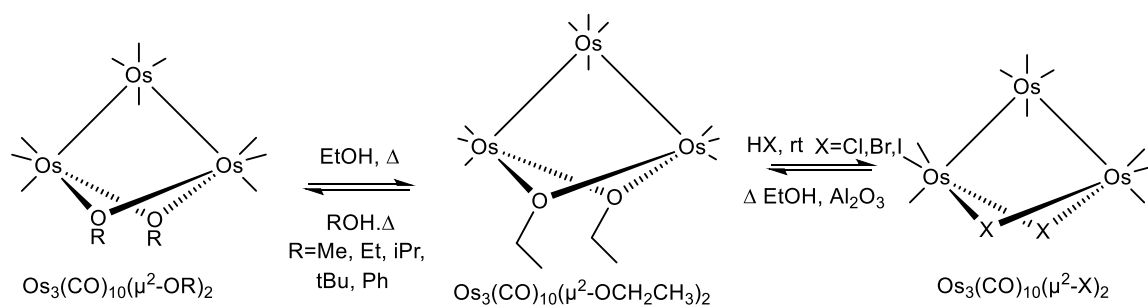


Figure 23- Reactions of $\text{Os}_3(\text{CO})_{10}(\mu^2\text{-OEt})_2$ with alcohols and strong acids HX ($\text{X}=\text{Cl}$, Br , I), $\text{R}=\text{OMe}$, OEt , OiPr , OtBu , OPh ²⁰

This is markedly different than the reaction of $\text{Os}_3(\text{CO})_{12}$ with halogens I_2 , Br_2 , and Cl_2 to produce $\text{Os}_3(\text{CO})_{12}(\text{X})_2$ which takes considerably longer to produce. First, the cluster undergoes oxidative addition of X_2 , to produce a linear cluster of the form $\text{Os}_3(\text{CO})_{12}(\text{X})_2$ and then, upon extended heating, the cluster closes to produce a cluster of the form $\text{Os}_3(\text{CO})_{10}(\mu^2\text{-L})_2$ (figure 24). During the closing of this cluster the X ligand goes from a $1e^-$ donor to a $3e^-$ donor to satisfy the $18e^-$ rule This reaction was first done with halogens I_2 , Br_2 , and Cl_2 , by Johnson and Lewis in 1970, and then in 2010 Shah of this laboratory was able to exchange the halide products of the form $\text{Os}_3(\text{CO})_{12}(\text{X})_2$ for alcohols, producing an alternative route to the starting material of the majority of the reactions of this laboratory.^{22,23} The optimization of the synthesis of this cluster was achieved by several members of this group.^{18, 23-26}

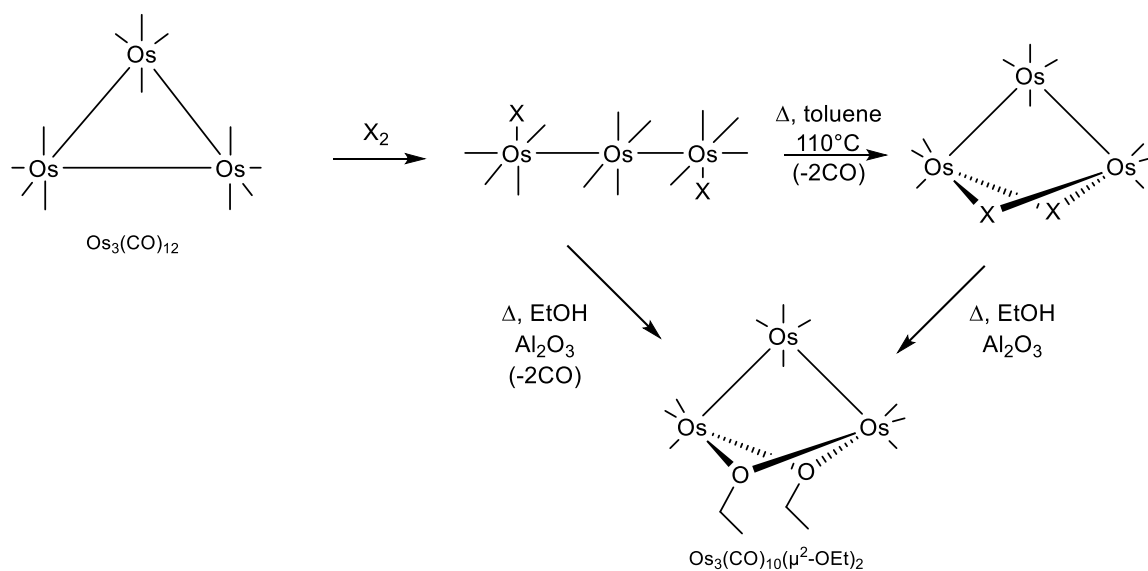


Figure 24- Synthetic routes to clusters of the form $\text{Os}_3(\text{CO})_{10}(\mu^2\text{-X})_2$ from $\text{Os}_3(\text{CO})_{12}$ passing through linear $\text{Os}_3(\text{CO})_{12}(\text{X})_2$ intermediate

Osmium Carbonyl Clusters with Carboxylate Ligands

For the purposes of this work, the most significant reactions of $\text{Os}_3(\text{CO})_{10}(\mu^2\text{-OEt})_2$ by our laboratory are the reactions with carboxylic acids. Carboxylic acids are different than other organic ligands studied by our group because they have the potential to act as either a mono or bidentate ligand like amides. Monodentate ligands are ones which coordinate to the cluster through only one atom. Bidentate ligands coordinate through two atoms of the ligand.

The electronic and coordination similarities between carboxylic acids and amides are the reason they were viewed as analogous ligands for the purposes of this investigation. However, it is important to note that the non-symmetrical aspects of amide chemistry allow them to both yield isomers and have potential to be hemilabile. Hemilabile ligands are simply bidentate ligands whose two sites of coordination are not equal, meaning one group could be more easily displaced than the other.

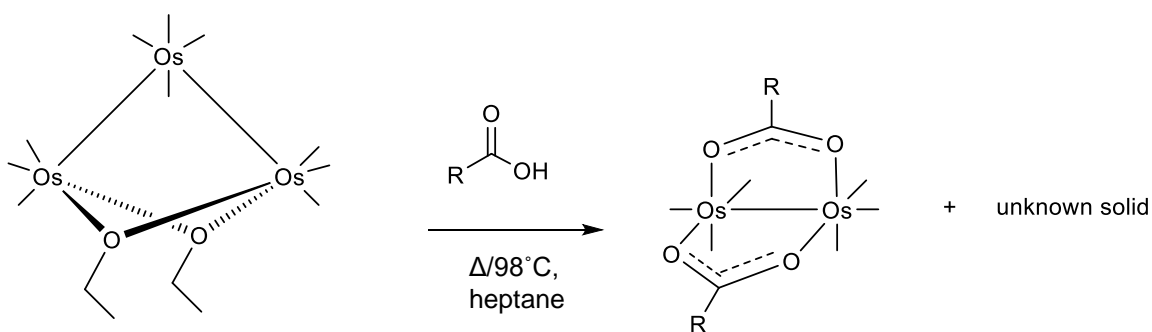


Figure 25– Reaction of $\text{Os}_3(\text{CO})_{10}(\mu^2\text{-OEt})_2$ with carboxylic acid in heptane

The results of the reactions between $\text{Os}_3(\text{CO})_{10}(\mu^2\text{-OEt})_2$ showed that the cluster breaks down to a dinuclear osmium compound with the carboxylate acting as a bidentate ligand which

was previously characterized by Billet and Cotton (Figure 25).²⁷ This reaction was originally reported by Crooks et.al 1969 and demonstrated that both osmium and ruthenium clusters $M_3(CO)_12$ broke down to this type of cluster, and interestingly enough the polymerization of the clusters through displacement of the CO ligands trans to the M-M was observed only for ruthenium clusters. This is seen in figure 26.²⁹

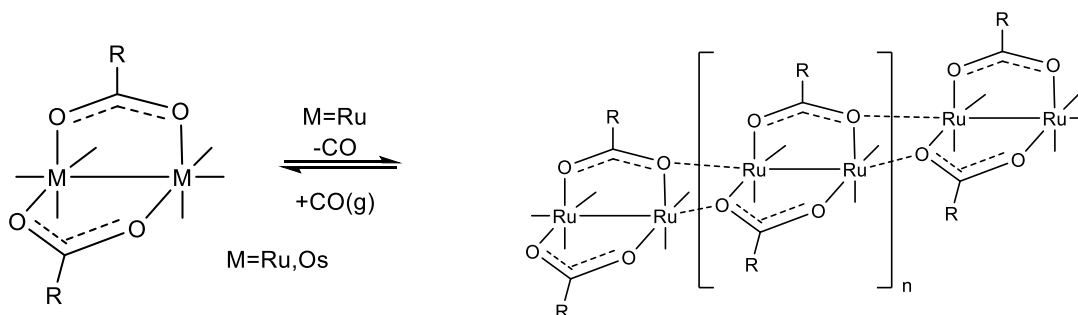


Figure 26- Products of the reaction of $M_3(CO)_12$ ($M=Os, Ru$) with carboxylic acids

The researchers Schmitt and Dunham of this lab who worked on reactions of $Os_3(CO)_{10}(\mu^2-OEt)_2$ with carboxylic acids also claim that $Os_3(CO)_12$ is produced as a byproduct of the reactions, however evidence presented in this work may refute that claim^{16,17}. By performing the reaction at lower temperatures, these researchers also showed that this happens via an intermediate where the cluster undergoes mono-substitution for a carboxy ligand. In this state, there is an equilibrium where the carboxylate is coordinated in either the mono or bidentate form. Additionally, the mono-substituted intermediate species maintains the Os_3 framework (Figure 27)^{16,17}. A second substitution then more readily yields the diosmium compound of the form $[cis-Os_2(CO)_6(RCOO)_2]$.

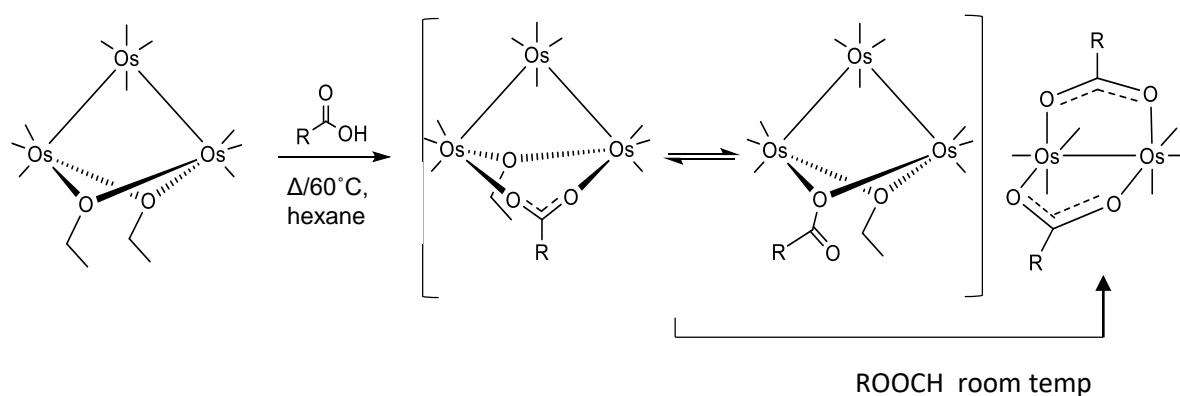


Figure 27– Intermediates of the reaction of $\text{Os}_3(\text{CO})_{10}(\mu^2\text{-OEt})_2$ with carboxylic acid

This result is consistent with the results of Greg Powell from Abilene Christian University in Texas, and his research team who performed a microwave reaction (180°C) with $\text{Os}_3(\text{CO})_{12}$ and carboxylic acids which directly yielded the same dioxmium bidentate compound without observing an intermediate (Figure 28).²⁹

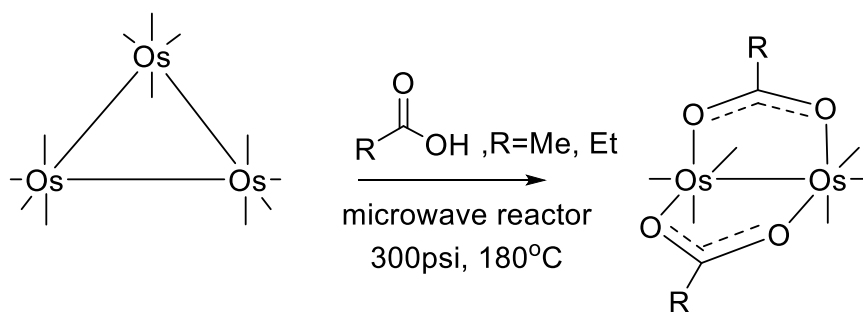


Figure 28- Microwave reaction of $\text{Os}_3(\text{CO})_{12}$ in carboxylic acids to produce dioxmium hexacarbonyl dicarboxylate products

Reactions of Osmium Carbonyl Clusters with Amides

In this work amides will be investigated with dibridged osmium carbonyl systems, something that to our knowledge has been unexplored. Similar reactivity was shown with amides as with carboxylic acids for the reaction with $\text{Ru}_3(\text{CO})_{12}$ (carboxylic acids discussed earlier and shown in figure 26). Just as with carboxylic acids, the amides cause the cluster to break down and labile ligands trans to the Ru-Ru bond are displaced for polymerization of the cluster as seen in figure 29.³⁰

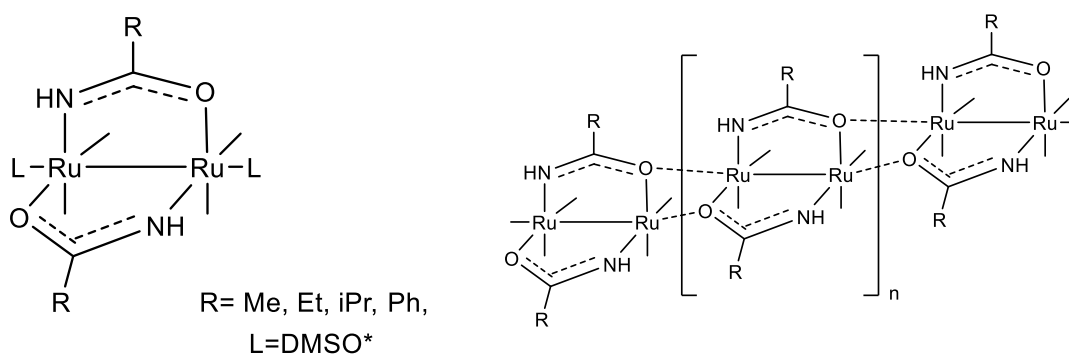


Figure 29- Monomeric and polymeric products of the reaction of $\text{Ru}_3(\text{CO})_{12}$ with amides

Carboxylic acids and amides were also shown to be analogous in the reaction of $\text{Os}_3(\text{CO})_{10}(\text{CH}_3\text{CN})_2$, a non-bridged functionalized cluster, with two small organic ligands. Amides were explored by Odiaka and his lab from the University of Ibadan. These reactions have been shown to yield major products of the form $[\text{Os}_3(\text{CO})_{10}(\mu^2\text{-H})(\text{NHCOR})]$ (figure 30).⁹ These results are consistent with products of $\text{Os}_3(\text{CO})_{10}(\text{CH}_3\text{CN})_2$ and carboxylic acids found by a lab group from Massey University

(figure 31).¹⁰ Both produce a cluster which has a single bridging bidentate ligand and a bridging hydride ligand coordinated to the triosmium frame supporting the claim that these ligands can be viewed as analogous.

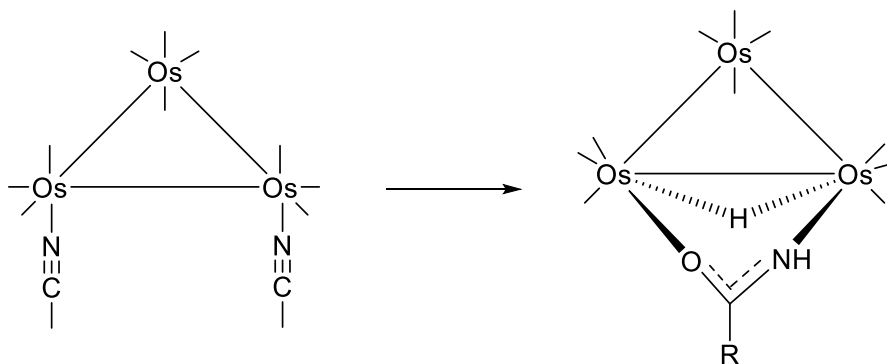


Figure 30- The major product of $\text{Os}_3(\text{CO})_{10}(\text{CH}_3\text{CN})_2$ with amides

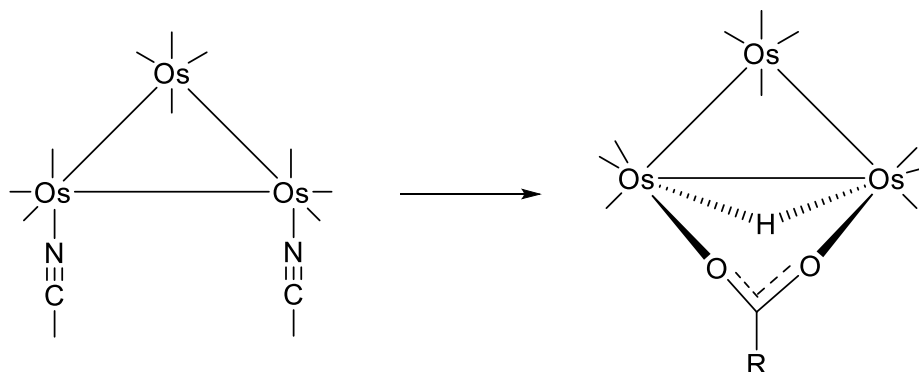


Figure 31- The major product of $\text{Os}_3(\text{CO})_{10}(\text{CH}_3\text{CN})_2$ with carboxylic acids

Preliminary investigations of $\text{Os}_3(\text{CO})_{10}(\mu^2\text{-OEt})_2$ with amides by our group in 2015, resulted in products were not fully characterized and due to the unconventional methods the results had yet to be reproduced³¹. Therefore, in this work reactions of triosmium decacarbonyl bisethoxide will be reacted with amides, specifically acetamide (CH_3CONH_2) and benzamide ($\text{C}_6\text{H}_5\text{CONH}_2$) to determine coordination modes of the

amide on the obtained product(s). The first goal will be to find a more conventional method to produce products, then to identify and characterize products. Based on knowledge of reactions of carboxylic acids with triosmium decacarbonyl bisethoxide it was hypothesized that amides would act as bidentate ligands and break down the triosmium framework into a diosmium cluster rather than coordinate as a monodentate ligand. Although a similar mechanism to carboxylic acids will be looked for to see if the first substitution will have coordination through the N or O alone, or a mixture of the two, while maintaining the triosmium frame. Working with amide also introduces the possibility of isomers which can be seen in the potential bonding modes shown in figure 32.

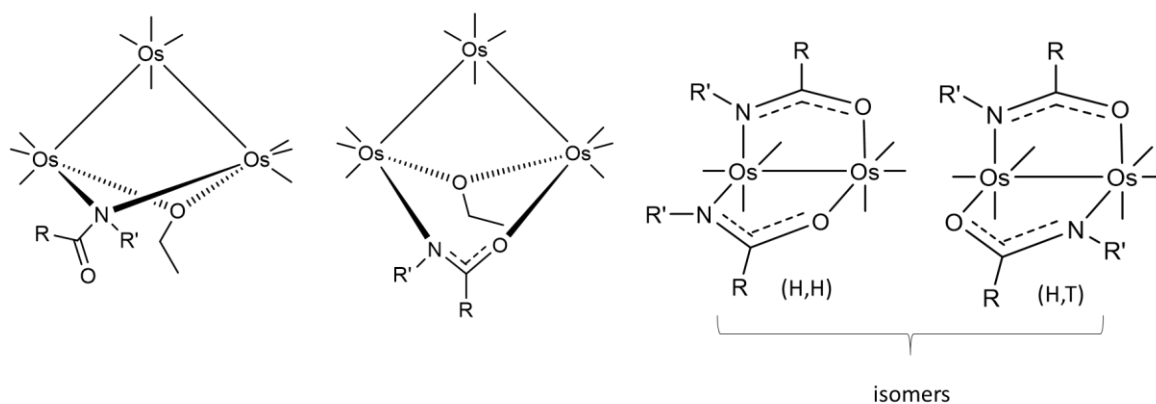


Figure 32- Some potential bonding modes of the reaction of $\text{Os}_3(\text{CO})_{10}(\mu^2\text{-OEt})_2$ with an amide

Experimental

Os₃(CO)₁₀ (μ²-OEt)₂ and acetamide in hexanes (68 °C)

Os₃(CO)₁₀ (μ²-OEt)₂, 24mg (0.0255 mmoles) and acetamide, 25 mg (0.423 mmoles, 10-fold excess) were added to 10 mL of hexanes and refluxed under nitrogen for two hours. The reaction was monitored by IR for the carbonyls in the range of (1600-2200) cm⁻¹ and for the amide in a full scan (400-4000) cm⁻¹. It was also monitored by TLC in a 20% dichloromethane/ 80% hexane solvent system. After two hours no changes were observed by TLC or in the IR. The acetamide peak in the IR (~1700 cm⁻¹) was not present indicating no acetamide in the reaction mixture.

Synthesis of new clusters of the type [Os₂(CO)₆ (RCONH)₂] using Os₃(CO)₁₀ (μ²-OEt)₂ and acetamide in toluene (110 °C)

Os₃(CO)₁₀ (μ²-OEt)₂, 24mg (0.0255 mmoles) and acetamide, 25 mg (0.423 mmoles, 10-fold excess) from the above failed reaction were removed from hexanes and added to 15mL of toluene and refluxed under nitrogen for six hours. The reaction was monitored by IR for the carbonyls in the range of (1600-2200) cm⁻¹ and for the amide in a full scan (400-4000) cm⁻¹. It was also monitored by TLC in a 20% dichloromethane/ 80% hexane solvent system and a 40% ethyl acetate/ 60% hexanes solvent system. Throughout the reflux, a color change in the reaction mixture was observed from a light yellow to a darker yellow. After cooling a brown slightly soluble precipitate was observed and the reaction mixture was decanted off. The IR (ν_{CO}, toluene) of reaction mixture 2086.7 cm⁻¹, 2066.7 cm⁻¹, 2049.0 cm⁻¹, 2025.4 cm⁻¹, 1992.3 cm⁻¹, 1972.78 cm⁻¹, 1709.0 cm⁻¹, and

1688.4 cm^{-1} . TLC in 40% ethyl acetate/ 60% hexanes shows a single moving compound (RF= 0.26) and a baseline.

The solution was run through a column 40% ethyl acetate/ 60% hexanes and a small amount of yellow $\text{Os}_3(\text{CO})_{10}(\mu^2\text{-OEt})_2$ was isolated as well as clear colorless products. Purified IR (ν_{CO} , dichloromethane) 2087.64 cm^{-1} , 2049.82 cm^{-1} , 1991.42 cm^{-1} , 1972.01 cm^{-1} . TLC in 40% ethyl acetate/ 60% hexanes shows a single moving compound (RF= 0.26). NMR (CDCl_3) δ - 6.319(1), 5.909(1.11), 2.020(3.57), 2.006(3.28). Several D_2O shakes were performed to determine exchangeable protons, slow exchange rates observed for both products, with the rate of C-H exchange being greater than N-H exchange in both.

Synthesis of clusters of the type $[\text{Os}_2(\text{CO})_6(\text{RCONH})_2]$ using $\text{Os}_3(\text{CO})_{10}(\mu^2\text{-OEt})_2$ and benzamide in toluene (110 $^\circ\text{C}$)

$\text{Os}_3(\text{CO})_{10}(\mu^2\text{-OEt})_2$, 23 mg (.024 mmoles) and benzamide, 59 mg (0.48 mmoles, 10-fold excess) were added to 10 mL of toluene and refluxed under nitrogen for 180 minutes. The reaction was monitored by IR for the carbonyls in the range of (1600-2200) cm^{-1} and for the amide in a full scan (400-4000) cm^{-1} . It was also monitored by TLC in a 20% ethyl acetate/ 80% hexanes solvent system. Throughout the reflux, a color change in the reaction mixture was observed from a light yellow to a darker yellow solution. After cooling a brown slightly soluble precipitate was observed and the reaction mixture was decanted off. The IR (ν_{CO} , toluene) of reaction mixture 2086.6 cm^{-1} , 2050.6 cm^{-1} , 1996.3 cm^{-1} , 1973.7 cm^{-1} , and 1689.4 cm^{-1} . TLC in 20% ethyl acetate/ 80% hexanes shows two

moving compounds (RF= 0.34 and 0.44) and a baseline. An NMR was taken of the crude reaction mixture, NMR (CDCl₃) δ- 7.1052(1.57), 6.6917(1.00), aromatics 7.3-7.8.

Preparatory TLC was done in 20% ethyl acetate/ 80% hexanes and the two clear colorless major products were collected, filtered and concentrated for fractional crystallization. Separated products demonstrated interconversion in solution through NMR spectra taken weekly for a month.

Gaussian09 DFT Calculations on optimized structure of the type [Os₂(CO)₆ (HCONH)₂]

Using Gaussian 09 software, a structure of [*cis*-(*H,H*) Os₂(CO)₆ (HCONH)₂] was optimized and frequencies were calculated using ground state DFT-B3LYP and basis set SDD in default solvation for heptane. IR (ν_{CO}, heptane^{theoretical}) 2037 cm⁻¹(w), 1995 cm⁻¹(s), 1944 cm⁻¹ (vs), 1941 cm⁻¹ (shoulder), 1919 cm⁻¹ (w), 1620 cm⁻¹ (w).

Using the same method above, a structure of [*cis*-(*H,T*) Os₂(CO)₆ (HCONH)₂] was optimized and frequencies were calculated. IR (ν_{CO}, heptane^{theoretical}) 2039 cm⁻¹(w), 1995 cm⁻¹(s), 1944 cm⁻¹ (vs), 1937 cm⁻¹ (shoulder), 1914 cm⁻¹ (w), 1620 cm⁻¹ (w).

Using the same method above, a structure of [*cis*- Os₂(CO)₆ (HCOO)₂] was optimized and frequencies were calculated. IR (ν_{CO}, heptane^{theoretical}) 2051 cm⁻¹(w), 2014 cm⁻¹(s), 1960 cm⁻¹ (vs), 1954 cm⁻¹ (m), 1941 cm⁻¹ (w), 1539 cm⁻¹ (w).

Methods

Infrared Spectroscopy

The more general use of infrared spectroscopy, or IR for short, involves excitation of a molecule with infrared light causing bond vibrations such as stretching and wagging which is characteristic of different functional groups on a molecule. While this technique can be useful for characterizing a molecule by identifying functional groups present or absent throughout a reaction, this work is primarily focused on IR in the carbonyl region ($\sim 1600\text{-}2200\text{ cm}^{-1}$) to characterize our products. This technique is used for metal carbonyl compounds because the symmetry of the carbonyl ligands about the cluster will dictate the band patterns observed in the IR. Uncoordinated CO ligands have a vibrational frequency of 2143 cm^{-1} , and when coordinated typically lower frequency vibrations are observed due to the back donation of the metal reducing the energy of the CO bond vibration. Additionally, when more than one carbonyl ligand is coordinated to a metal they can vibrate in different modes with each other creating several vibrational bands which depend on the symmetry. Looking at simple mono-nuclear compounds with more than one carbonyl ligand for example, one can see that a high symmetry compounds like (O_h) has only one band as all the carbonyl ligands are in the same environment, while lower symmetry $\text{cis-Mo(CO)}_4(\text{PH}_3)_2$ (C_{2v}) has several vibrational modes creating four distinct bands in its pattern (figure M. 1).

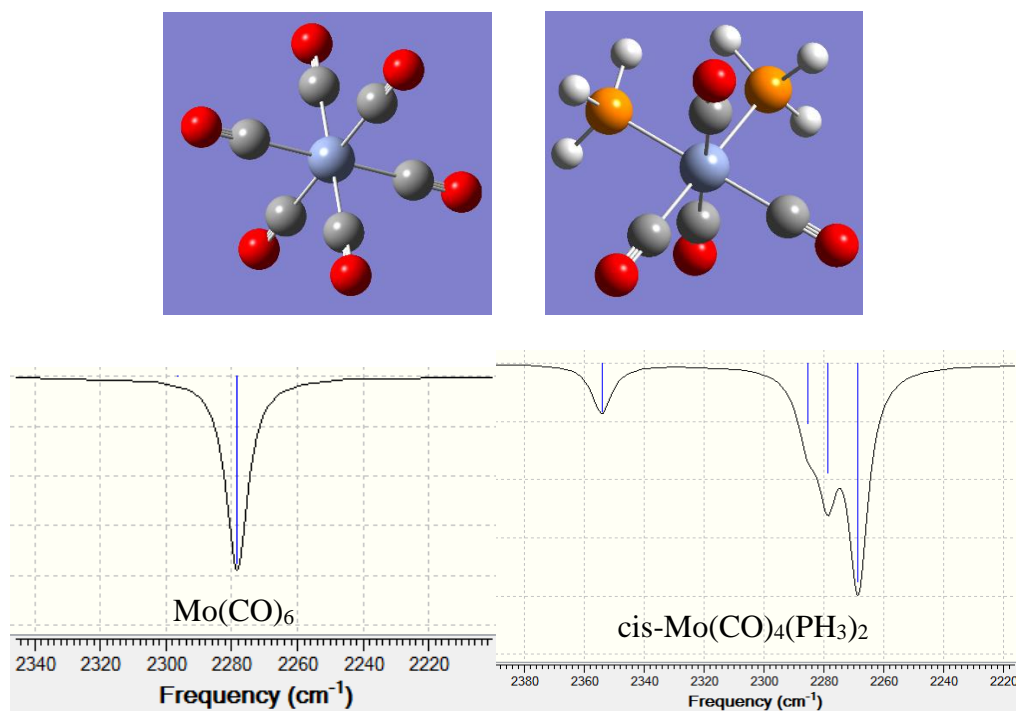


Figure M.1- Calculated vibrational band patterns of $\text{Mo}(\text{CO})_6$ (left) and $\text{Mo}(\text{CO})_4(\text{PH}_3)_2$ (right) demonstrating the effect of symmetry of the carbonyls on the band pattern

Extending this concept to higher nuclearity clusters it is possible to monitor a reaction and characterize products based on the symmetry of the carbonyl ligands. For example, an $\text{Os}_3(\text{CO})_{10}(\mu^2\text{-X})_2$ cluster will have a band pattern as shown in figure 11, and this pattern will remain consistent for each X, where X could be OEt, OMe, Cl, Br, I, although the wavenumbers will shift depending on the strength of the ligand X. In

comparison, a $\text{cis-Os}_2(\text{CO})_6(\mu^2\text{-X})_2$ cluster has a higher level of symmetry, so its observed band pattern is different than an $\text{Os}_3(\text{CO})_{10}(\mu^2\text{-X})_2$ as seen in figure M.2.

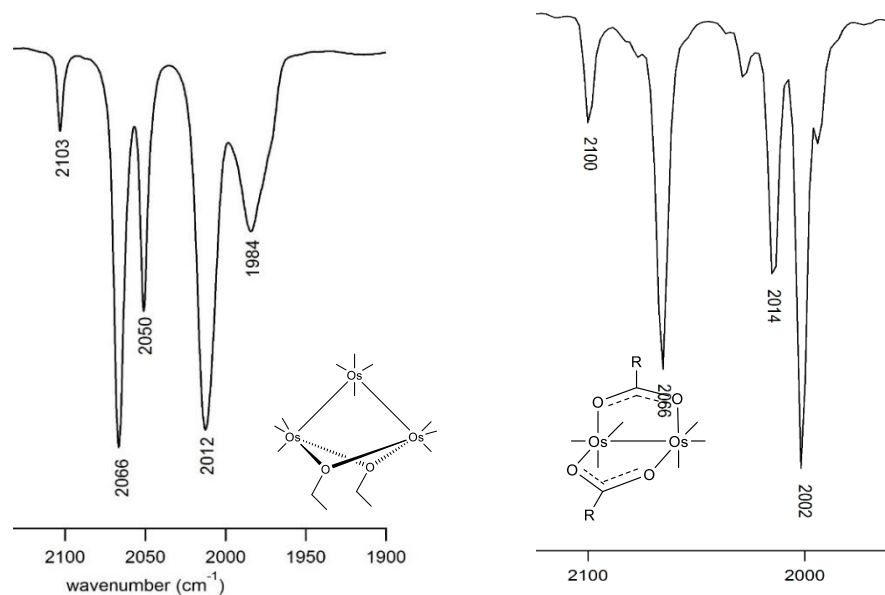


Figure M.2- Example of band patterns $\text{Os}_3(\text{CO})_{10}(\mu^2\text{-X})_2$ class of cluster (left) and $\text{cis-Os}_2(\text{CO})_6(\mu^2\text{-X})_2$ class of cluster (right) demonstrating the change in band pattern.

Thin Layer Chromatography

Chromatography is a technique used to separate compounds based on a physical property. In the case of this work all osmium carbonyl clusters are separated using thin layer or preparative thin layer chromatography which separates compound based on their polarity. This technique involves a thin layer of silica coated on a plate which acts as the polar stationary phase, the bottom of this is then placed into a mixture of relatively non-polar solvents making up the mobile phase. The compound is spotted near the bottom of the plate so that it will lie just above the level of the mobile phase. Then as the mobile phase travels up the vertical plate the compounds will travel with it, with more polar compounds interacting more with the polar stationary phase and therefore remaining

closer to the bottom of the plate than less polar compounds which travel more with the mobile phase. This setup can be seen in figure M.3.

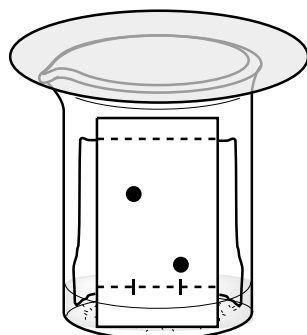


Figure M.3- TLC plate set up

The TLC plate can also give quantitative data with a property called the retardation factor, or R_f value, which describes the amount a compound moved up the plate compared to the amount the mobile phase moved (equation 1). This can be seen in figure M.4.

$$R_f = \frac{\text{Distance compound traveled}}{\text{Distance mobile phase traveled}} \quad (\text{Equation 1})$$

Compounds with higher R_f values are more non-polar than compounds with lower R_f values, and in the same mobile phase it can serve as a way to identify a compounds.

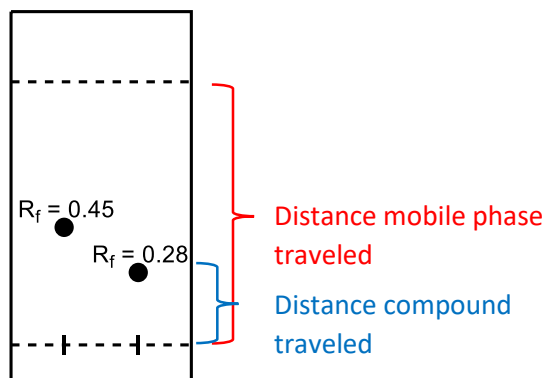


Figure M.4- Sample TLC plate with R_f parameters shown.

In general, this technique is used to monitor reactions to check for new product formation and consumption of the starting material. This technique can also be done on a larger scale, called preparative TLC, where the plate is considerably larger and made of glass, so at the end separated compounds can be scraped off and extracted from the silica. This was used in this investigation as a means of purification as well as separation of products.

Nuclear Magnetic Resonance Spectroscopy

Proton nuclear magnetic resonance spectroscopy, or NMR, is a powerful tool in the characterization of compounds. This technique relies on the spin state of a nucleus and location in the molecule relative to other atoms in a molecule. In the presence of a powerful magnetic field some atom's nuclear spins will align with this field and then a perpendicular pulse of magnetic energy is applied and the received change on the magnetic coil gives insight to the structure of the molecule. For ^1H -NMR, specifically the protons in a molecule are what is being observed, and in the resulting spectrum, each

cluster of peaks represents a chemically unique proton which relies on three things: chemical shift, integration, and multiplicity.

Chemical shift is dependent on the shielding or deshielding that a proton experiences in the presence or absence of electron withdrawing groups. For example, protons near to an electron withdrawing atom like oxygen, is considered deshielded and is shifted downfield, or to higher ppm. The opposite is true for electron donating groups which shield the proton and therefore it will have lower chemical shifts and be more upfield.

Integration depends on the number of protons that are associated with a peak in the spectrum. For example, a methyl group (CH_3) in n-propanol has three protons that are all in the same chemical environment so the peak associated with that group would have a relative integration of three, where the adjacent CH_2 would have a relative integration of 2. It is important to note that these integrations are relative to the other integrations in the spectrum, so symmetry in a molecule like butane would maintain a ratio of 3:2 even though there are 6 H that are chemically equivalent for the two terminal methyls and 4 for the two CH_2 groups inside the chain. Integration can also be used to determine the ratios of more than one substance in an impure sample because the integrations are proportional to the amount of substance in a sample.

Multiplicity has to do with the “neighbors” of each chemically unique proton. This means the number of protons on each adjacent atom (with few exceptions) which interact with the proton in question and split the peak. In the propanol example the

terminal methyl group has one adjacent carbon which has two protons bonded to it. These protons will split the single signal of the methyl protons into three. The splitting or multiplicity is $1 + \text{\#of neighboring Hs}$, making protons with no neighbors a single peak called a singlet, one neighbor a doublet, two neighbors a triplet, three neighbors a quartet and so on. There also exists the possibility of two different neighbors which causes more complicated splitting. For example, in propanol one of the CH_2 has an adjacent methyl and another CH_2 which would create a triplet of quartets.

Density Functional Theory Calculations

Electronic structure calculations can be used to gain insight into the energy of a system, optimized structures, and the theoretical vibrational spectrum which is what is most significant to this paper. In order to do this, density functional theory (DFT) calculations are used to approximate Schrödinger's equation and find the ground state electronic energy which Hohenberg and Kohn, developers of DFT, demonstrated to depend on the electron density of the system.³² A commonly used hybrid functional was also employed, Becke 3-parameter Lee- Yang-Parr (B3LYP). The basis set used for these calculations also plays a significant role in the accuracy of the results. The Stuttgart group effective core potential (SDD) basis set was employed because it takes into account the high computational demand that would be required for such a large atom like osmium and reduces the core electrons to an electrical potential rather than as approximate wave functions.³³ This reduces the number of basis set functions and therefore alleviates the computational demand for third row transition metal elements. This approximation is valid because the inner core electrons of third row transition metals

are well shielded and therefore the chemistry is occurring at the frontier orbitals. SDD treats the valence electrons with a double zeta basis set, looking into the chemistry of 20 or fewer electrons on transition metal atoms which have total electrons ranging from 58-80 electrons and approximates the core electrons as an electronic potential.³³ The vibrational frequencies are computed by taking the second derivatives of energy with respect to the nuclear coordinates of the structure with a subsequent transformation to mass-weighted coordinates. This is then converted to a readable theoretical IR spectrum.

This process treats the vibrations as harmonic rather than anharmonic, and this approximation can cause theoretical wave numbers to be higher in energy than experimental. As one can see in figure M.5, the harmonic approximation is a parabola where all energy transitions are equivalent, however due to nuclear repulsions the energy of a bond as a function of internuclear separation is anharmonic and is represented by the Morse potential. Here vibrational energy levels decrease with vibrational levels and there is a limit to the r before the bond dissociates.

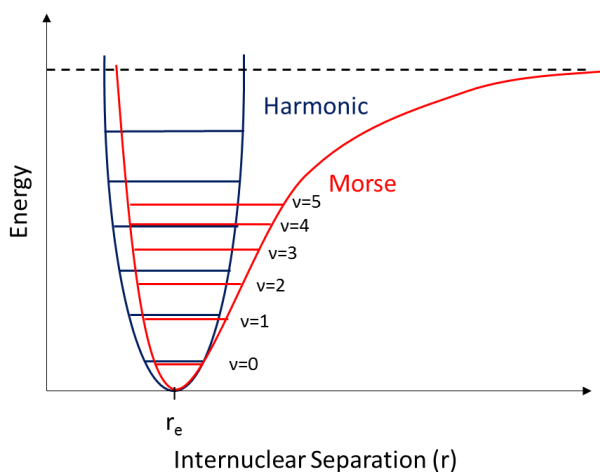


Figure M.5- The Harmonic Oscillator approximation as it relates to Morse potential

Results and Discussion

Reaction of $Os_3(CO)_{10}(\mu^2-OEt)_2$ and acetamide

The first amide to be explored is acetamide, where the R group of the amide is a simple methyl group. Due to its simplicity it is easy to handle and thus it should give foundational information about the coordination of amides in general to this class of organometallic clusters.

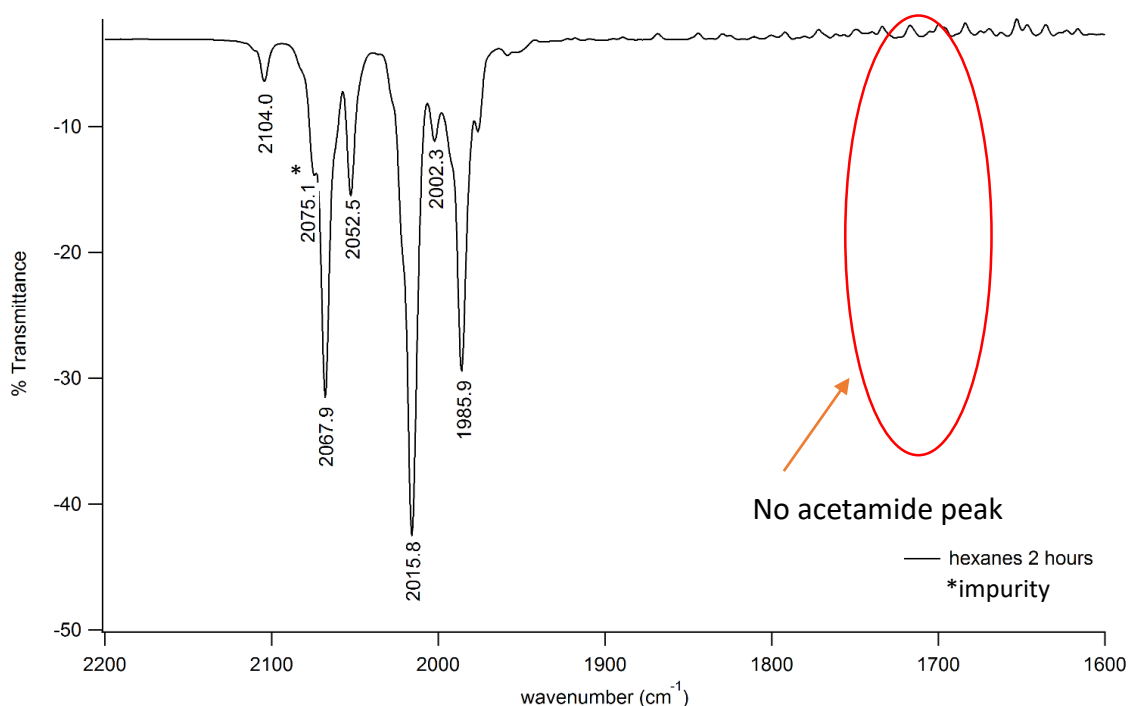


Figure R.1 IR of crude reaction mixture of $Os_3(CO)_{10}(\mu^2-OEt)_2$ and acetamide in hexanes (68°C) showing no reaction

This reaction had been attempted previously with unconventional methods to produce products. In order to improve the method of reacting $Os_3(CO)_{10}(\mu^2-OEt)_2$ with amides, the same reaction conditions previously investigated by Katterman were again

repeated to determine why no products formed until the solvent was unintentionally removed and reactants formed a tar like sludge containing new cluster IR patterns¹¹. Upon refluxing in hexanes with acetamide, no changes were observed in the IR or the TLC. The IR (figure R.1) of the reaction mixture after 2 hours shows no changes from spectra of the starting $\text{Os}_3(\text{CO})_{10}(\mu^2\text{-OEt})_2$, but more significantly it also showed no peak at $\sim 1700\text{ cm}^{-1}$ which is indicative of acetamide in solution. From this, we gathered that acetamide is not soluble enough in hexanes to allow for a reaction so toluene was selected as a more practical solvent in which acetamide is reasonably soluble.

On heating of $\text{Os}_3(\text{CO})_{10}(\mu^2\text{-OEt})_2$ with acetamide in toluene for six hours, complete reaction was observed as indicated by no more spectral changes in the IR and a TLC which showed disappearance of starting material and new product formation (figure R.2). Upon cooling a brown solid precipitated out of the yellow solution in toluene, the solid will be referred to as product B and the product(s) in solution will be referred to as solution A.

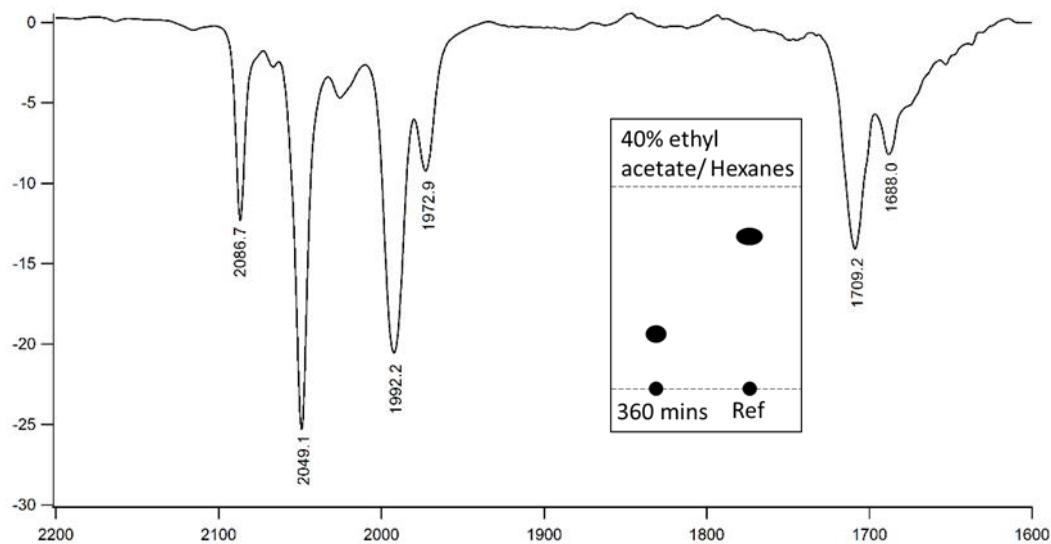


Figure R.2- Reaction of $\text{Os}_3(\text{CO})_{10}(\mu^2\text{-OEt})_2$ and acetamide IR and TLC of crude reaction mixture after 6 hours in toluene against impure $\text{Os}_3(\text{CO})_{10}(\mu^2\text{-OEt})_2$

Comparing the IR of the crude final reaction mixture to the crude starting mixture in toluene (figure R.3) a total transformation of band pattern is observed. Not only does this indicate reaction completion, but also that there has been a change in cluster symmetry. This is because clusters of similar frame have similar band patterns although they may have different wave numbers depending on other coordinated ligands.

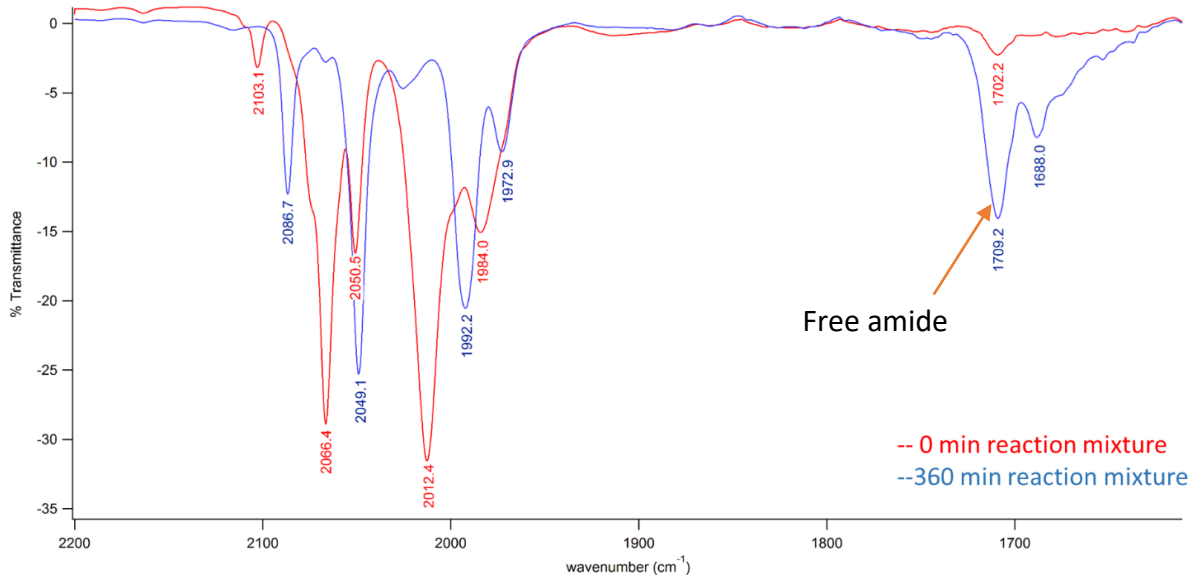


Figure R.3- Overlaid spectra of crude reaction mixture of $\text{Os}_3(\text{CO})_{10}(\mu^2\text{-OEt})_2$ and acetamide in toluene (110°C) at 0 minutes (red) and 6 hours (blue).

The simplicity of the new band pattern indicates a transformation of the cluster to a new cluster-type which is likely of the form $\text{cis-Os}_2(\text{CO})_6(\mu^2\text{-X})_2$.

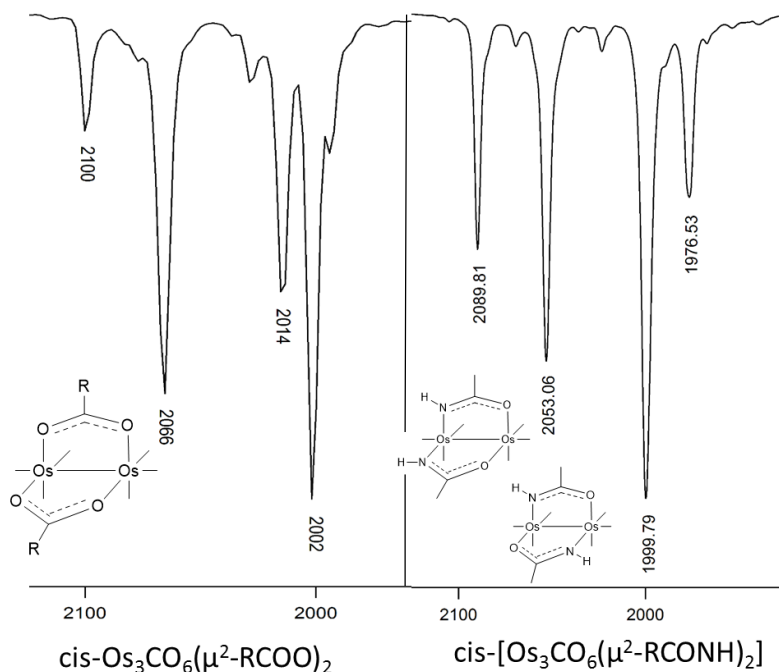


Figure R.4 IR Comparison of product(s) of acetamide reaction to a $\text{cis-Os}_2(\text{CO})_6(\mu^2\text{-RCOO})_2$ both in hexanes

This is because the band pattern produced by mixture A is similar to that of $\text{cis-Os}_2(\text{CO})_6(\mu^2\text{-RCOO})_2$ as seen in figure R.4. The $\text{cis-Os}_2(\text{CO})_6(\mu^2\text{-RCOO})_2$ band pattern consists of 5 bands w, m, m, s, w(shoulder) while the spectrum of mixture A has only 4 bands m, m, s, w, although nonetheless visually similar. If the identification of the product(s) in mixture A is correct, this raises the possibility of isomers of the form $\text{cis-[Os}_2(\text{CO})_6(\mu^2\text{-CH}_3\text{CONH})_2]$ with the H,T confirmation of the amidate ligands and the H,H confirmation (figure R.5) which will be referred to as compounds I and II respectively throughout this paper. However, the band pattern is quite sharp in hexanes

and indicates that if both isomers are present then they are not distinguishable by IR spectroscopy.

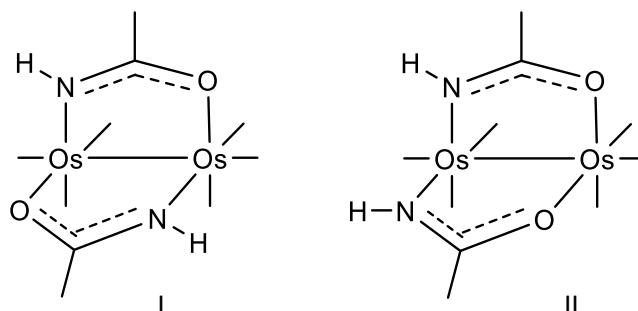


Figure R.5- The possible isomer configurations of $\text{cis-}[\text{Os}_2(\text{CO})_6(\mu^2\text{-CH}_3\text{CONH})_2]$ of mixture A

Another technique that can be used to determine the number of products in a solution is thin layer chromatography. This reaction was also monitored by TLC (mobile phase 40% ethyl acetate/ 60% hexanes) and indicated complete consumption of the starting material after 6 hours refluxing with one eluting product spot and increasing intensity of baseline forming throughout (figure R.6). The reference all products are run against throughout this paper is one of impure starting material $\text{Os}_3\text{CO}_{10}(\mu^2\text{-OEt})_2$ with the impurity at the baseline. The spot that ran ($\text{RF}=0.26$), is mixture A, and could correspond to one or both isomers of $\text{cis-}[\text{Os}_2(\text{CO})_6(\mu^2\text{-CH}_3\text{CONH})_2]$ since they would not be polar enough to be at the baseline, and they may be similar enough in polarity to not be separated. Several mobile phases were investigated trying to separate mixture A by TLC to no avail. The baseline spot designated as product B, may either be highly polar or, since it appears to be an incredibly fine powder, it may have just been suspended in

the solution and deposited on the TLC plate at the baseline without being soluble in the mobile phase.

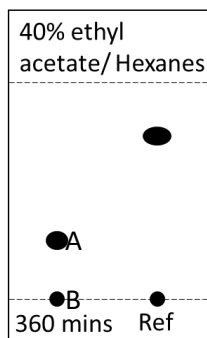


Figure R.6- TLC of crude reaction mixture of $\text{Os}_3(\text{CO})_{10}(\mu^2\text{-OEt})_2$ and acetamide 360 minutes

Attempts to further characterize and identify product B have been unsuccessful as it is not soluble in organic solvents and nujol mol was inconclusive though the broadness and indistinguishable bands may indicate some sort of anion has been formed as a byproduct. Additionally, as supported by the reactions with ruthenium, it is possible that this side product is a polymer, though there was not considerable reduction in IR intensity suggesting it is not a major byproduct.

The crude reaction mixture was then purified by prep-TLC and aliquots of both $\text{Os}_3(\text{CO})_{10}(\mu^2\text{-OEt})_2$, the source of the mixture's yellow color, and mixture A were recovered. Mixture A in solution is clear and colorless, and as a solid it is colorless. This further supports the identification of this cluster being of the form $\text{cis-}[\text{Os}_2(\text{CO})_6(\mu^2\text{-CH}_3\text{CONH})_2]$ because clusters of the form $\text{cis-}[\text{Os}_2(\text{CO})_6(\mu^2\text{-RCOO})_2]$ that have been

observed are generally colorless while triosmium carbonyl clusters are typically yellow-yellow orange.

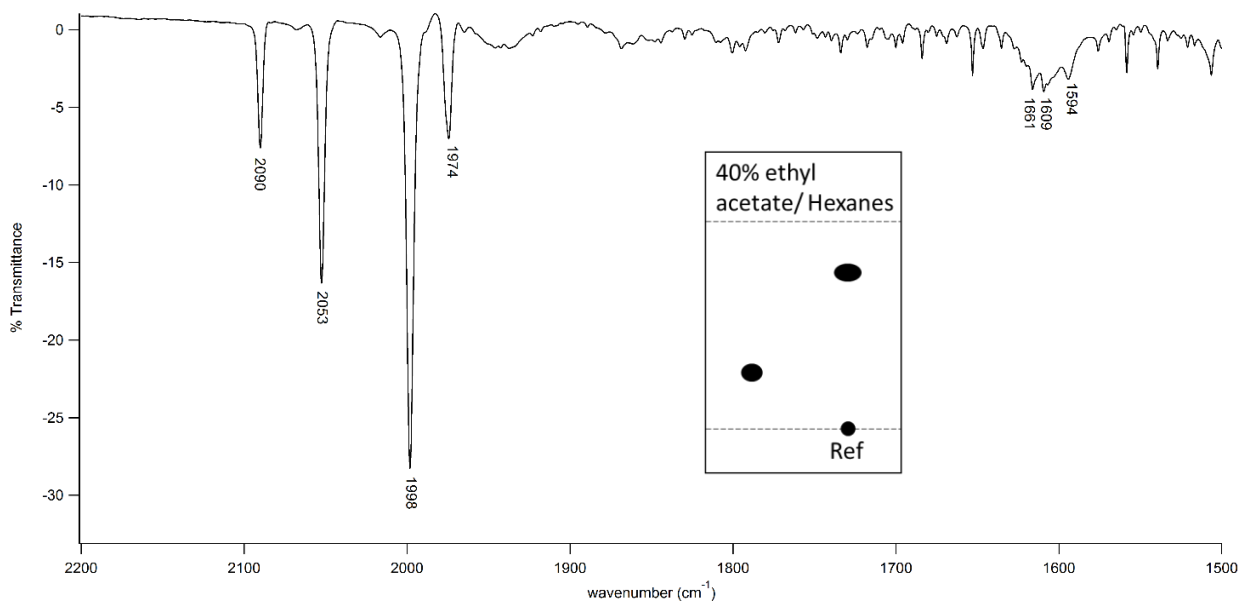


Figure R.7- IR and TLC of purified product A in hexanes

The IR of purified product A (figure R.7) is very clean and the sharpness of the spectrum again suggests one isomer, or if both isomers (I,II) were formed then the isomers are not different enough to distinguish spectroscopically. Looking in the lower wavenumber range for the coordinated amide, which was reported in Odiaka's work with amides and $\text{Os}_3(\text{CO})_{10}(\text{NCMe})_2$ to be $\sim 1590 \text{ cm}^{-1}$ there are several possibilities in this spectrum.⁹ Unfortunately, the solvents appear to be wet, which makes this region of the IR difficult to resolve through subtraction of the solvent and determination of the coordinated amide has not been reached, although it is likely between $1594\text{-}1661 \text{ cm}^{-1}$.

The TLC of the purified product also supports the identity of product A as the product with $R_f=0.26$ since the baseline spot is not observed as it was removed by the column.

Reaction of $Os_3(CO)_{10}(\mu^2-OEt)_2$ and benzamide

A larger substituted amide was also attempted, benzamide, whose R group is a phenyl ring. This is still a relatively simple ligand, so no complications to the reaction were anticipated. Under the same reaction conditions as above, $Os_3CO_{10}(\mu^2-OEt)_2$ was reacted with benzamide ($PhCONH_2$) completely in 150 minutes as indicated by no further spectral changes in the IR and disappearance of the starting material in the TLC with three new spots observed. This is considerably faster than with acetamide and suggests the phenyl ring serves to activate the mechanism of conversion likely due to the enhanced acidity of benzamide over acetamide with pK_{as} of 13 and 15.1 respectively. Throughout the reaction, the mixture went from a pale yellow solution to a darker orange/yellow. Upon cooling a dark brown precipitate was formed, similar to that formed with acetamide, which will be referred to as product C. Product C was insoluble in other organic solvents therefore was unable to be fully characterized.

TLC indicates that the remaining supernatant, D, contains two products (figure R.8) although like the acetamide reaction, the IR was sharp and clear indicating one unique band pattern for these clusters in spite of the fact that mixture D consists of two compounds which are likely isomers. The crude reaction mixture (figure R.8) has a very similar band pattern to that of acetamide which suggests that primary amides will react

similarly despite the R substituent. Similar to the problem with the acetamide reaction, the coordinated amide could not be distinguished from the noise due to water in the solvent.

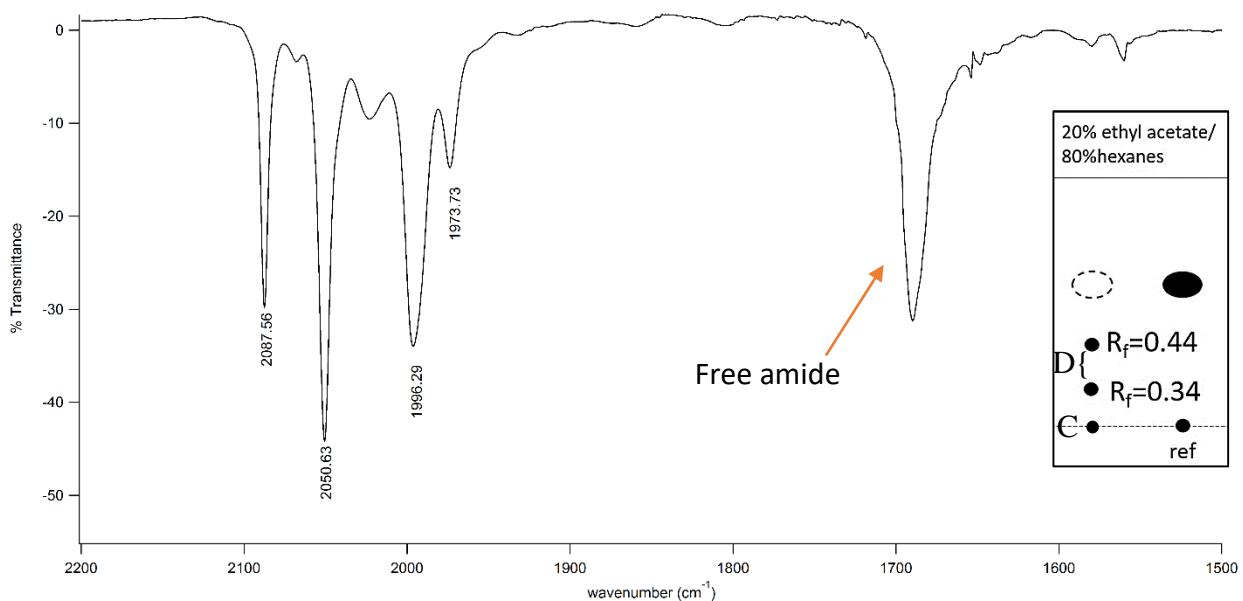


Figure R.8- Crude IR of reaction mixture of benzamide and $\text{Os}_3(\text{CO})_{10}(\text{u}^2\text{-OEt})_2$ after 150 minutes in toluene

Preparative TLC was done to separate the isomers. The less polar isomer will be referred to as compound III and the more polar isomer will be referred to as IV. Based on the orientation of the amidato ligands, (H,H) is proposed to be the more polar isomer (IV) as the dipoles of both amide ligand will be in the same direction and (H,T) the less polar isomer (III) as the dipoles will be pointing opposite. These assignments are shown in figure R.9.

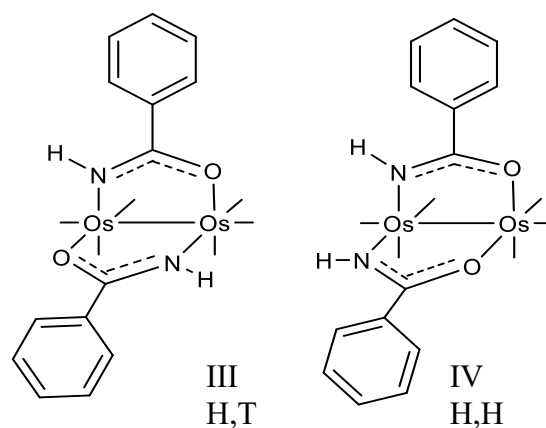


Figure R.9- Isomers in mixture D of the form $\text{cis-}[\text{Os}_2(\text{CO})_6(\mu^2\text{-PhCONH})_2]$

The TLC in 20% ethyl acetate/80% hexanes showed that isomers had been separated successfully, and the baseline product C was removed during the preparative TLC process. Looking at the overlaid IR spectra, figure R.10, of the two separated isomers, it is very apparent that they are not distinguishable by IR as hypothesized with the acetamide isomers. This makes sense because the distribution of the carbonyls is the same in both isomers, and each isomer has two CO ligands trans to an O, N and the M-M bond, meaning overall the vibrations of the CO ligands should not be effected significantly.

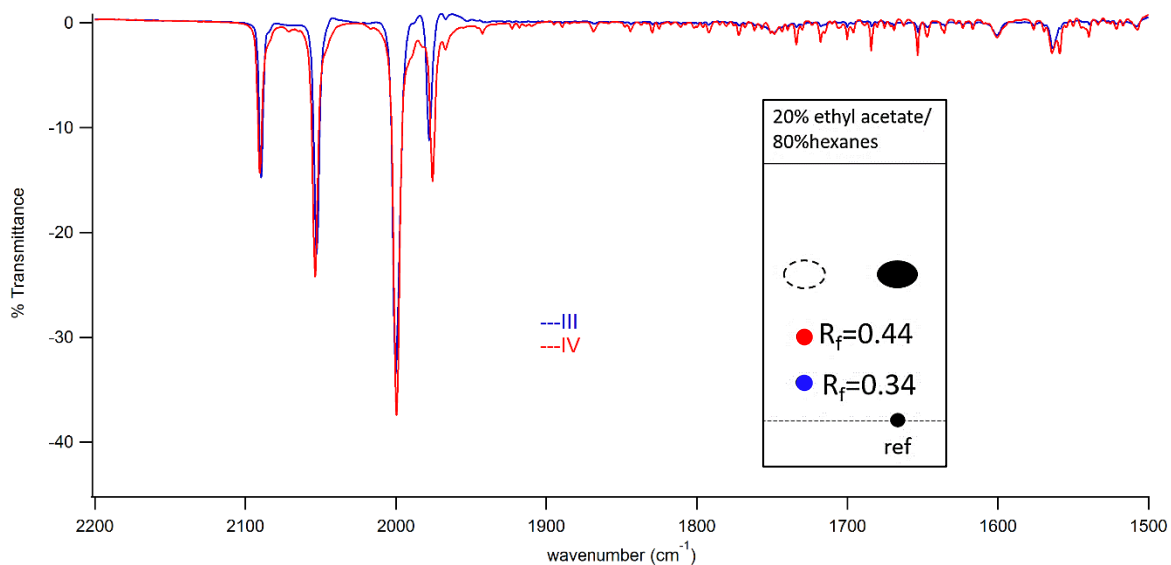


Figure R.10- Overlaid IR spectra of isomers of $\text{cis-}[\text{Os}_2(\text{CO})_6(\mu^2\text{-PhCONH})_2]$ along with TLC **III** blue and **IV** red in hexanes

Reaction comparison of amides and carboxylic acids as ligands.

Since this work is also concerned with the comparison of amide ligands and carboxylic acids as ligand, a reaction was performed under the same conditions with acetic acid. Although work with carboxylic acids has been done already by this lab group, it was performed in hexanes and heptanes which reflux at a lower temperature than toluene making it impossible to compare the reactivity.^{6,7} This reaction of $\text{Os}_3\text{CO}_{10}(\mu^2\text{-OEt})_2$ with acetic acid in toluene was complete in 30 minutes as indicated by no more changes in the IR spectra and no more starting material on the TLC. The mono-substituted intermediate observed by Dunham and Schmitt was not observed. This indicates that in this cluster system carboxylic acids are more reactive than amides. The reactions investigated are summarized in table 1.

Bidentate Ligand	Reaction time in Δ toluene (min)
CH ₃ COOH	30
CH ₃ CONH ₂	360
PhCONH ₂	150

Table1- Bidentate ligand reactivity summary table

Computational Vibrational Analysis:

Since diosmium diamidate carbonyl clusters have not been observed previously in literature, a computational vibrational analysis was done on the formamide derivative of the product clusters, both H,T and H,H, in order to further support the structural determination. Several attempts were made to optimize the input file to yield an adequate result, and all of them will be discussed in this section.

Initially, unoptimized structures of both isomers were used with 90° angles and overall octahedral geometry about both osmium clusters. The frequency calculations for the two isomers were nearly identical in pattern further supporting the rational that both isomers are present although only one clean IR of the products is observed. However, as one can see in figure R.11, the wavenumbers and the pattern are off from the experimental IR (Figures R.7 and R.8) which strongly suggests that a modification to the method was needed.

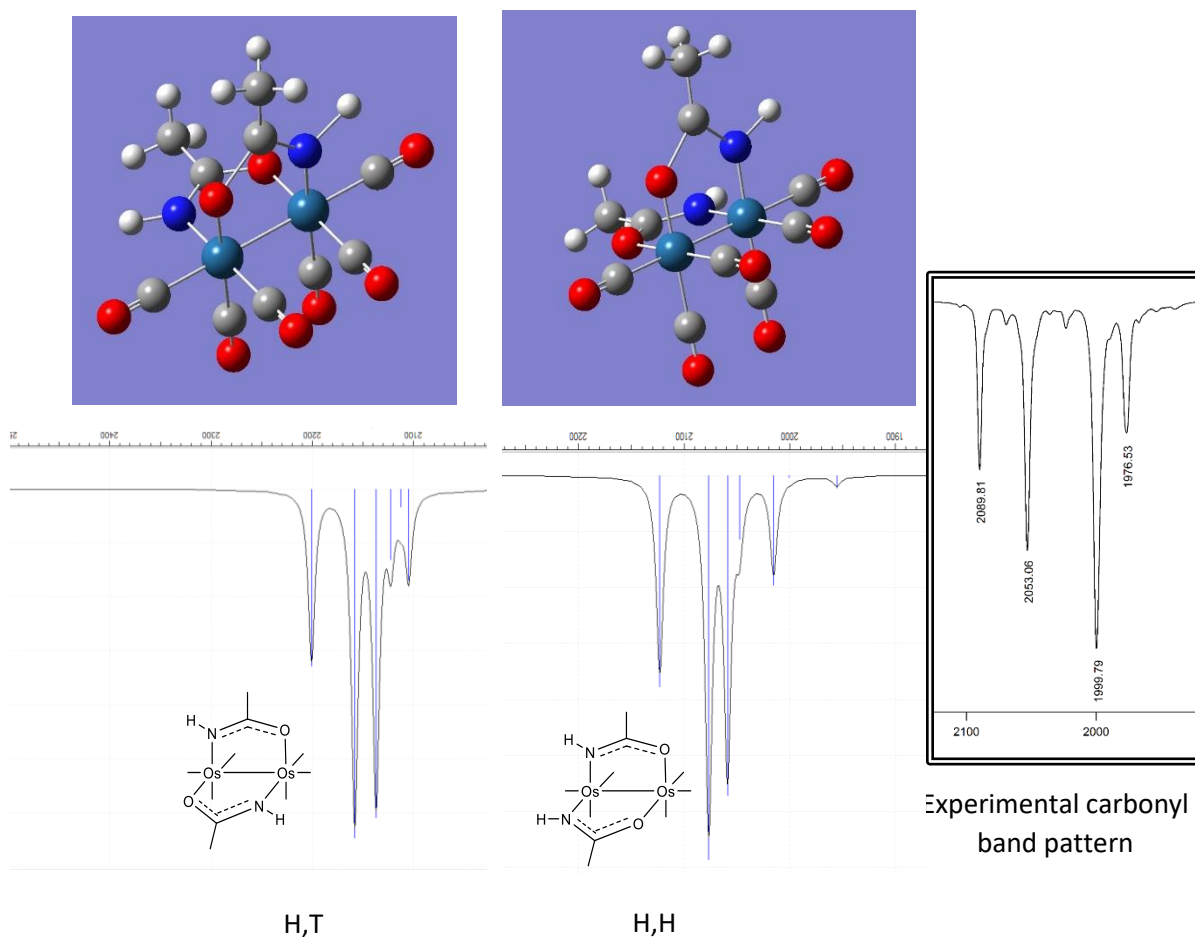


Figure R.11 Gaussian 09 unoptimized structures and theoretical frequency calculations for both isomers, cis-(H,T) $\text{Os}_2(\text{CO})_6(\text{HCONH})_2$ (left) and cis-(H,H) $\text{Os}_2(\text{CO})_6(\text{HCONH})_2$ (right). Experimental carbonyl pattern boxed far right.

Attempts were made to optimize the structure with the same parameters as above, but those resulted in the cluster being broken apart. Therefore, modifications were made to the cluster input structure for frequency calculations by using a structure adapted from X-ray crystal data of $\text{Os}_2(\mu^2\text{-sebacate})(\text{CO})_4(\text{dmsO})_2$.¹² Having these bond angles and bond lengths produced a pattern much more similar to experimental. However, the wave

numbers were off by more than one could attribute to anharmonic stretching, with the highest frequency less than 1700cm^{-1} compared to almost 2100cm^{-1} in the experimental (Figure R.12).

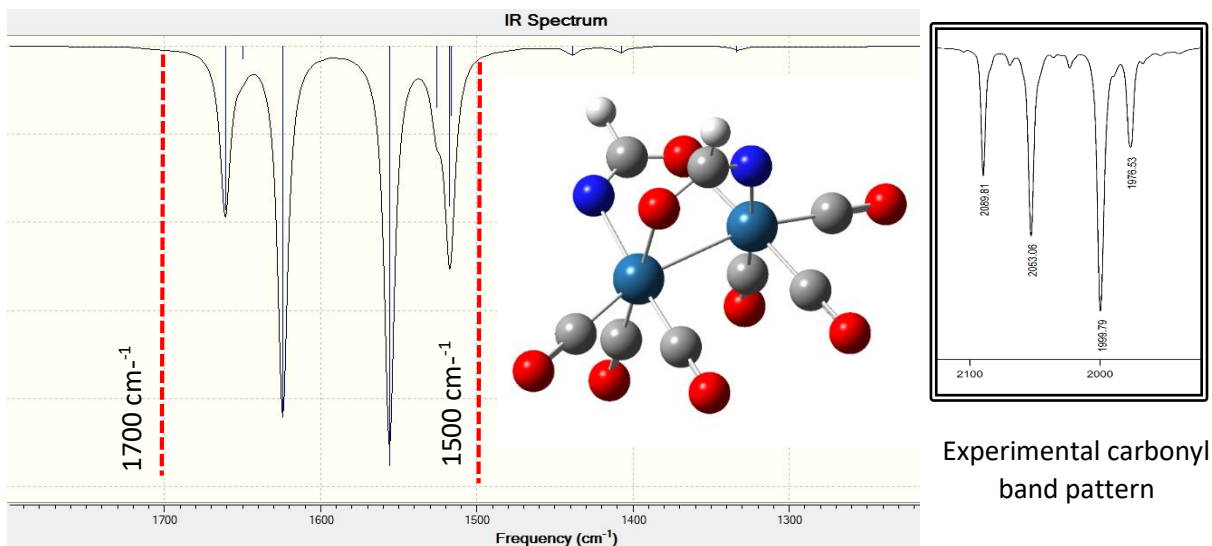


Figure R.12- Frequency calculation of modified structure of cis-(H,T) $\text{Os}_2(\text{CO})_6(\text{HCONH})_2$ showing similar pattern to experimental (right) but poor wavenumber correlation

In order to account for the shift in wavenumbers, a modification was made to the “solvation” parameter in the calculation set-up. By taking the structures as compounds in heptane, whose dielectric constant is most similar to experimental hexane, rather than the default gas phase, successful optimization and frequency calculations were achieved. These parameters were used for both cis-(H,T) $\text{Os}_2(\text{CO})_6(\text{HCONH})_2$ and cis-(H,H) $\text{Os}_2(\text{CO})_6(\text{HCONH})_2$. The resulting structures can be seen in figure R.13, and resultant theoretical vibrational spectra can be seen in figures R.14 and R.15 respectively. All iterations of these calculations resulted in different final structures whose bond lengths and angles are summarized in table 2.

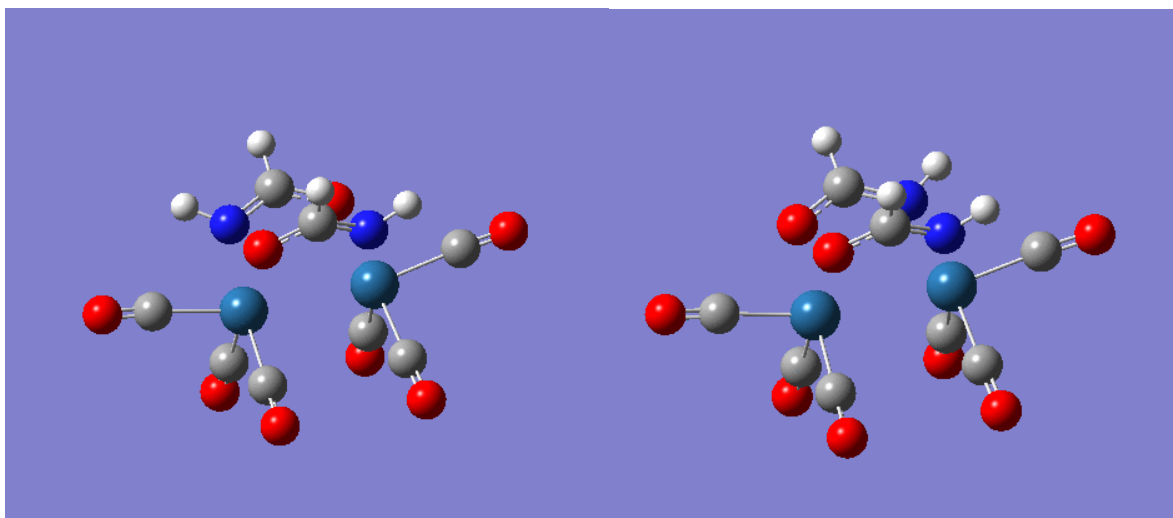


Figure R.13- Optimized structures of (cis H,T) $\text{Os}_2(\text{CO})_6(\text{HCONH})_2$ (left) and (cis H,H) $\text{Os}_2(\text{CO})_6(\text{HCONH})_2$ (right)

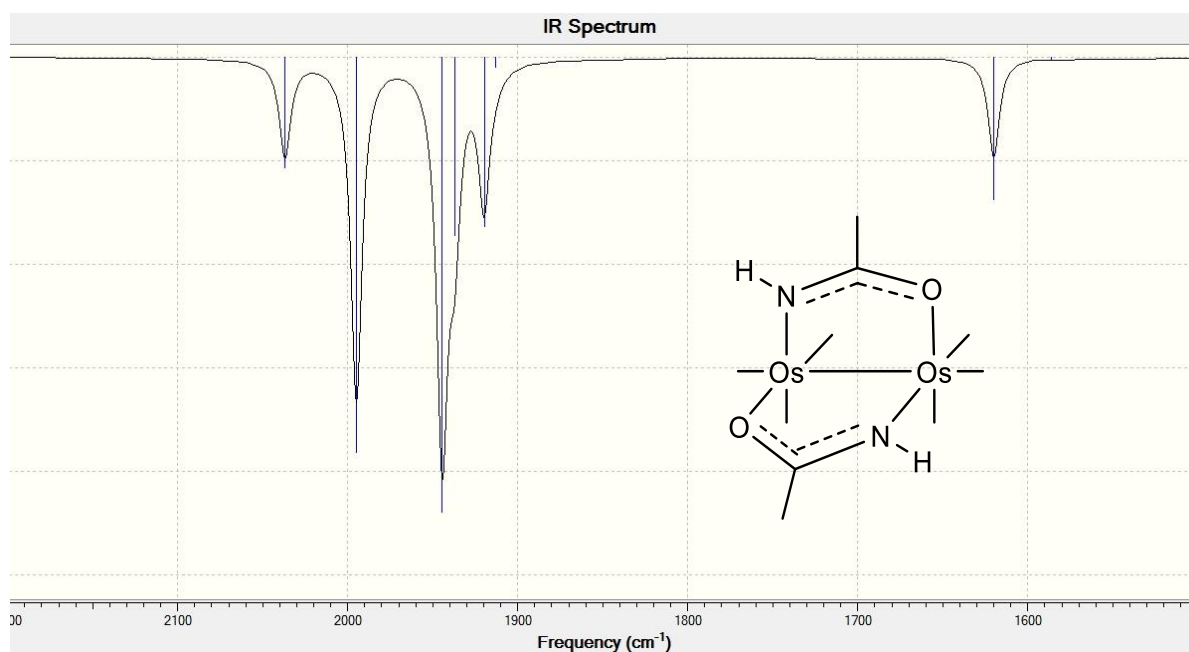


Figure R.14- Theoretical vibrational frequencies for (cis H,T) $\text{Os}_2(\text{CO})_6(\text{HCONH})_2$

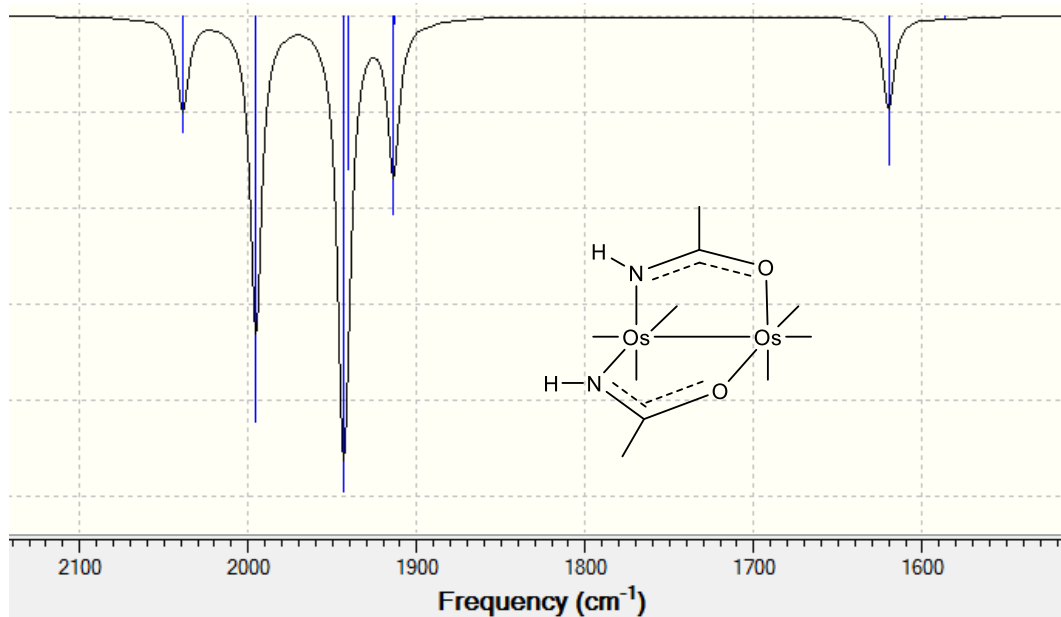


Figure R.15- Theoretical vibrational frequencies for (cis H,H) Os₂(CO)₆(HCONH)₂

To further validate this method, and explore the spectral differences in the band patterns, the same computational vibrational analysis was done on a diosmium dicarboxylate carbonyl cluster, Os₂(CO)₆(μ²-HCOO)₂. The resulting theoretical IR and optimized molecular structure can be seen in figures R.16 and R.17 respectively and showed good correlation with experimental data. This provides further evidence that the analysis and structural assignments of the bisamidato clusters are reasonable and valid.

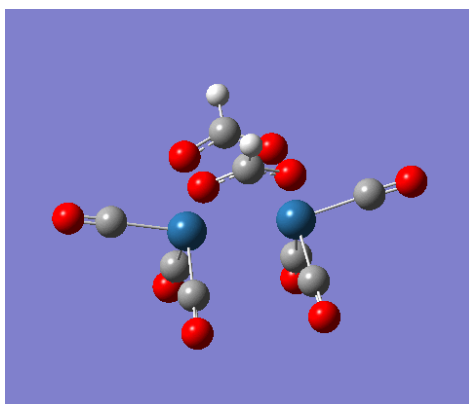


Figure R.16- Optimized structure of cis- $\text{Os}_2(\text{CO})_6(\mu^2\text{-HCOO})_2$

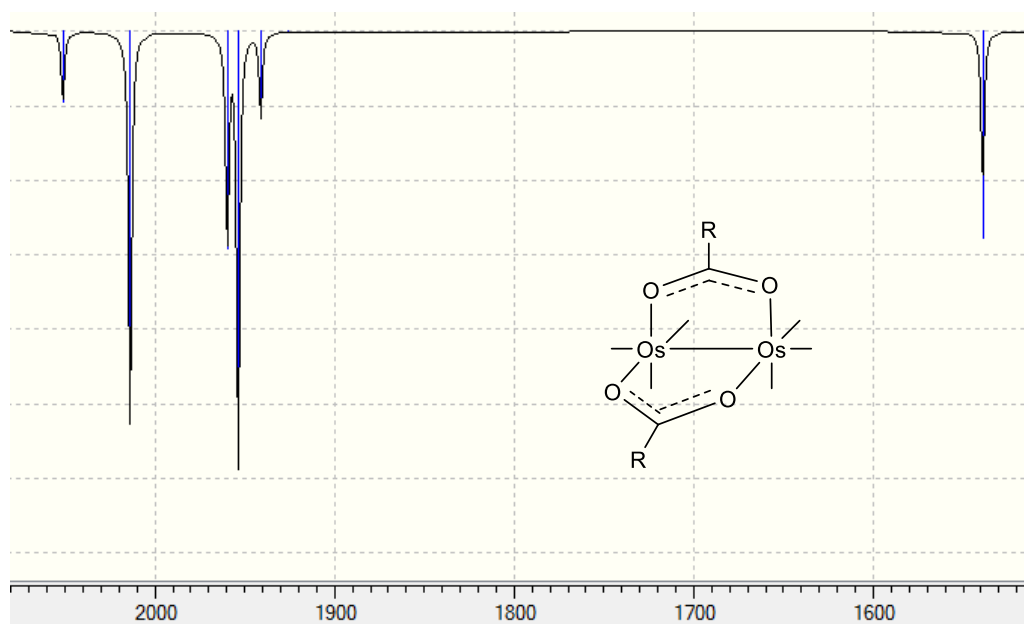


Figure R.17- Theoretical vibrational spectrum of cis- $\text{Os}_2(\text{CO})_6(\text{HCOO})_2$

Bond lengths	(H,T)	(H,H)	non-solvated	C_2V
Os-Os	2.88262	2.88387	2.712	2.52
Os-C(O)1	1.9582	1.97001	1.854	2.03
Os-C(O)2	1.89497	1.89728	1.854	2.03
Os-C(O)3	1.91991	1.9171	1.854	2.03
Os-N	2.13453	2.14534	2.118	1.8902
Os-O	2.14989	2.13828	2.118	1.8902

Bond angles

Os-Os-C(O)1	168.7462	170.2794	164.87001	180
N-Os-C(O)3	172.2781	173.257	175.4648	180
O-Os-C(O)2	176.6369	175.409	179.1548	180
N-C(R)-O	124.651	124.5529	130.81353	96.20308

Table 2- Summary of computational bond lengths and angles

With all three of the $\text{cis-Os}_2(\text{CO})_6(\mu^2\text{-X})_2$ calculations successful, a further vibrational analysis was performed to determine the effect of the NH group on the vibrational spectra. When looking at a comparison of experimental $\text{cis-Os}_2(\text{CO})_6(\text{RCOO})_2$ and $[\text{cis-Os}_2(\text{CO})_6(\text{RCONH})_2]$ IR band patterns there seems to be band shifting occurring in the lower wavenumber bands from 2014 to 1976 (figure R.18). In order to probe this difference in the spectra, a detailed look at the vibrations responsible for each band was done and this is summarized in table 3. When looking at the structures in table 3, CO ligands that are contributing to the vibration are replaced with an arrow representing their motion with respect to the other ligands. For the sake of clarity RCOO and RCONH ligands are represented as L for all but the coordinated amide frequency.

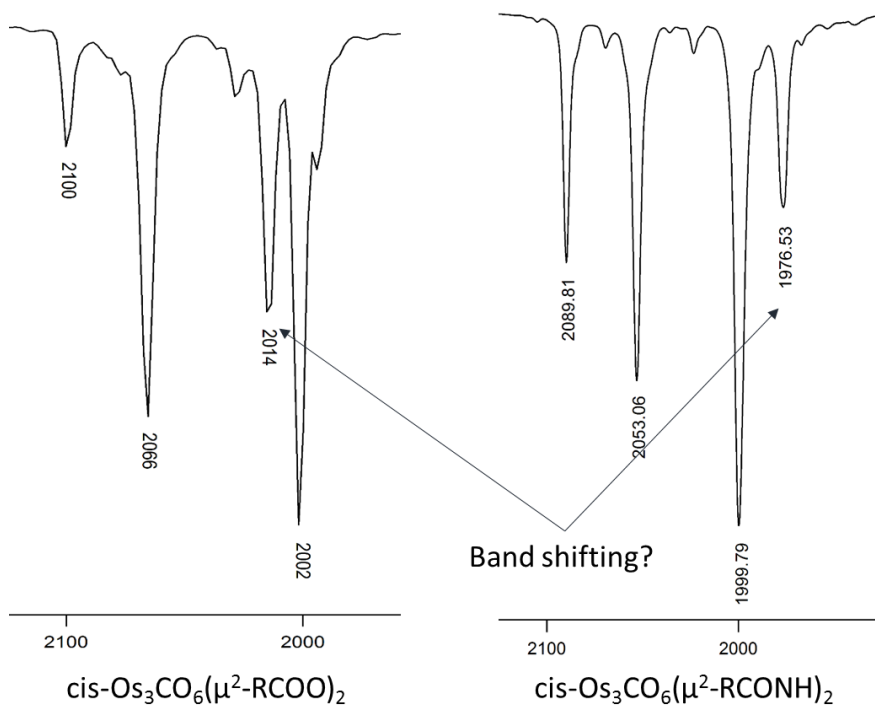


Figure R.18- General regions of hypothesized band shifting as evident by the difference in experimental pattern between $\text{Os}_2(\text{CO})_6(\text{RCOO})_2$ (left) and $[\text{cis- Os}_2(\text{CO})_6(\text{RCONH})_2]$ clusters (right).

Placing the wavenumbers of each type of vibration into the table, it becomes evident which bands are causing the shift in the overall band pattern. The most notable shift is summarized in figure R.19 which shows the theoretical bands that have shifted in comparison to the rest of the pattern which remains similar for carboxylate and amidate ligands and figure R.20 which shows experimentally the band that breaks the pattern. The vibration responsible for this band is one where COs trans to the organic ligand are moving symmetrically with respect to each other while moving asymmetrically with respect to the ligands trans to the M-M bond. It would make sense that this band would

be affected since the CO ligands trans to the amidate or carboxylate ligands are contributing greatly and the ligands trans to the N-H group in particular are weakened in the intensity of their stretching.

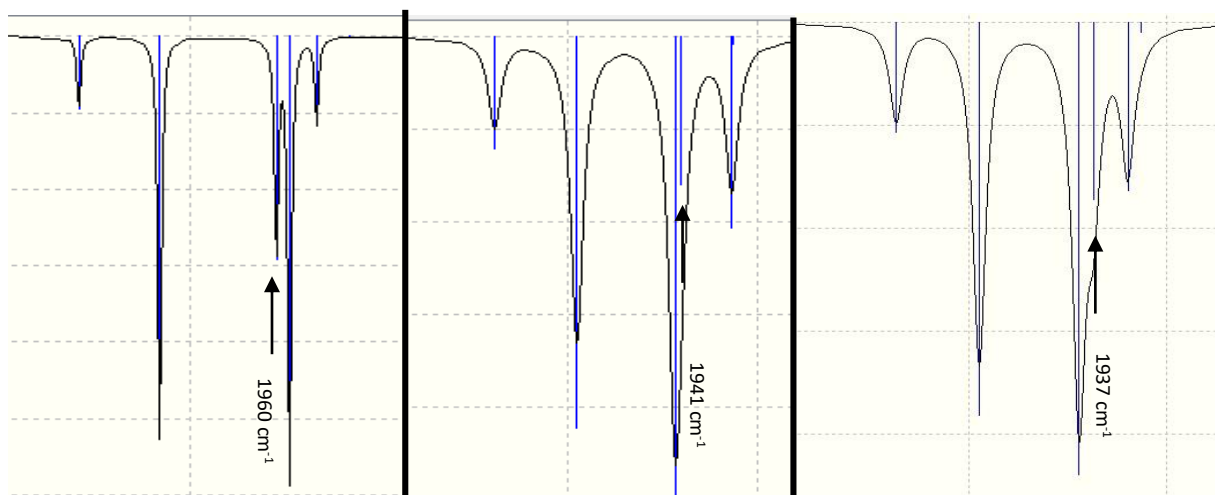


Figure R.19- Theoretical mid intensity band of $\text{Os}_2(\text{CO})_6(\text{RCOO})_2$ (left) shifting to become lower energy shoulder in $[\text{cis- Os}_2(\text{CO})_6(\text{RCONH})_2]$ clusters (right).

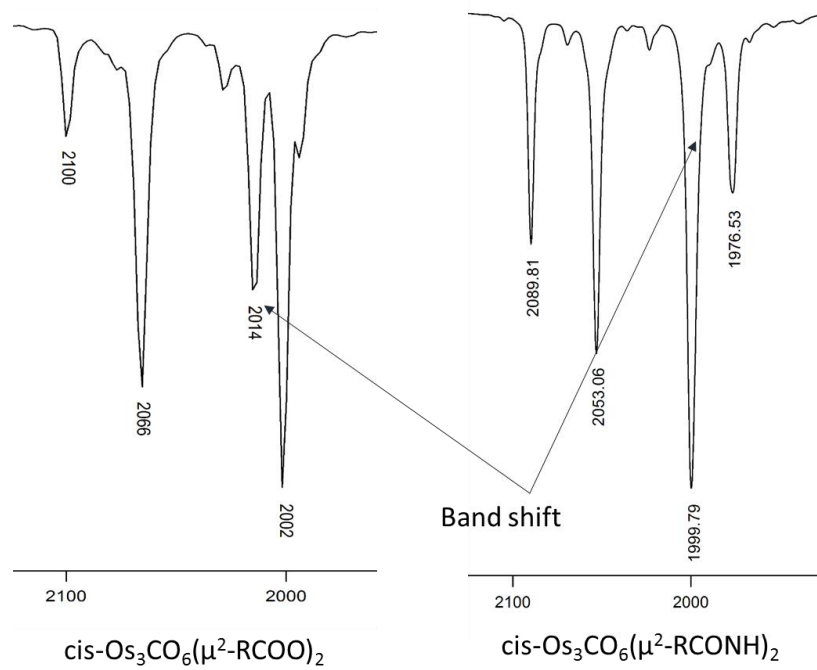


Figure R.20- Experimental band shifting to become lower energy shoulder

Table 3

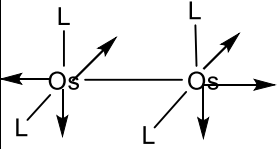
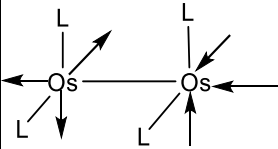
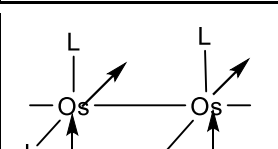
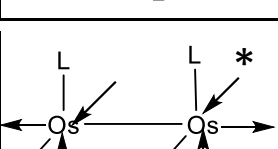
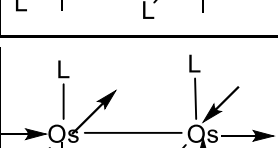
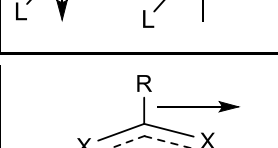
	cis-(H,H) $\text{Os}_2(\text{CO})_6(\text{HCONH})_2$	cis-(H,T) $\text{Os}_2(\text{CO})_6(\text{HCONH})_2$	cis- $\text{Os}_2(\text{CO})_6(\text{HCOO})_2$
	2037 cm^{-1}	2039 cm^{-1}	2051 cm^{-1}
	1995 cm^{-1}	1995 cm^{-1}	2014 cm^{-1}
	1944 cm^{-1}	1944 cm^{-1}	1954 cm^{-1}
	1941 cm^{-1}	1937 cm^{-1}	1960 cm^{-1}
	1919 cm^{-1}	1914 cm^{-1}	1941 cm^{-1}
	1620 cm^{-1}	1620 cm^{-1}	1539 cm^{-1}

Table 3- Frequency calculation summary table for clusters the three clusters.

* in cis-(H,H) $\text{Os}_2(\text{CO})_6(\text{HCONH})_2$ the CO ligands trans to the nitrogen group do not contribute at all to the vibration, otherwise the same carbonyl vibrations are observed.

These optimization/ frequency calculations also allow for mapping of molecular orbitals. In particular, looking at the LUMO or lowest unoccupied molecular orbital, can indicate the likelihood of new bond formation and also where in a molecule a bond is likely to break. The LUMO of cis-(H,T) Os₂(CO)₆(HCONH)₂ shows two significant things (figure R.21). First, the lack of a molecular orbital on the proton of the NH group helps to corroborate the finding that the NH can be displaced more readily than the CH₃ protons by deuterium. The second finding is the hole in the molecular orbital under the NH group, especially notable in comparison to cis- Os₂(CO)₆(HCOO)₂ (Figure R.21). This hole suggests that these amidates are in fact hemilabile ligands with a preference to break at the Os-N side of the coordination as hypothesized. Although, the gap in molecular orbitals on both the head and tail side of the ligand suggests the whole ligand is labile.

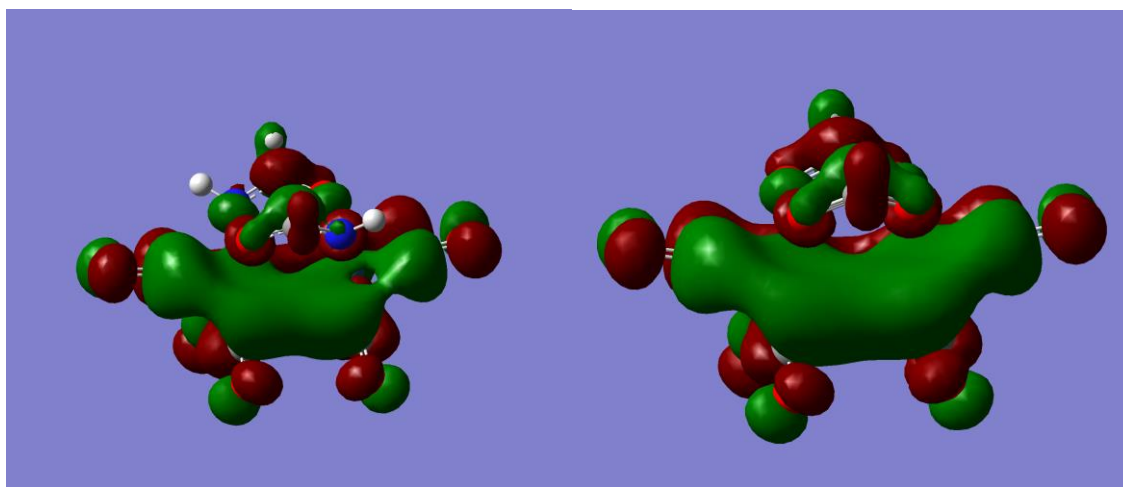


Figure R.21- LUMO of cis-(H,T) Os₂(CO)₆(HCONH)₂ (left) and to cis- Os₂(CO)₆(HCOO)₂ (right).

¹H-NMR analysis of products I-IV

Since the isomers cannot be distinguished using IR spectroscopy, proton nuclear magnetic resonance or ¹H-NMR was done on all products for characterization and also, by using spectra of the crude reaction mixtures, A and D, determination of the ratios of the isomers. ¹H-NMR spectra for each of the separated isomers III and IV once characterized could be used to determine which isomer was more prevalent under thermodynamic conditions and to assign peaks in the NMR spectrum of mixture D (I,II). The spectrum of isomer III (H,T), the less polar isomer, can be seen in figure R.22 and the proton NMR spectrum of isomer IV (H,H), the more polar isomer, can be seen in figure R.23. The NH peak is shifted further downfield in isomer III with a chemical shift of 7.099 compared to 6.686 of isomer IV, the less polar isomer. These were identified as NH peaks through the broadness and integration in comparison to the aromatics. It should also be noted that in both cases there is good resolution in the aromatic region and the integrations are fairly consistent with expected ratios which have been identified in figures R.22 and R.23.

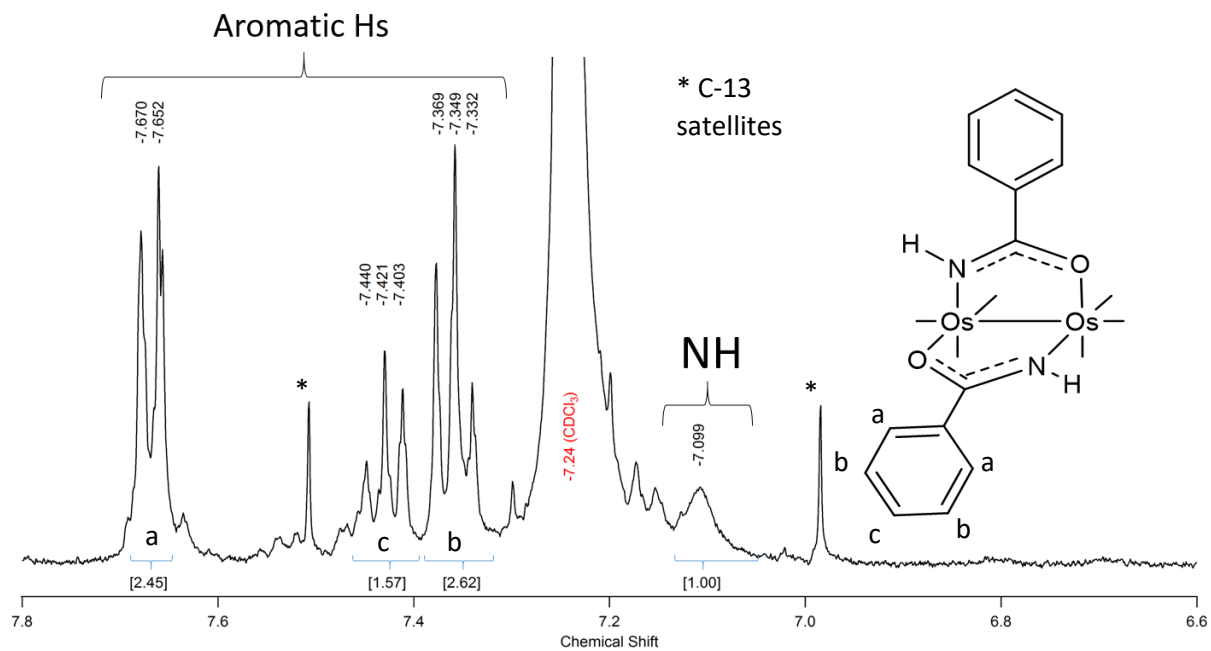


Figure R.22- ^1H NMR of isomer III, $\text{cis (H,T) Os}_2(\text{CO})_6(\mu^2\text{-C}_6\text{H}_5\text{CONH})_2$ with relative integrations and chemical shifts (δ).

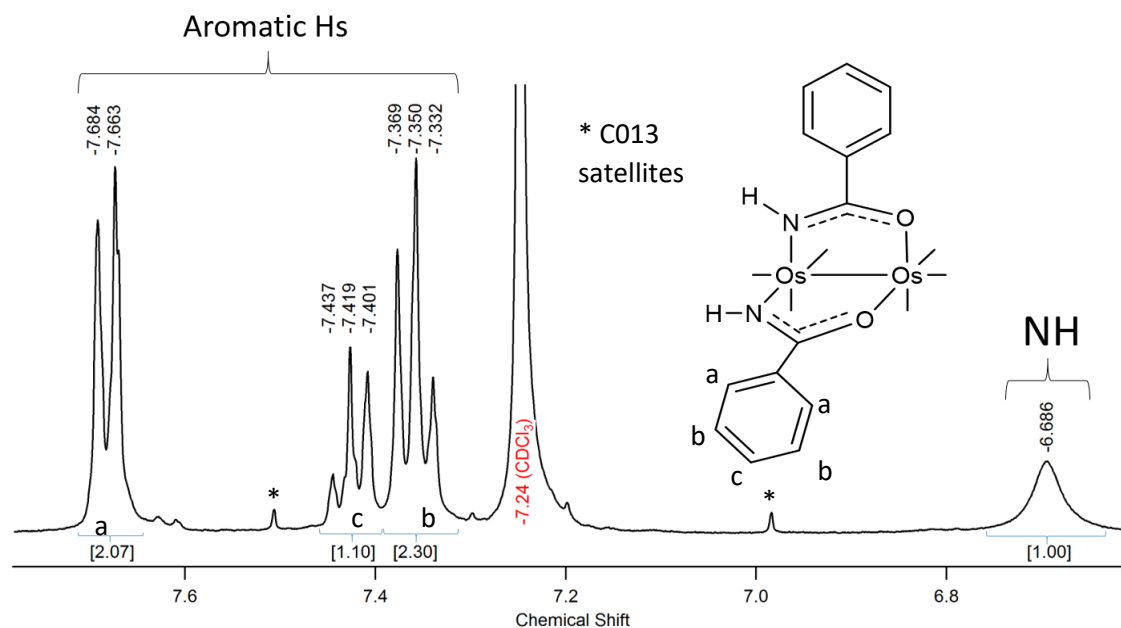


Figure R.23- ^1H NMR of IV cis (H,H) $\text{Os}_2(\text{CO})_6(\mu^2\text{-C}_6\text{H}_5\text{CONH})_2$ with relative integrations and chemical shifts (δ).

With the knowledge of what effect coordination of the ligand to the cluster has on the NH protons depending on the isomer, the peaks in the ^1H -NMR mixture A ($\text{R}=\text{CH}_3$) and D ($\text{R}=\text{Ph}$) can be assigned and the ratios can be determined. The ^1H -NMR spectrum of mixture D ($\text{R}=\text{Ph}$) is shown in figure R.24. By integrating the peaks, the protons which correspond to the proton bonded to the nitrogen can be determined and thus the relative concentrations of the isomers were determined. In this case the ratio of the isomers is 61:39 favoring the isomer whose NH peak is shifted further downfield at 7.1052 (δ) over the more shielded NH peak at 6.6917(δ). This informs us that product III (H,T) is the more favored isomer under thermodynamic conditions relative to isomer IV (H,H).

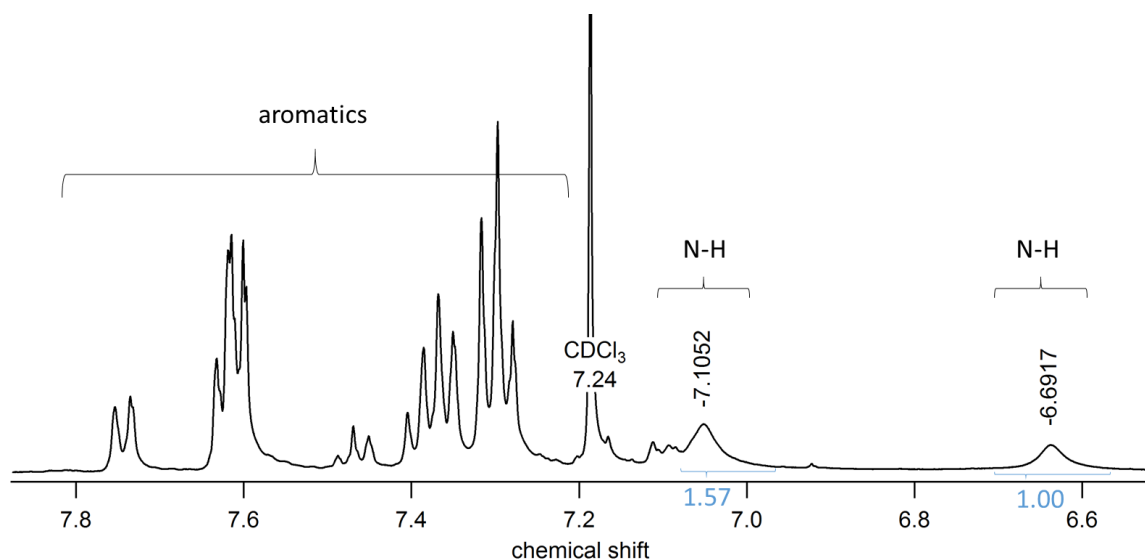


Figure R.24- $^1\text{H-NMR}$ of mixture D, cis (H,H) and cis (H,T) $\text{Os}_2(\text{CO})_6(\mu^2\text{-C}_6\text{H}_5\text{CONH})_2$ with relative integrations of NH peaks.

The $^1\text{H-NMR}$ of mixture D, cis (H,H) and cis (H,T) $\text{Os}_2(\text{CO})_6(\mu^2\text{-C}_6\text{H}_5\text{CONH})_2$ is shown in figure R.25. The peaks at 6.319 (1) and 5.909 (2) correspond to the NH protons because their chemical shifts and broadness are consistent and their relative integrations are 1 and 1.11 respectively. The peaks at 2.020(3) and 2.006(4) correspond to the CH_3 protons because the chemical shift is appropriate for a methyl amide and each has an integration close to 3 times the NH peak integrations, 3.57 and 3.28 respectively. The isomers were assigned with the more downfield NH peak and corresponding methyl protons belonging to the less polar isomer, (H,T) isomer I, shown in red in figure R.25, and the less shifted NH and corresponding methyl protons assigned to the more polar isomer, (H,H) II shown in blue. Using the NH integrations, the ratio was determined to be 52:48 (H,H):(H,T) favoring the more polar isomer, isomer II slightly.

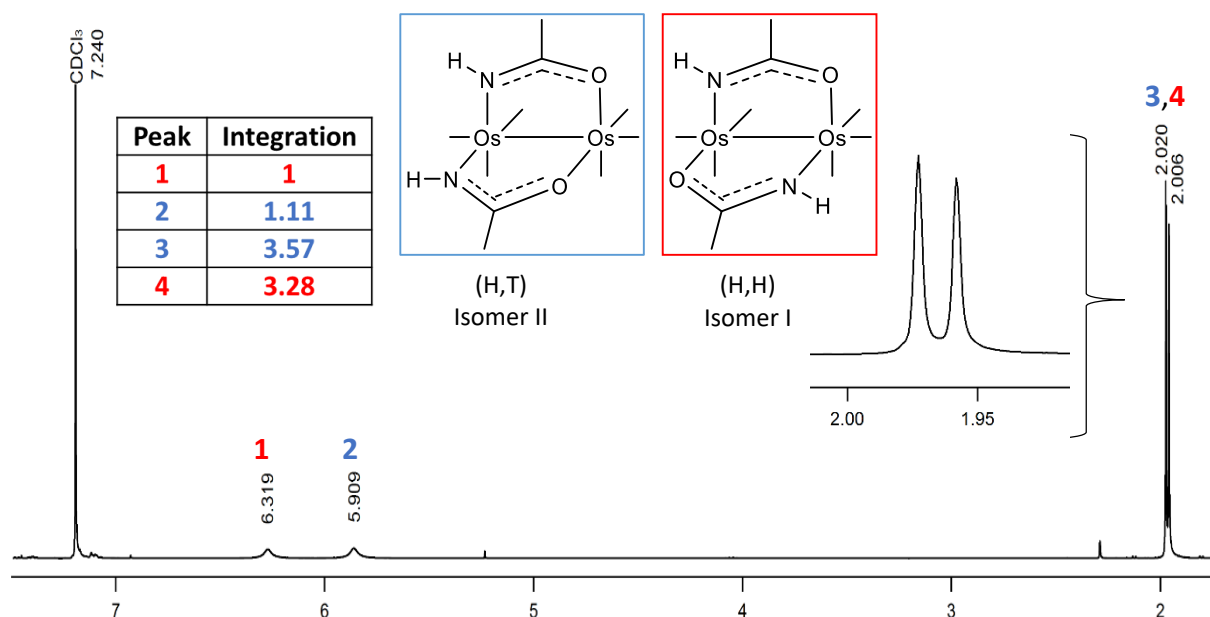


Figure R.25- ^1H -NMR of mixture A highlighting peaks corresponding to isomer I in red and peaks corresponding to isomer II in blue.

D₂O exchange to find exchangeable protons

One technique to determine the acidity of a proton is to look at how readily it exchanges with D_2O . Several D_2O shakes were performed on a solution of $\text{Os}_3(\text{CO})_6(\mu^2\text{-CH}_3\text{CONH})_2$ in CDCl_3 with one drop of D_2O monitoring the change in integration of the NH peak using ^1H NMR over the span of a month. It was determined that after the initial change in the ^1H NMR, no further deuterium exchanged without another violent shake of the tube and therefore the tube was successively shaken over the course of a month. The data was collected by integration of the NH peaks of both isomers I and II with respect to an internal reference of grease. The results of the shakes are summarized in figure R.26 which shows a graph of the integration ratios of the NH and CH_3 peaks in each isomer

(peaks 1,2,3,4 from figure R.25) compared to an internal reference peak (δ 1.24) integration. Because we don't expect the grease to have exchangeable protons we will be able to use it as a reference to see how the relative amounts of the product peaks decrease after each shake. Looking at the chart, the x axis is number of shakes, which is simply the number of times the sealed NMR tube was shaken. While this seems like an unreliable method to display the data, the exchange happened so minimally, and nothing was observed to happen to the ratios other than immediately following a shake of the NMR tube, thus time is not an acceptable axis. Additionally, the data is presented on a single proton basis, meaning the CH_3 integration ratios are divided by three to compare the likelihood of a single proton exchanging. We can see from the graph that all of the protons are exchanging, though fairly slowly, however isomer I (H,T) is exchanging at a faster rate than isomer II (H,H) for both the NH and CH_3 protons. This is an unexpected result since mechanistically we would expect both isomers to be able to exhibit exchange at equal rates. One explanation of this could be the low miscibility of D_2O and CDCl_3 meaning exchange is only happening on the surface, and due to differences in polarity this may cause the less polar, (H,T) isomer to preferentially exchange. Additionally, in both isomers, the NH proton exchanges more readily than one of the CH_3 protons. This preliminary data indicates that the NH protons are exchangeable, but slowly, and further investigation is necessary.

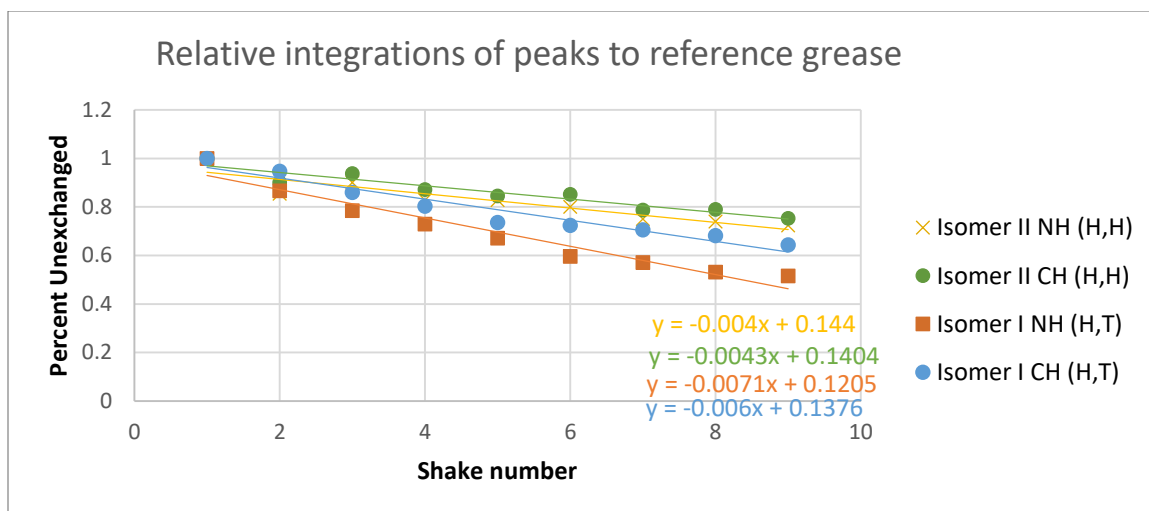


Figure R.26- Graphs of D₂O shakes' ¹H-NMR integration ratio data to a grease reference

Interconversion of the isomers in solution of CDCl₃

Another interesting finding is the interconversion of the isomers of cis-Os₃(CO)₆(μ²-PhCONH)₂ in solution. By interconversion it is meant that if isolated isomer III (H,T) was left in solution it would begin to interconvert back to some ratio of both isomers III (H,T) and IV (H,H). This interconversion was monitored for two solutions A and B, which began as pure compounds III (H,T) and IV (H,H) respectively. As the isomers interconverted over time their relative ratios to each other were monitored using the NH peaks in the NMR. In the figure R.27 the baseline in ¹H-NMR where the other isomer's NH peak would appear is in green. The colored lines show the same region after a period of time, and the grey is a reference for the location of the other isomer that is not initially in solution. A chart of the relative ratios is shown to the right. This data shows solution A, starting as (H,T), is interconverting at a slower rate which makes sense as it is comprised of mostly the more thermodynamic product, isomer III which is therefore

more stable. This data is also represented graphically in figure R.28 which clearly shows a faster rate of interconversion for solution B.

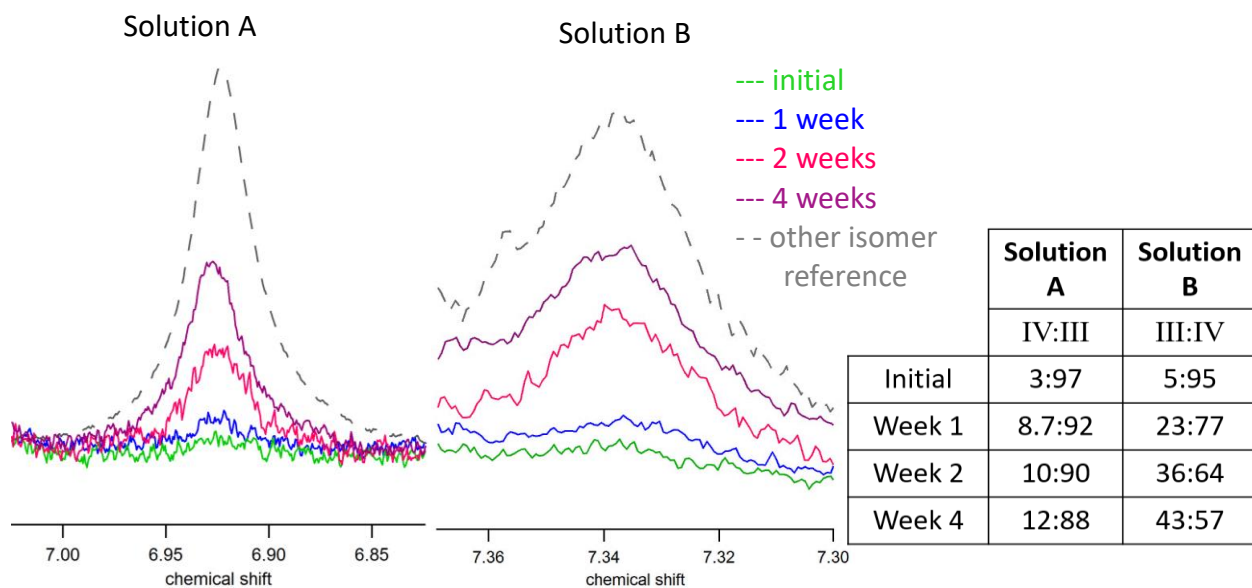


Figure R.27- Evidence of isomers III (H,T) and IV (H,H) interconversion in solution.

Solution A, left primarily isomer III, and solution B, primarily isomer IV. accompanied by isomer ratios across four weeks.

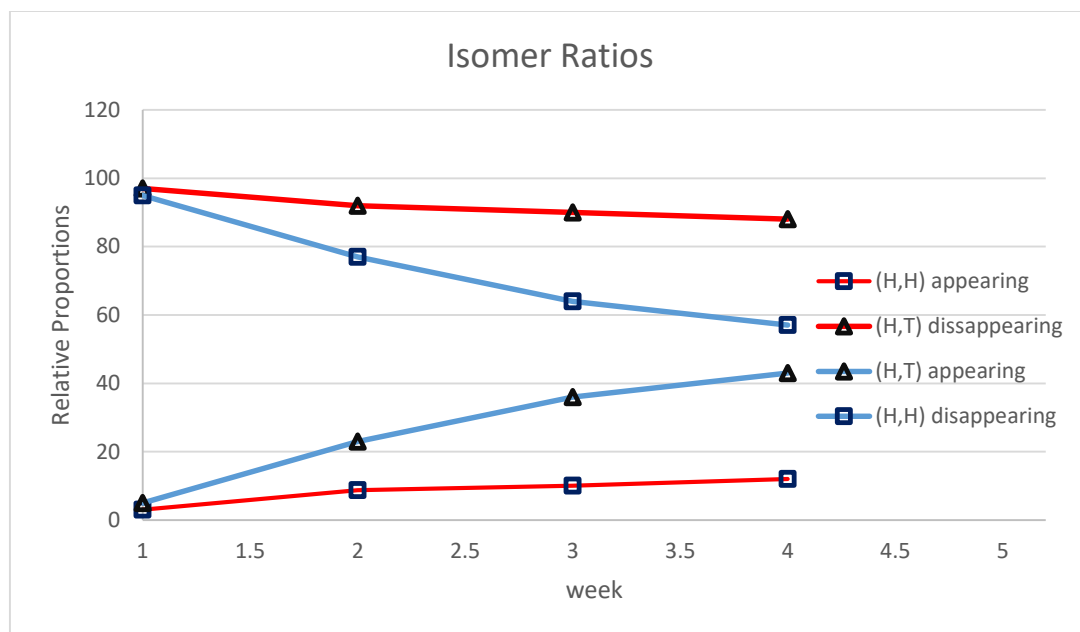


Figure R.28 Isomer ratios of solutions A and B as they change across weeks. Solution A is shown in red and clearly interconverts less rapidly than solution B. Isomer III is represented by a triangle and isomer IV by a square.

There are a few possible mechanisms for the interconversion. One involves the amide completely dissociating in solution and then reattaching switching between (H,H) and (H,T) confirmations. This is the most unlikely as ligand dissociation is not probable at room temperature and there is nothing to stabilize the ligand in solution. Another possibility involves the partial dissociation of the amidato ligand via the NH group to form a mono dentate intermediate. The nitrogen could then re-coordinate in either the H,H or H,T configuration. This model is more plausible as the activation energy would be lower and amides are already suspected to be a hemilabile ligands, meaning that one coordination site is weaker than the other. Also, since it does not involve complete

dissociation it does not need something in solution to stabilize the free ligand. This model is demonstrated in figure R.29.

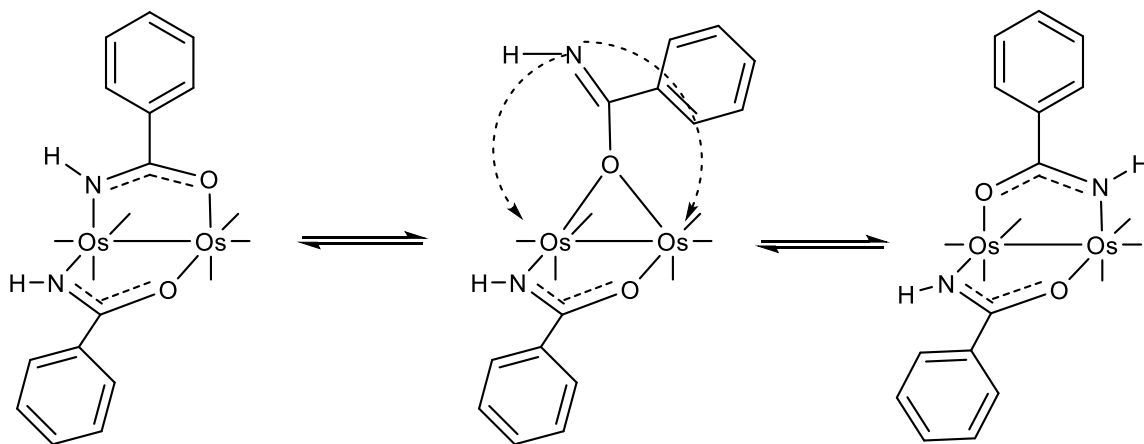
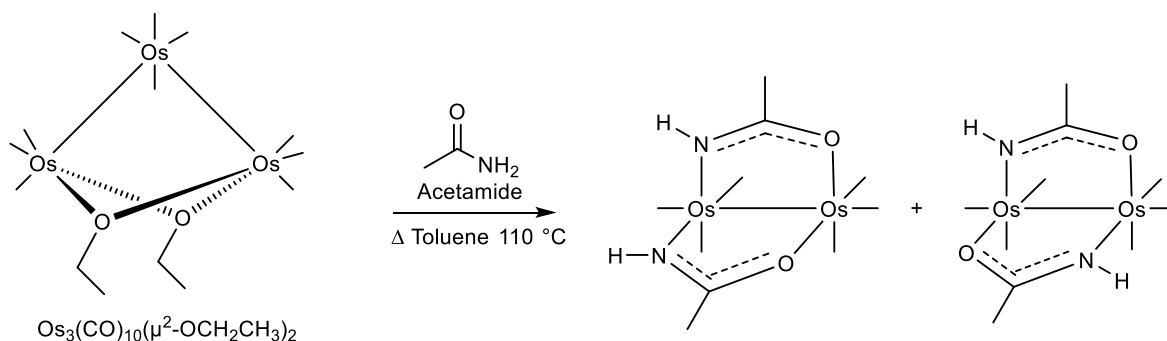


Figure R.29- Potential mechanism for interconversion of isomers III and IV

Conclusion-

Based on the analysis of data presented in this research paper, the proposed structures of the products of $\text{Os}_3(\text{CO})_{10}(\mu^2\text{-OEt})_2$ with acetamide and benzamide are presented in figure 33. From the NMR integrations we concluded that both possible isomers, *cis*-(H,H) and (H,T), are observed in a 52:48 (R=CH₃) and 61:39 (R=Ph) ratio respectively. The identity of these products were supported by DFT vibration calculations which corresponded to experimental IR spectra. In the future we would like to separate the isomers of the acetamide reaction to completely identify and characterize them. The group would also like to perform the reaction at lower temperatures to try to isolate an intermediate step before cluster breakdown as observed for carboxylates. Additionally, it will be interesting to find if the coordinated amides are exchangeable for carboxylates which have been found to be more reactive in forming diosmium products. Also characterization of the unknown insoluble product produced by these reactions would help to provide insight into the mechanism of product formation. This could also be aided by further DFT calculations which could help to explain why in the benzamide reaction there is a favored isomer but not for acetamide. This is summarized in table 4.



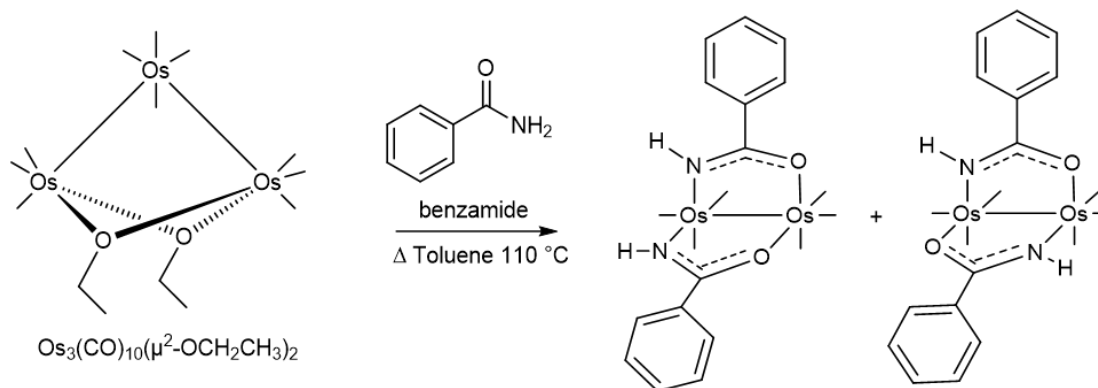


Figure 33- Proposed products of reaction of $\text{Os}_3(\text{CO})_{10}(\mu^2\text{-OEt})_2$ with acetamide and benzamide in toluene

Bidentate Ligand	Reaction time in Δ toluene (min)	Ratio (H:T):(H,H)	Other
CH_3COOH	30	N/A	N/A
CH_3CONH_2	360	48:52	D_2O exchange-very slow
PhCONH_2	150	61:39	Isomers interconvert in solution

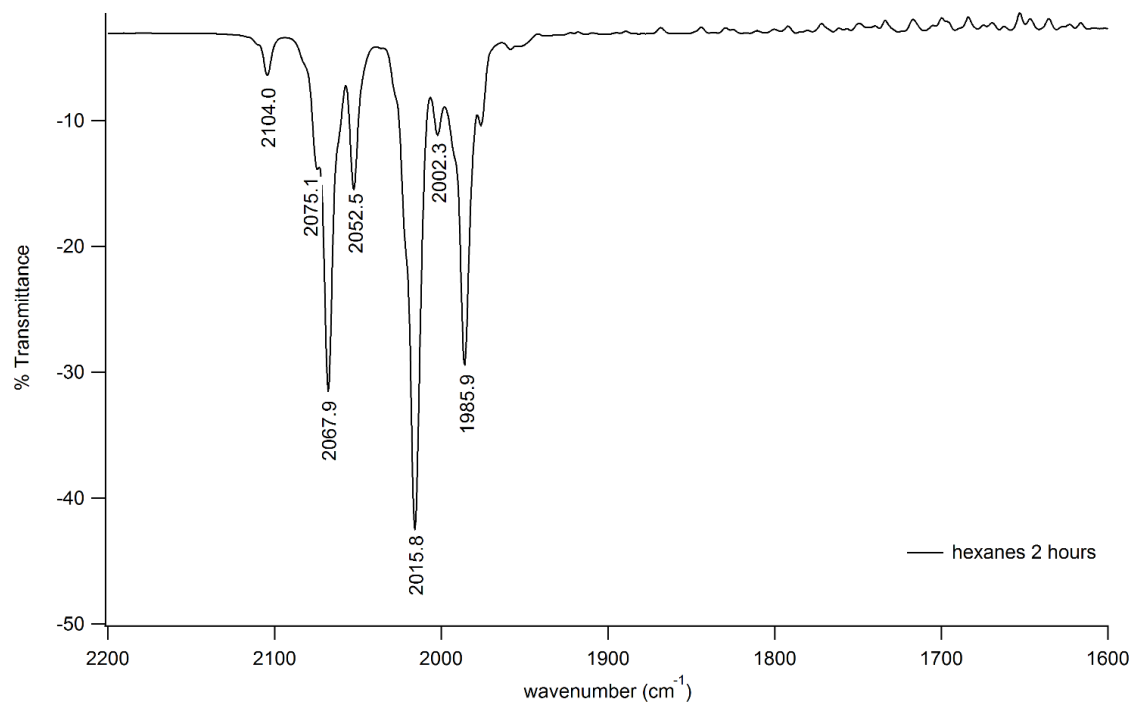
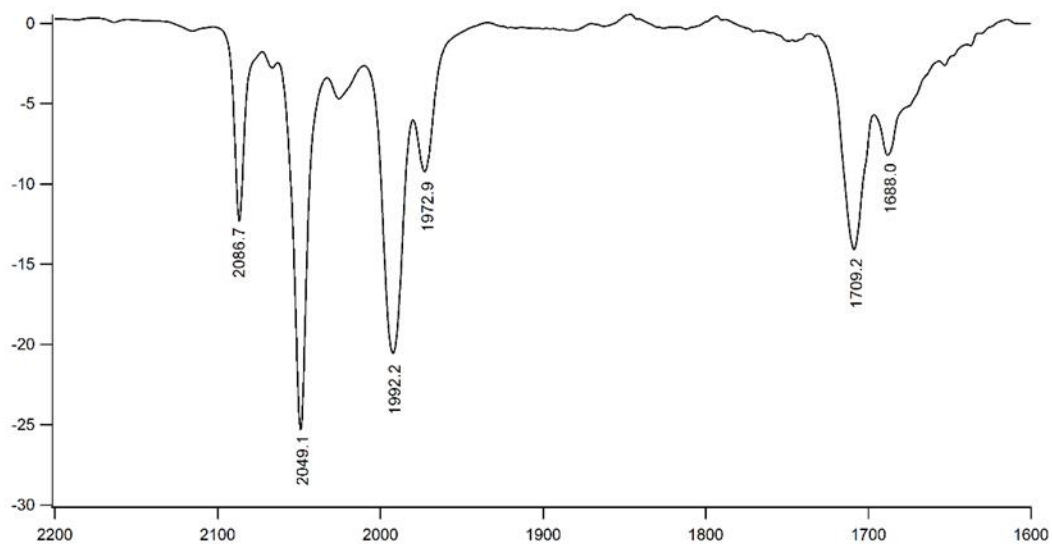
Table 4- Reactions summary of $\text{Os}_3(\text{CO})_{10}(\mu^2\text{-OEt})_2$ with bidentate ligands

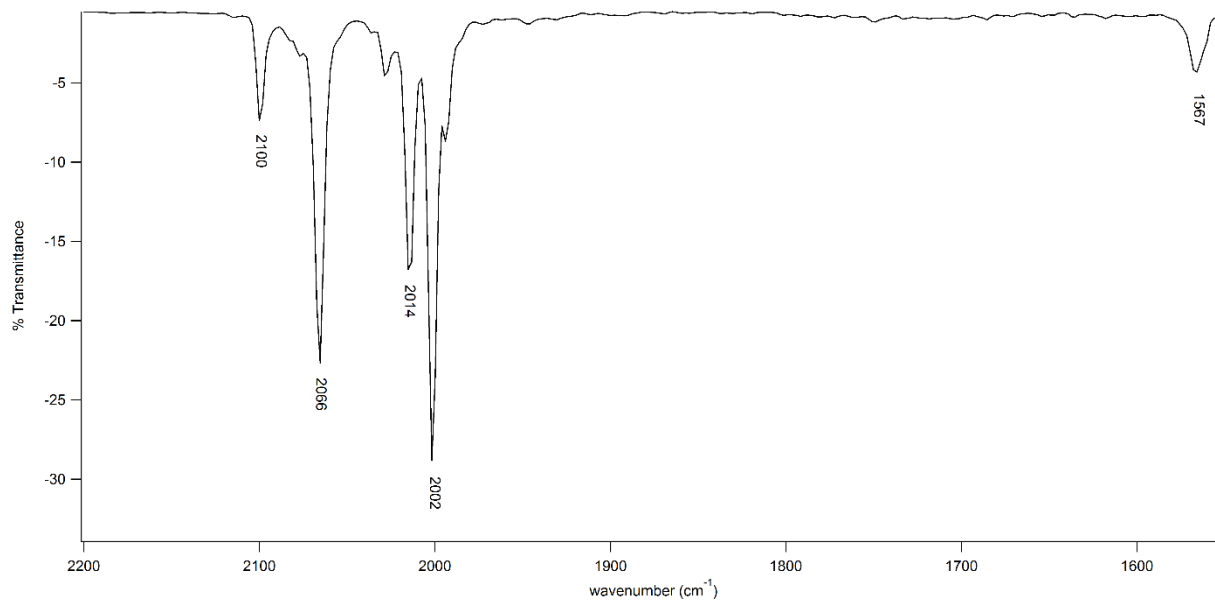
Works Cited

1. Miessler, G. L.; Tarr, D. A. *Inorganic Chemistry*. 4th ed.; Pearson Prentice Hall: 2011.
2. Andriotis, A. N.; Lathiotakis, N.; Menon, M. Magnetic properties of Ni and Fe clusters: a tight binding molecular dynamics study, *Chemical Physics Letters*, 260(1), **1996**, 15-20
3. Krämer, J.; Redel, E.; Thomann, R.; Janiak, C. Use of Ionic Liquids for the Synthesis of Iron, Ruthenium, and Osmium Nanoparticles from Their Metal Carbonyl Precursors. *Organometallics*, **2008**, 27 (9), pp 1976–1978
4. Konga, K.V; Leong, W. K.; Lim, L.H.K. Induction of apoptosis by hexaosmium carbonyl clusters. *J. Organomet. Chem.* **2009**, 694(6), 834–839.
5. Burya, S.J; Palmer, A.M.; Gallucci, J.C.; Turro, C. Photoinduced Ligand Exchange and Covalent DNA Binding by Two New Dirhodium Bis-Amidato Complexes. *Inorg. Chem.* **2012**, 51, 11882–11890
6. Deeming, A. J. Triosmium Clusters. *Adv. Organomet. Chem.*, **1986**, 26, 1-96.
7. Burgess, K. Reactions of triosmium clusters with organic compounds. *Polyhedron*, **1984**, 11, 1175-1225.
8. Braga, D.; Lewis, J.; Johnson, B. F. G.; McPartin, M.; Nelson, W. J. H.; Vargas, M. D. Synthesis and x-ray analysis of the tetrahydrido dianion $[\text{H}_4\text{Os}_{10}(\text{CO})_{24}]^{2-}$, the first noncarbido decaosmium cluster. *J. Chem. Soc., Chem. Commun.* **1983**, 241.
9. Odiaka, T. I., New triosmium metal clusters derived from the reactions between $[\text{Os}_3(\text{CO})_{10}(\text{NCMe})_2]$ and amides. *J. Organomet. Chem.* **1985**, 284(1), 95-99.
10. Ainscough, E. W.; Brodie, A. M.; Coll, R. K.; Coombridge, B. A.; Waters, J. M., The reaction of $[\text{Os}_3(\text{CO})_{10}(\text{CH}_3\text{CN})_2]$ with carboxylic acids: the crystal and molecular structures of $[\text{Os}_3\text{H}(\text{CO})_{10}(\text{C}_6\text{H}_4(\text{OH})\text{CO}_2)]$ and $[\text{Os}_3\text{H}(\text{CO})_{10}(\text{C}_6\text{H}_5\text{COS})]$. *J. Organomet. Chem.* **1998**, 556 (1), 197–205.
11. Fikes, Audrey G.; Gwini, Nigel, Powell, Gregory L.; Yoon, Soo Hun; Nesterov, Vladimir N. *J. Organomet. Chem.* **2014**, 772-773, 188-191
12. Chunxiang Li, W. K. L., The reaction of triosmium and -ruthenium clusters with bifunctional ligands. *J. Organomet. Chem.* **2008**, 693 (7), 1292–1300.

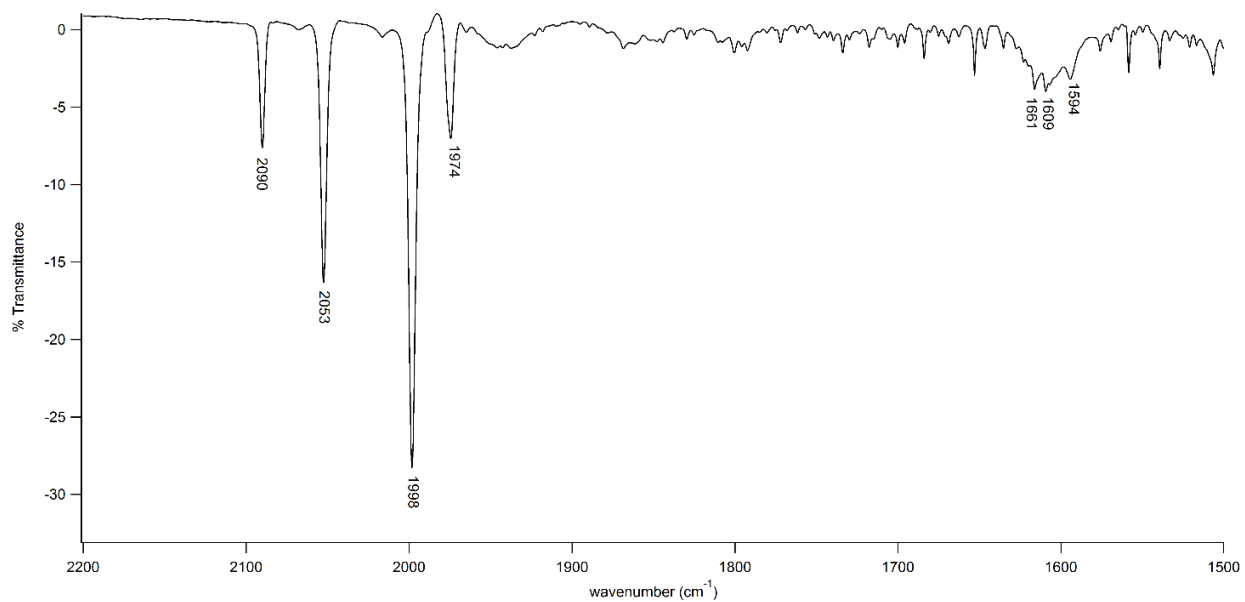
13. Knox, S. A. R.; Koepke, J. W.; Andrews, M. A.; Kaesz, H. D. *J. Am. Chem. Soc.* **1975**, *97*, 3942
14. Deeming, A.J.; Hasso, S.; Underhill, M. Insertion of acetylene into osmium-hydrogen bonds in cluster complexes, *J. Organomet. Chem.* **1974**, *80* (3), C53-C55
15. Clauss, A. D.; Tachikawa, M.; Shapley, J. R.; Pierpont, C. G. Crystal structure and solution dynamics of $(\mu\text{-H})\text{Os}_3(\text{CO})_{10}(\mu\text{-}\eta^2\text{-CPh:CHPh})$, *Inorg. Chem.* **1981** *20* (5), 1528-1533
16. Lynn Schmitt. Unpublished results. Drew University. **2012**.
17. Shari Dunham. Unpublished results. Drew University. **1990**
18. Sommerhalter, Robert. "New Synthetic Approaches to Triosmium Decacarbonyl Bisethoxide and the Systematic Design of Linked Triosmium Clusters via Bridging Diols" Honors Thesis, Drew University, May 2016.
19. Quintos, Christian. Unpublished Results. Drew University, Madison, NJ, 2017.
20. Baum, Brian. "An Investigation of the Kinetics of the Disubstitution Reaction of Triosmium Complexes of type $\text{Os}_3(\text{CO})_{10}(\mu\text{-X})_2$, X=Cl, Br, I, OMe, OEt, OiPr, OtBu, OPh with Trimethyl Phosphite." Honors Thesis, Drew University, May **2004**.
21. Pearsall, M.A. "Synthesis and Reactivity of Some Osmium Carbonyl Clusters." Ph.D. Thesis, University of Cambridge
22. Johnson, B.F.G.; Lewis, J.; Pippard, D.A. *J. Chem. Soc. Dalton Trans.* **1981**, 407.
23. Shah, Ashish.; Crotty, Joe. Unpublished Results. Drew University, Madison, NJ, 2010.
24. Patel, Runi. Unpublished Results. Drew University, Madison, NJ, 2011.
25. Reuger, Caitlyn. Unpublished Results. Drew University, Madison, NJ, 2016.
26. Marak, Katherine. Unpublished Results. Drew University, Madison, NJ, 2016.
27. Bullitt, J.G, Cotton, F.A. The Structure of a Dinuclear Complex of Osmium(I) with a Metal-to-Metal Single Bond: Bis-(p-acetato)hexacarbonyldiosmium. *Theor Chim Act.* **1971**. *5*(3), 406-411
28. Crooks, G. R.; Johnson, B. F. G.; Lewis, J.; Williams, I. G.; Gamlen, G. *Journal of the Chemical Society A: Inorganic, Physical, Theoretical*, **1969**, p2761-2766

29. Pyper , K.J.; Jung, J.Y.; Newton, B.S.; Nesterov, V. N. and Powell, G.L. *J. Organomet. Chem.* **2013**, 723, 103-107.7
30. Neumann, F.; Stoeckli-Evans, H.; Süss-Fink, G. *J. Organomet. Chem.* **1989**, 379. 139-150
31. Katterman, Alex. Unpublished Work, Drew University, **2015**
32. Hohenberg, P.; Kohn, W.; Inhomogeneous electron gas. *Phys Rev.* **1964**, 136(3B). 864-871
33. Haubermann, A.D.; Dolg, M.; Stoll, H.; Preub, H. Energy-adjusted *ab initio* pseudopotentials for the second and third row transition elements. *Theor Chim Act.* **1990**. 77(2), 123-141

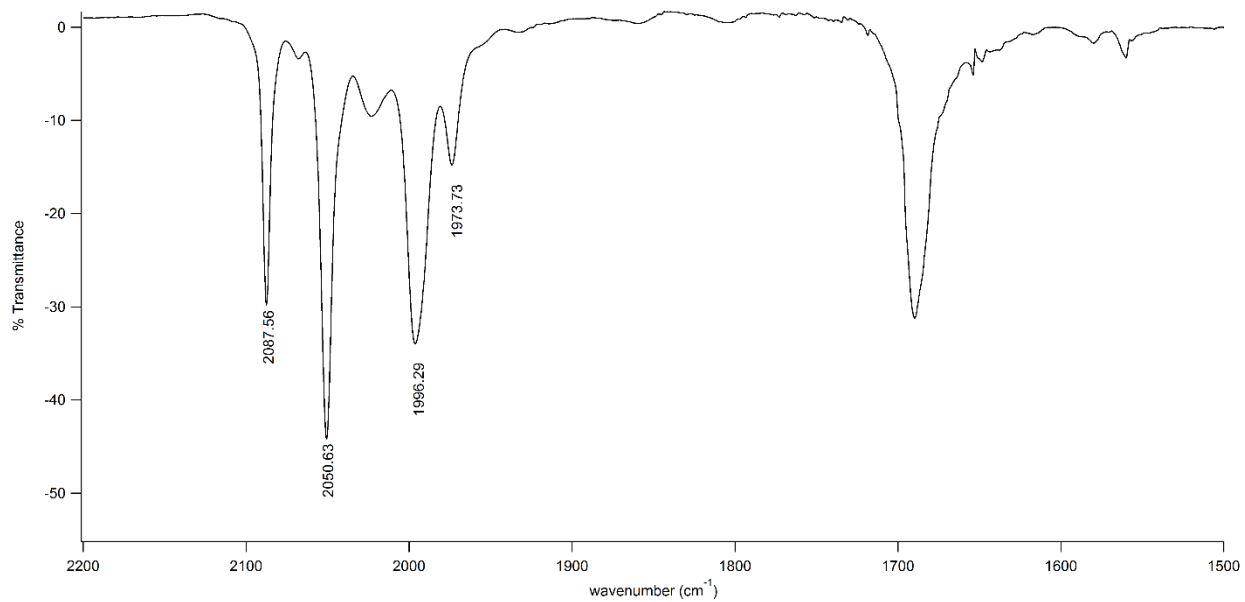
Spectral Appendix:IR1- IR of crude reaction mixture of Os₃(CO)₁₀(μ²-OEt)₂ and acetamide in hexanesIR2- IR of crude reaction mixture of Os₃(CO)₁₀(μ²-OEt)₂ and acetamide after 6 hours in toluene



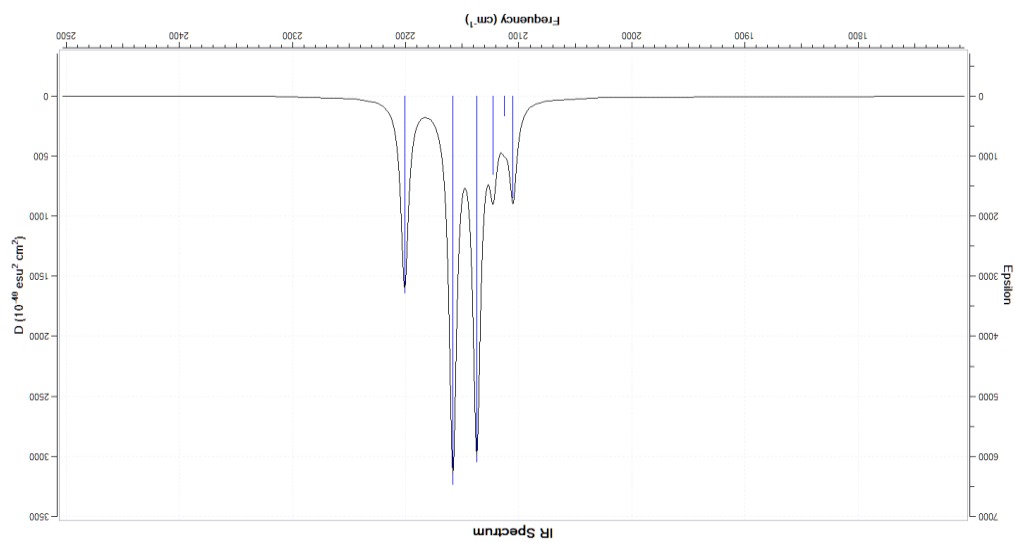
IR3- IR spectrum of Os₂(CO)₆(μ²-RCOO)₂ in hexanes



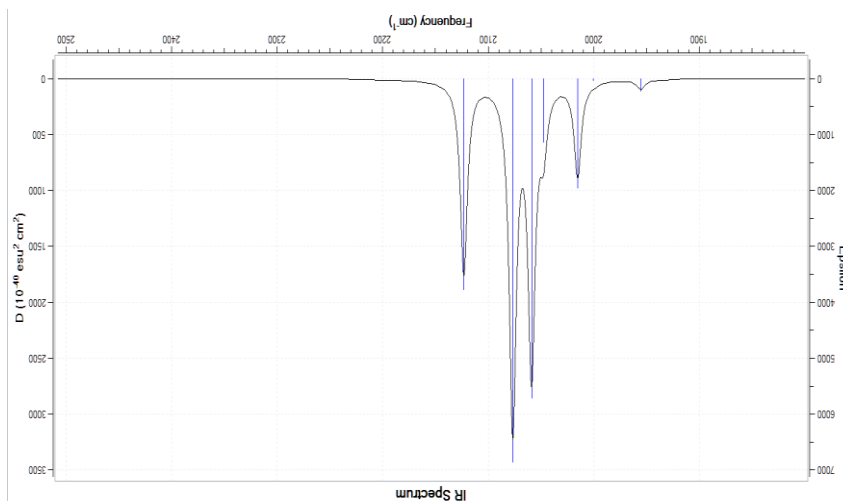
IR 4- IR purified mixture of cis-(H,H) and (H,T) Os₂(CO)₆(μ²-CH₃CONH)₂ in hexanes



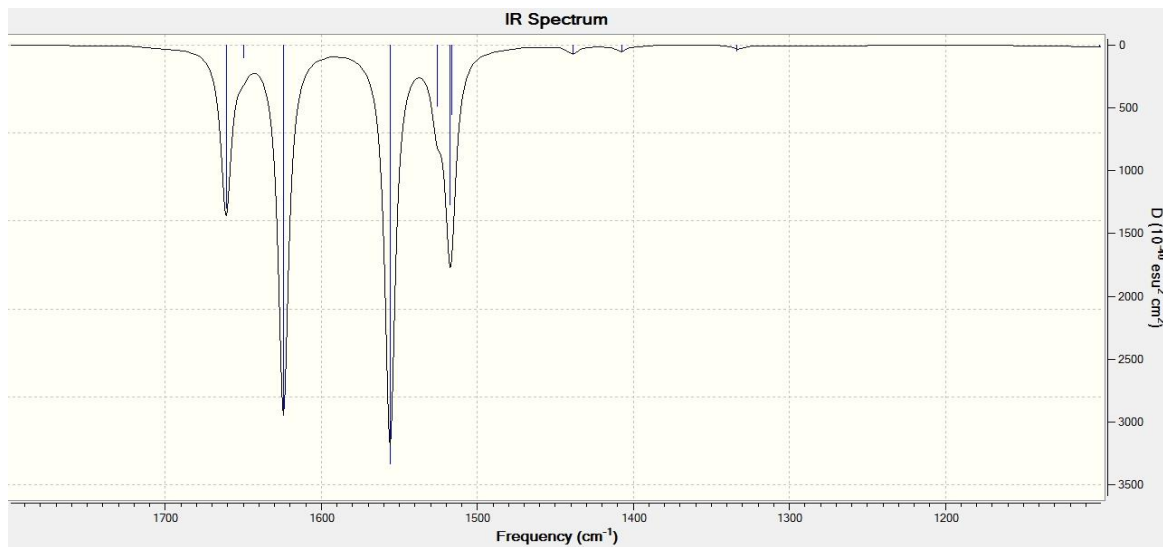
IR5- Crude IR of reaction mixture of benzimide and Os₃(CO)₁₀(u²-OEt)₂ after 150 minutes in toluene



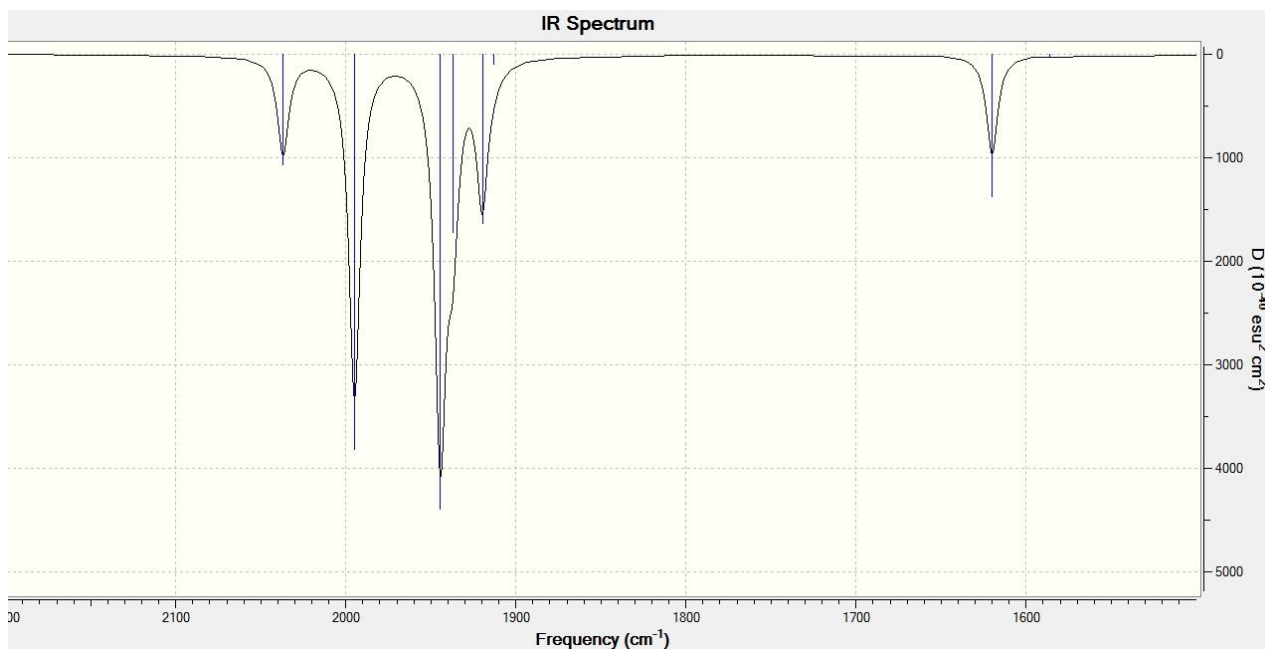
IR6- Computational unoptimized cis-(H,T) Os₂(CO)₆(HCONH)₂ without solvation



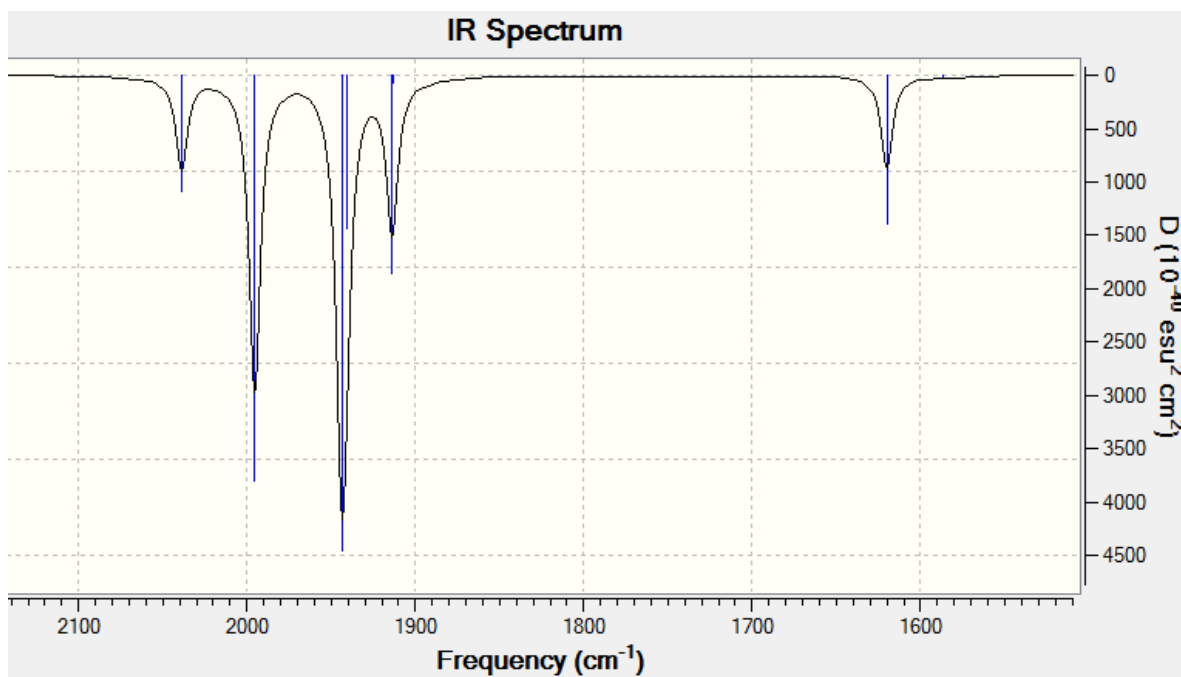
IR7- Computational unoptimized cis-(H,H) Os₂(CO)₆(HCONH)₂ without solvation



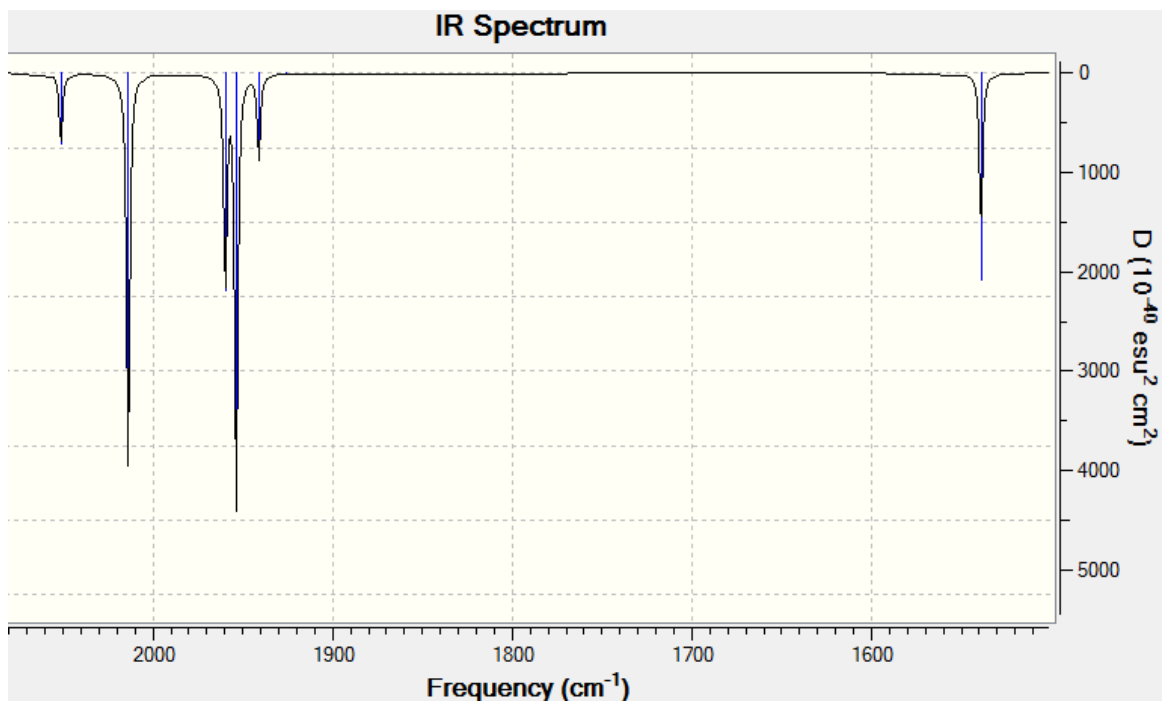
IR8- Frequency calculation of modified structure of cis-(H,T) Os₂(CO)₆(HCONH)₂ without solvation



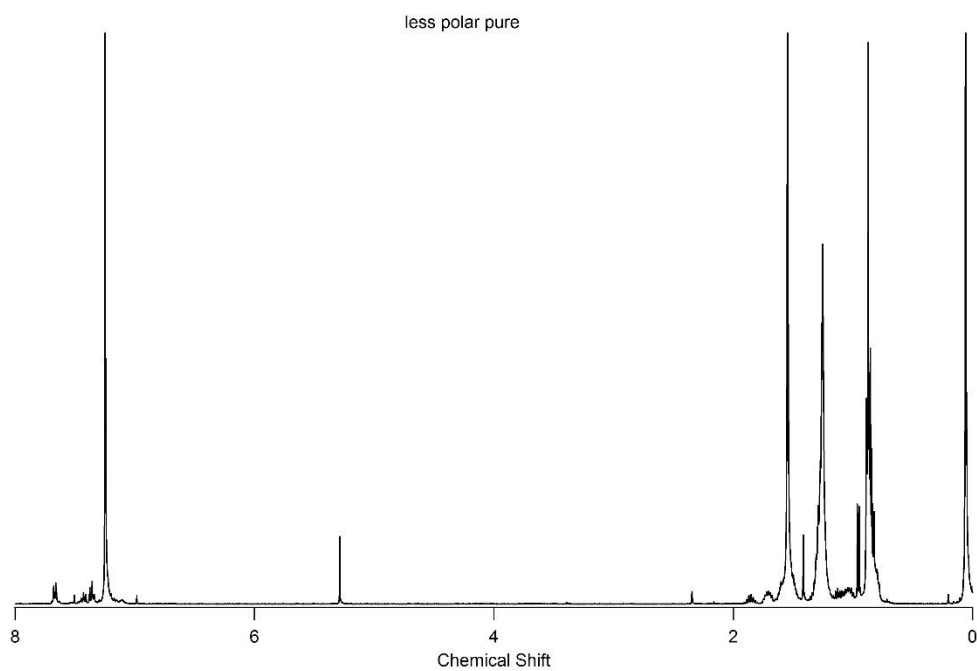
IR9- Theoretical vibrational frequencies for (cis H,T) Os₂(CO)₆(HCONH)₂ solvation heptanes



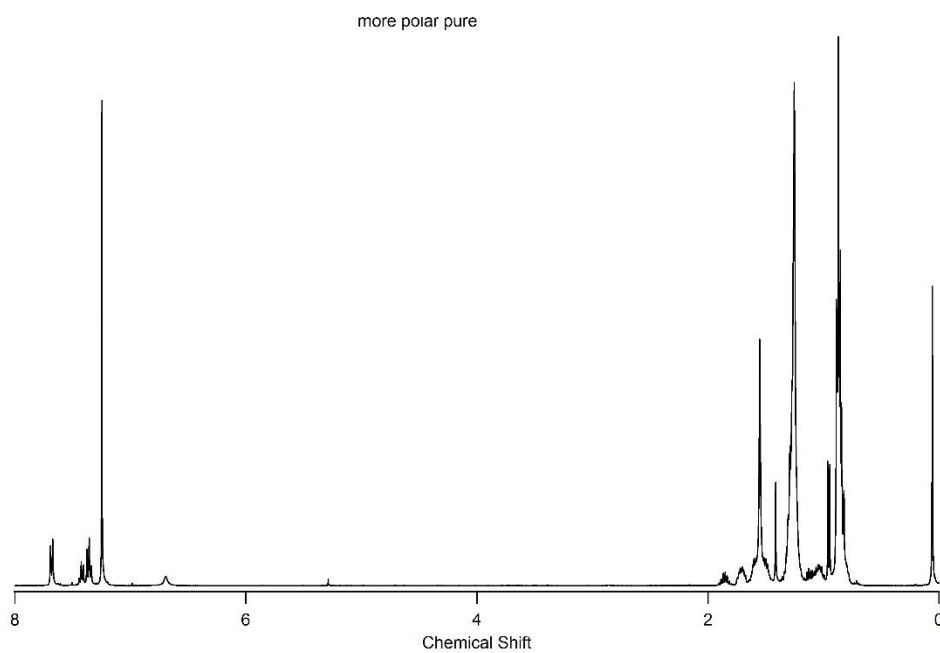
IR10- Theoretical vibrational frequencies for (cis H,H) Os₂(CO)₆(HCONH)₂ solvation heptanes



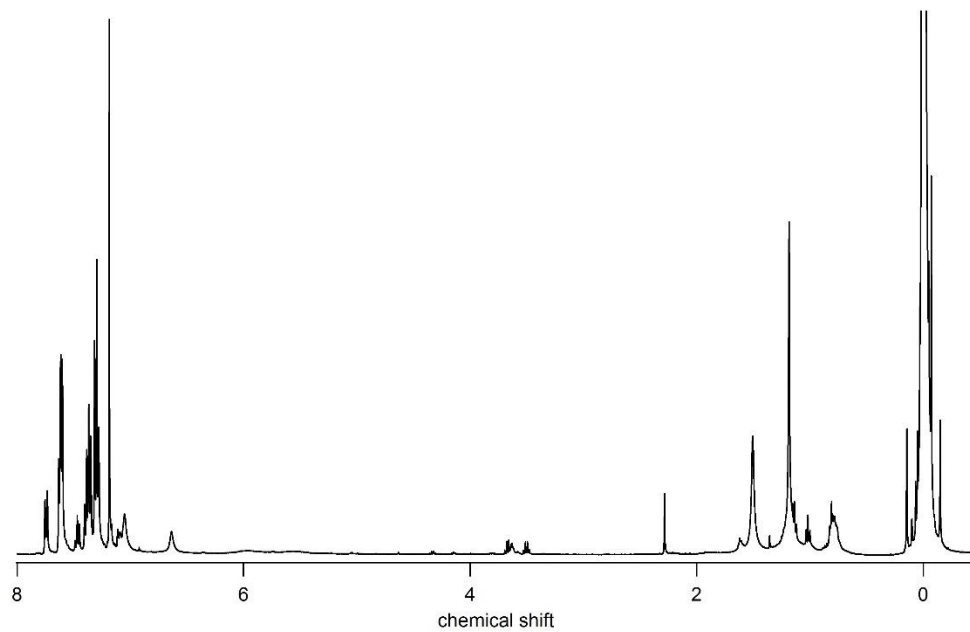
IR11- Theoretical vibrational spectrum of cis- Os₂(CO)₆(HCOO)₂ solvation heptanes



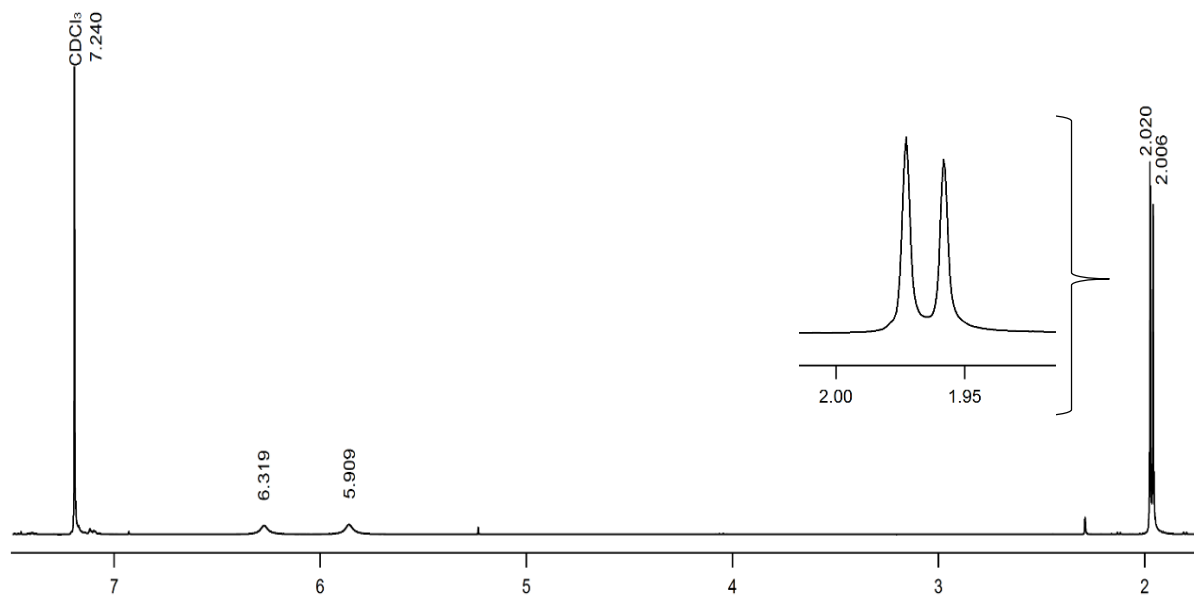
NMR1-¹H NMR of isomer III, cis (H,T) Os₂(CO)₆(μ²-C₆H₅CONH)₂



NMR2- ¹H NMR of IV cis (H,H) Os₂(CO)₆(μ²-C₆H₅CONH)₂



NMR3- ¹H-NMR of mixture D, cis (H,H) and cis (H,T) Os₂(CO)₆(μ²-C₆H₅CONH)₂



NMR4- $^1\text{H-NMR}$ of mixture A corresponding to isomer I,
 $\text{cis (H,T) Os}_2(\text{CO})_6(\mu^2\text{-CH}_3\text{CONH})_2$ and isomer II, $\text{cis (H,H) Os}_2(\text{CO})_6(\mu^2\text{-CH}_3\text{CONH})_2$